AD_____

Award Number: W81XWH-08-1-0203

TITLE: Ovarian autoantibodies predict ovarian cancer

PRINCIPAL INVESTIGATOR: Judith Luborsky, PhD

CONTRACTING ORGANIZATION: Rush Presybeterian St. Lukes Medical Center
Chicago, IL 60612

REPORT DATE: November 2010

TYPE OF REPORT: Final

PREPARED FOR: U.S. Army Medical Research and Materiel Command
Fort Detrick, Maryland 21702-5012

REPORT DOCUMENTATION PAGE

Form Approved
OMB No. 0704-0188

1. REPORT DATE *(DD-MM-YYYY)*	2. REPORT TYPE	3. DATES COVERED *(From - To)*
01-11-2010	Final	1 MAY 2008 - 31 OCT 2010

4. TITLE AND SUBTITLE
Ovarian autoantibodies predict ovarian cancer

5a. CONTRACT NUMBER

5b. GRANT NUMBER
W81XWH-08-1-0203

5c. PROGRAM ELEMENT NUMBER

6. AUTHOR(S)
Judith Luborsky, PhD

E-Mail: jluborsk@rush.edu

5d. PROJECT NUMBER

5e. TASK NUMBER

5f. WORK UNIT NUMBER

7. PERFORMING ORGANIZATION NAME(S) AND ADDRESS(ES)
Rush Presybeterian St. Lukes Medical Center
Chicago, IL 60612

8. PERFORMING ORGANIZATION REPORT NUMBER

9. SPONSORING / MONITORING AGENCY NAME(S) AND ADDRESS(ES)
U.S. Army Medical Research and Materiel Command
Fort Detrick, Maryland 21702-5012

10. SPONSOR/MONITOR'S ACRONYM(S)

11. SPONSOR/MONITOR'S REPORT NUMBER(S)

12. DISTRIBUTION / AVAILABILITY STATEMENT
Approved for Public Release; Distribution Unlimited

13. SUPPLEMENTARY NOTES

14. ABSTRACT

Ovarian cancer (OVCA) affects about 25,000 women annually. Most cases are diagnosed at a late stage with less than a 20% probability of survival. We used the egg-laying hen, a spontaneous animal model of OVCA, to test the hypothesis that hens with AOA are more likely to develop OVCA, and therefore that AOA can be used as a predictor of OVCA. We compared the proportion of hens with AOA to those without AOA that developed OVCA. Serum AOA was measured by immunoassay by standard methods. Angiogenesis (new blood vessel formation) is a hallmark of tumor pathology and was measured in serial assessments as blood flow resistance by color Doppler ultrasound. Only hens with anti-tumor antibodies showed significant evidence of angiogenesis, a surrogate marker of early OvCa. We also demonstrated that specific antibodies to mesothelin, a specific antigen in human OVCA, are found in hens with OVCA. Demonstrating that AOA precedes OVCA would expand the number of measurable risk factors for OVCA, revolutionize screening for OVCA, and make it possible to detect OVCA prior to its development, or in its early stages when effective treatments are available.

15. SUBJECT TERMS
Ovarian cancer, autoantibodies, animal model, chicken

16. SECURITY CLASSIFICATION OF:			17. LIMITATION OF ABSTRACT	18. NUMBER OF PAGES	19a. NAME OF RESPONSIBLE PERSON
a. REPORT	b. ABSTRACT	c. THIS PAGE			USAMRMC
U	U	U	UU	87	19b. TELEPHONE NUMBER *(include area code)*

Table of Contents

INTRODUCTION

Subject: The objective of this study was to determine if anti-ovarian autoantibodies (AOA) precede ovarian cancer (OVCA) in the laying hen model of OVCA. In humans, AOA are associated with infertility [1, 2]. infertility is also an epidemiologic risk factor for OVCA that has not been explored [3]. Since the same group of women have both AOA and OVCA risk, AOA may be a risk factor that can be used to predict OVCA, and this will be tested in the hen model.

Purpose: We will test the hypothesis that hens with AOA are more likely to develop OVCA, and therefore that AOA can be used as a predictor of OVCA.

Scope: The study design is longitudinal. We developed ultrasound detection of hen OVCA that permits longitudinal evaluation of early events associated with tumor initiation and progression. Since hens with reduced egg production have declining ovarian function, similar to human infertility, we use egg production as a selection factor, in addition to the presence or absence of AOA. Thus, to test the hypothesis that AOA precede ovarian pathology, we will select hens with low egg production, and with and without AOA, and monitor ovarian pathology by ultrasound in middle aged hens (2.5-3 year old) at intervals for 9 months.

Addendum: At the term of this we project we requested and received an extension (reasons detailed below). This report describes additional progress in the last 12 months. The additional information is underlined.

BODY

Research accomplishments associated with each task in the Statement of Work

The plan was dependent on access to an ultrasound machine; the pilot data was obtained with a z-one (Zonaire Medical Systems) and was loaned by the company for the pilot data that led to the study. However, in the first 3 months, the company that we were collaborating with was closed. We applied for and received an institutional capital equipment grant and purchased a Micromax 2D Ultrasound (Sonosite Inc.). This took about 10 months. Therefore, we have also applied for a no-cost extension for this project (letter submitted to contract officer, Susan.Dellinger@Amedd.Army.Mil). The original progress report represented the 3 months of initial work (June 2008-September 2008) and 4 recent months of work (August 2009-October 2009). The "Addendum" sections report work since the last report and covers one year (November 2009-Novmeber 2010). A summary of final activity is included in the Addendum. The tasks associated with the original SOW were accomplished and are summarized below.

Personnel supported by this project include: Judith Luborsky, PhD, Professor (Principal Investigator), Animesh Barua, PhD, Assistant Professor (co-investigator) and Seby Edassery, MS (Research Associate).

SOW Task 1: Select 120 hens for longitudinal study of risk factors for OVCA (months 1-3) by selecting White leghorn hens (Gallus domesticus) hens with normal (5-6 eggs/clutch) or low egg production (< 3 eggs/clutch) with normal ultrasound morphology.

1. Perform Gray scale ultrasound to assess morphology for normal follicles and absence of ovarian mass or cysts. *Progress: 117 hens were examined for inclusion in the study. 85 hens were screened by gray scale ultrasound to determine normal morphology; 57 without an apparent mass and several follicles were select for further monitoring.* As of this report all morphology by ultrasound is completed.

2. Perform Doppler ultrasound to assess blood flow indices in comparison to same aged hens with normal egg production. *Progress: 85 hens were screened by color Doppler ultrasound and the Resistive (RI) and Pulsatility Index (PI) measured as an indication of blood flow velocity and tumor associated neo-angiogenesis.* As of this report all measurement of angiogenesis by Doppler ultrasound is completed.

3. Analyze data and determine baseline values. *Progress: Baseline data, summarized below, was analyzed and was presented at the regional Reproductive Biology Symposium (abstract appended).* As of this report initial data analysis of ultrasound is completed.

b. Measure serum AOA by immunoassay and 2D Western blot by standard methods in serum samples. *Progress: Baseline data for AOA was analyzed and was summarized in the attached abstract presented at the regional Reproductive Biology Symposium.* Serum AOA measurement was completed.

c. Form 3 groups as follows: (group A, n= 40) low egg production with AOA; (group B, n=40) low egg production negative for AOA; and (group C, n=40) normal egg production without AOA. Assign random numbers (1 to 40) to hens in each group so that hens in control groups (B, C) will be sacrificed when the same numbered hen is sacrificed in experimental group A. *Progress: Three hen groups were formed, as reported in the attached abstract. The study is not complete as explained above.* As of this report hen groups were determined; they may be modified for analysis according to final histological categories as a secondary analysis. The final adjustments are 90% complete.

SOW Task 2: Follow animals to detect tumor initiation (months 3-12):

a. Measure ultrasound and AOA by immunoassay and Western blot monthly. *Progress: Ultrasound scans were performed; 85 hens were scanned once and 57 hens were scanned twice. Serum was obtained at each scan. Western blot will be completed at the end of the study for those hens with at least three ultrasound scans and serum samples.*

b. Sacrifice animals when Doppler ultrasound indices (RI and PI values reflecting reduced resistance associated with angiogenesis) decline significantly compared to values for normal hens. After the first change, evaluate hens again the next month and if the values remain abnormal, sacrifice hens and collect serum and tissue. *Progress: Hens have been sacrificed or died (n=7). The plan is to continue monitoring the 50 remaining hens in the next 6 months.*

SOW Task 3: Determine if AOA predicts OVCA (months 10-18):

a. Confirm the presence or absence of ovarian tumors in ovarian tissue. For histological evaluation, ovaries will be cut into 8 segments, fixed in formalin, paraffin embedded and sectioned for H and E staining. Every third section (10μm) from the entire ovary will be evaluated, photographed and scored. Ovarian histology will be examined for focal lesions exhibiting OVCA histology and for the number of inclusion cysts. Any pathological change observed by ultrasound and confirmed by histology will be scored as OVCA. *Progress: A systematic study of tumor histology was completed and published [4] as a basis for this task (manuscript appended).* This task is completed.

b. Review and compile data and perform statistical analysis to determine if AOA is a significant predictor of OVCA. The proportion of hens with AOA that develop OVCA (group A) will be compared with those without AOA (groups B, C) using Chi square analysis with $p < .05$ considered significant. *Progress: This task remains to be completed.* This task remains to be completed.

The data obtained as of September 2009 was presented at a regional meeting (30th Annual Minisymposium on Reproductive Biology, October 2009). The data is presented in Table 1. In brief, hens (n=50) were assessed initially by ultrasound and color Doppler ultrasound and then again at about 14 months. AOA were determined in serum taken at the same time using a pooled extract of three tumors in immunoassay.

At the second assessment, there were 3 groups of hens: (A) anti-tumor antibody negative (n=20) at both time points, (B) anti-tumor antibody negative at the first assessment and antibody positive at the second assessment (n=18) and (C) anti-tumor antibody positive/borderline at both assessments (n=12). In hens that remained antibody negative (group A), the average blood flow resistance declined non-significantly from 0.52±0.14 (RI) and 0.86±0.37 (PI) to 0.47±0.11 (RI) and 0.68±0.22 (PI) (p=0.2 and 0.07 respectively). In group B, hens that transitioned from negative to positive, the average RI and PI values declined significantly (p=0.04 and 0.01 respectively). In hens that remained positive (group C), values also declined significantly (p=0.05 and 0.02) from 0.55±0.17 (RI) and 0.89±0.38 (PI) to 0.43±0.10 (RI) and 0.57±0.16 (PI). Thus only hens with anti-tumor antibodies showed significant evidence of angiogenesis, a surrogate marker of early OvCa.

Table 1. Comparison of Blood Flow Velocity (angiogenesis) by AOA

Antibody group	1st scan		2nd scan	
	RI	PI	RI	PI
negative (n=20)				
average±SD	0.52±0.14	0.86±0.37	0.47±0.11	0.68±0.22
p value (t test)	ref	ref	0.20	0.07
changed (n=18)				
average±SD	0.62±0.19	1.02±0.40	0.51±0.10	0.73±0.21
p value (t test)	ref	ref	0.04	0.01
positive(n=12)				
average±SD	0.55±0.17	0.89±0.38	0.43±0.10	0.57±0.16
p value (t test)	ref	ref	0.05	0.02

Addendum: Overall 119 hens were examined by ultrasound to determine ovarian morphology and evidence of angiogenesis (defined by a decrease of RI and PI values below 0.4). Of these 42 already had OvCa and were excluded, died naturally or were euthanized due to other illness during the course of the study; 77 were monitored further. 52 hens had three or more ultrasound scans and usable data during 16 months. 21 were initially positive for AOA and 13 hens progressed to OVCA (62%); 31 were initially negative for AOA and 12 of these hens progressed to OVCA (39%). However, of the 31 hens that were initially negative, 7 became positive for AOA during surveillance bringing the total AOA negative hens (n=24) that developed OVCA to 5 out of 24 (20%). Therefore we proved our original hypothesis, although further work remains to be completed.

Relationship of the most recent findings with that of previously reported findings

The concept that autoantibodies precede overt signs of carcinogenesis is supported by literature reports; for example, in patients with chronic hepatitis (which predisposes to liver cancer) specific antibodies appeared a year or more before patients went on to develop hepatocellular carcinoma [5]; the same antibodies reappeared before recurrence in these patients. The increase in antibodies occurred either as an increase in titer of a pre-existing antibody or as the appearance of a novel reaction. Similarly, studies suggest that anti-p53 appears before lung cancer develops in groups at high risk [5]. The link between autoimmunity (e.g., rheumatoid arthritis, SLE, Sjogrens's syndrome) and non-Hodgkin's lymphoma is well established. Furthermore, a role for B cell hyperactivity in carcinogenesis was suggested by a small study in which the anti-B cell drug rituximab reduced tumor burden in colon cancer [6]. Thus, although the role of antibodies and B cells in cancer etiology is not well understood, the phenomenology is apparent, and supports the concept that antibodies could be used as very early "reporters" of incipient cancer.

The results are consistent with our pilot study which showed that low egg laying hens with and without AOAs followed prospectively for up to 45 weeks using Doppler ultrasound as reported previously [7] (*Figure 7*) . Briefly, we monitored Resistive and Pulsatile Indices generated by the Micromax 2D Ultrasound (Sonosite Inc.) at 15 week intervals in hens (n=9) that were either AOA positive or negative at the initial reading. The blood flow indices reflect ovarian blood flow velocities and detect changes in vascular architecture related to neo-angiogenesis. Neo-angiogenesis is an early change in tumor development. Tumor tissue revealed lower indices reflecting increased vascularization and flow velocity. Significantly, 83% of hens with antibodies developed OVCA and this was accompanied by a characteristic decrease in blood flow resistance (angiogenesis) similar to women with ovarian tumors [8].

This study will be the first to show that AOA predicts OVCA. This suggests the possibility of developing a screening test for early detection of OVCA based on antibody detection. In order to translate these findings to

humans we are submitting applications to repositories with serial serum collections that include pre-diagnostic sera.

Problems in accomplishing tasks

- The plan was dependent on access to an ultrasound machine; the pilot data was obtained with a Zonaire and was loaned by the company for the pilot data that led to the study. However, in the first 3 months, the company that we were collaborating with closed. We applied for and received an institutional capital equipment grant and purchased a Micromax 2D Ultrasound (Sonosite Inc.). This took about 10 months. Therefore, we have also applied for a no-cost extension for this project.
- Since the assay we are using for antibodies is an ovarian tumor extract, it may not efficiently monitor all relevant antibodies. During this study we developed additional information on specific antigens in the hen, relevant to this project using Western blots and mass spectrometry [9] and using immunoassays with recombinant proteins to detect antibodies [10]. We found that mesothelin is expressed in hen ovarian tumors with a similar pattern of expression as in humans (manuscript appended). Furthermore, we detected antibodies to recombinant mesothelin in serum from hens with ovarian tumors, similar to humans [10]. Thus we conducted the pilot study and found an increase in mesothelin antibody in two hens before OVCA (Figure 3). This suggests that a positive AOA result may reflect changing antibody specificities during tumor progression since of the two hens one was initially AOA positive and the other was initially AOA negative, but neither had mesothelin antibodies at the outset.

Recommended changes or future work to better address the research topic

We suggest that in addition to using the AOA antibody assay, we will test for several specific antibodies that are relevant to human OvCa to gain additional information on early reactions that would predict OvCa. Currently, it is not clear which antibody reactions might occur early and if the antibody specificity or titer changes with tumor stage, as shown for liver cancer [5]. Thus the serum and data collected for this study could be used to define the timing of specific antibody appearance.

Ultrasound has proven useful for assessing general morphology but selecting hens with reduced egg-laying (reduced ovarian function) leads to lower initial values for blood flow velocity and we may be missing initial angiogenic changes. Other parameters can be assessed.

KEY RESEARCH ACCOMPLISHMENTS

- Hens were selected using ultrasound and AOA immunoassay. Mid-study results show hens with AOA are more likely to show evidence of neo-angiogenesis (used as a surrogate marker of OVCA), consistent with the results of a pilot study. The results were presented at a regional meeting.
- A systematic study of tumor histology and tumor classification was completed as a baseline for evaluation of tumor pathology. The manuscript was published.
- The expression of mesothelin, a relatively specific antigen in OVCA was demonstrated and corresponding circulating mesothelin antibodies were found specifically associated with ovarian tumors in the hen .
- **Addendum**: From this study
    - Hens were followed serially for morphology and angiogenesis by ultrasound and for the presence of AOA up to 20 months
    - 95% of the diagnostic histology is completed
    - pilot data was obtained showing an increase in mesothelin antibody in two hens before OVCA
    - cellular immunology foundation study showed immune cell content in ovaries and tumors and that hens express S1P1 (which regulates lymphocyte trafficking)

REPORTABLE OUTCOMES

- Manuscripts: seven manuscripts were produced
    - Barua, A., et al., *Histopathology of Malignant Ovarian Tumors in Laying Hens, a Preclinical Model of Human Ovarian Cancer. Int J Gyn Cancer,* 2009. **19**(4): p. 531-539.
    - Yu, Y., et al., *Mesothelin expression in ovarian tumors of the laying hen model is similar to human ovarian cancer.* revisions submitted December 2010.
    - Barua A, Bitterman P, Bahr JM, Bradaric MJ, Hales DB, Luborsky JL, Abramowicz JS (2010) *Detection of tumor-associated neoangiogenesis by Doppler ultrasonography during early-stage ovarian cancer in laying hens: a preclinical model of human spontaneous ovarian cancer.* J Ultrasound Med. 2010 Feb;29(2):173-82.
    - Barua A, P Bitterman, JM Bahr, S Basu, E Sheiner, MJ Bradaric, DB Hales, JL Luborsky, JS Abramowicz (2010) *Contrast Enhanced Ultrasonography Detects Spontaneous 1 Ovarian Cancer at Early Stage in a Preclinical Animal Model,* J Ultrasound Med, in press
    - Bradaric, MJ, Barua, A, Penumatsa, K, Yi,Y, Edassery,SL, Sharma S, Abramowicz,JS, Bahr, JM, Luborsky, J (2010) *Sphingosine-1 Phosphate Receptor (S1p1), a Critical Receptor Controlling Human Lymphocyte Trafficking, is Expressed in Hen and Human Ovaries and Ovarian Tumors*, submitted December 2010.
    - Bradaric, MJ; Barua, A; Penumatsa, K; Bitterman, P; Abramowicz, JS; Bahr, JM; and Luborsky, JL (2011) *Analysis of lymphocytes in spontaneous ovarian tumors in the laying hen show altered B cell content in early stage tumors*, in preparation (submission January 2011)
- Abstracts & Presentations: five meeting abstracts were produced
    - J. E. Nam, S.L. Edassery, A. Barua, J. Abramowicz, P. Bitterman, J.M. Bahr and J.L. Luborsky, *Anti-tumor antibodies may precede ovarian tumors in the laying hen model of ovarian cancer,* 30th Annual Minisymposium on Reproductive Biology, Chicago, IL, October, 2009 (poster)
    - J. E. Nam, S.L. Edassery, A. Barua, J. Abramowicz, P. Bitterman, J.M. Bahr and J.L. Luborsky, *Anti-tumor antibodies may precede ovarian tumors in the laying hen model of ovarian cancer,* 30th Annual Minisymposium on Reproductive Biology, Chicago, IL, October, 2009 (poster)
    - Judith L Luborsky, Seby L Edassery, Krishna Penumatsa, M Bradaric, Yi Yu , Karl Eric Hellstrom, Animesh Barua, Pincas Bitterman, Ingegerd Hellstrom, *Common autoantibodies in ovarian cancer (OvCa) and infertility may define biomarkers for OvCa risk,* American Association for Cancer Research (annual meeting), Washington, DC, abstract #2737
    - Yi Yu; Seby L Edassery; Animesh Barua; Pincas Bitterman; Jacques S. Abramowicz; Janice M Bahr; Ingegerd Hellstrom and Judith L Luborsky, *Mesothelin expression in ovarian tumors and serum autoantibodies of the laying hen model is similar to human ovarian cancer,* American Association for Cancer Research (annual meeting), Washington, DC, abstract #3264
    - Bradaric, MJ; Barua, A; Penumatsa, K; Bitterman, P; Abramowicz, JS; Bahr, JM; Luborsky, JL *Lymphocyte content differs in normal ovaries and ovarian tumor stages in spontaneous ovarian cancer in the chicken*. American Association for Cancer Research (annual meeting), Washington, DC, #1918
- Patents and licenses applied for and/or issued; degrees obtained that are supported by this award:
    - none
- Development of cell lines, tissue or serum repositories:

- Hen serum is archived for additional tests.

- Funding applied for based on work supported by this award
  - Awarded: NIH 1R01CA134487-01 (I Hellstrom, PI), J Luborsky (co-invest & PI, subcontract), "Mesothelin as a marker and therapeutic target for ovarian cancer", 9/15/08-9/14/12. The subcontract objective is to use the hen model for preclinical studies of a vaccine against mesothelin.
  - NIH R01CA143457-01, J Luborsky (PI), "Antibodies as predictors of ovarian cancer and role of B cells in tumor etiology" (submitted February 2009; not funded)
  - NIH (RFA-CA-09-017, The Early Detection Research Network: Biomarker Developmental Laboratories (U01)) , J Luborsky (PI), "Novel cancer risk groups: biomarkers for ovarian cancer risk in infertility," (submitted October, 2009; not funded)
  - NIH RFA-OD-09-003 for (03) Biomarker Discovery and Validation and specific Challenge Topic, 03-CA-110 Validation of Known Biomarkers", J Luborsky (PI) "Antibodies to ovarian cancer markers in infertility define ovarian cancer risk" (score 7 percentile; not funded)
  - NIH R01, J Luborsky (PI) "Autoantibodies predict ovarian cancer risk in women with infertility" re-submission February 2011 (Aims based on the Challenge grant with a 7 percentile)
  - Marsha Rivkin Center for Ovarian Cancer Research, "Specific ovarian autoantibodies predict ovarian cancer", submitted December 2010

- Employment or research opportunities applied for and/or received based on experience/training supported by this award :
  - Dr Barua, co-investigator, was promoted from postdoctoral fellow to Assistant Professor (2008)

CONCLUSION

This study will be the first to show that AOA predicts OVCA. This suggests the possibility of developing a screening test for early detection of OVCA based on antibody detection. A suggested change to future work is to relate the development of ovarian tumors to specific antibodies using recombinant protein antigens for detection. Since we found that many of the antigens associated with human OVCA are also found in hens with OVCA (e.g., mesothelin antibodies) identification of the predictive value of these antibodies in the hen has a direct application to patients at risk of OVCA and development of these tests is a marketable product.

REFERENCES

1. Luborsky, J., *Ovarian autoimmune disease and ovarian autoantibodies.* J Womens Health Gend Based Med, 2002. **11**(7): 585-99.
2. Forges, T., et al., *Autoimmunity and antigenic targets in ovarian pathology.* Hum Reprod Update, 2004. **10**(2): 163-75.
3. Runnebaum, I.B. and E. Stickeler, *Epidemiological and molecular aspects of ovarian cancer risk.* J Cancer Res Clin Oncol, 2001. **127**(2): 73-79.
4. Barua, A., et al., *Histopathology of Malignant Ovarian Tumors in Laying Hens, a Preclinical Model of Human Ovarian Cancer. Int J Gyn Cancer*, 2009. **19**(4): 531-539.
5. Tan, E.M. and J. Zhang, *Autoantibodies to tumor-associated antigens: reporters from the immune system.* Immunol Rev, 2008. **222**: 328-40.
6. Barbera-Guillem, E., et al., *B lymphocyte pathology in human colorectal cancer. Experimental and clinical therapeutic effects of partial B cell depletion.* Cancer Immunol Immunother, 2000. **48**(10): 541-549.

7. Barua, A., et al., *Anti-ovarian and anti-tumor antibodies in women with ovarian cancer.* Am J Reprod Immunol, 2007. **57**: 243-249.
8. Barua, A., et al., *Detection of Ovarian Tumors in Chicken by Ultrasonography - a Step towards Early Diagnosis in Humans?* J Ultrasound Med 2007. **26**: 909-919.
9. Barua, A., et al., *Prevalence of anti-tumor antibodies in the laying hen model of human ovarian cancer.* International Journal of Gynecological Cancer, 2009. ***18(4)****: 500-507.*
10. Yu, Y., et al., *Mesothelin expression in ovarian tumors of the laying hen model is similar to human ovarian cancer.* Gynecol Oncol, 2009. submitted October 2009.

APPENDICES

- Barua A, Bitterman P, Bahr JM, Bradaric MJ, Hales DB, Luborsky JL, Abramowicz JS (2010) *Detection of tumor-associated neoangiogenesis by Doppler ultrasonography during early-stage ovarian cancer in laying hens: a preclinical model of human spontaneous ovarian cancer.* J Ultrasound Med. 2010 Feb;29(2):173-82.
- Barua A, P Bitterman, JM Bahr, S Basu, E Sheiner, MJ Bradaric, DB Hales, JL Luborsky, JS Abramowicz (2010) *Contrast Enhanced Ultrasonography Detects Spontaneous 1 Ovarian Cancer at Early Stage in a Preclinical Animal Model*, J Ultrasound Med, in press
- Bradaric, MJ, Barua, A, Penumatsa, K, Yi,Y, Edassery,SL, Sharma S, Abramowicz,JS, Bahr, JM, Luborsky, J (2010) *Sphingosine-1 Phosphate Receptor (S1p1), a Critical Receptor Controlling Human Lymphocyte Trafficking, is Expressed in Hen and Human Ovaries and Ovarian Tumors*, submitted December 2010.

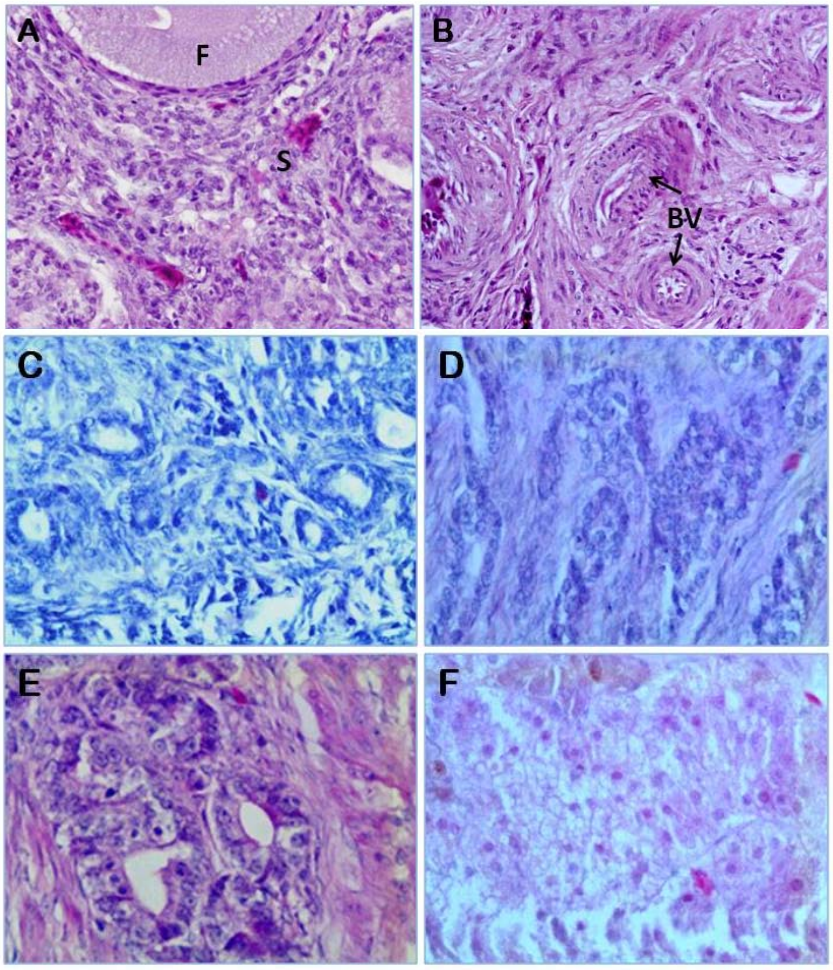

Figure 1. Examples of the diagnostic histology of hen ovaries showing normal ovaries (A-B) and ovarian tumors (C-F). (A) Normal ovary showing follicle (F) and stroma (S). (B) Normal ovary showing the medullary (M) region with large central blood vessels (BV). (C) Endometrioid ovarian tumor (D) Serous ovarian tumor (E) mucinous ovarian tumor (F) clear cell ovarian tumor. Original magnification = 40x.

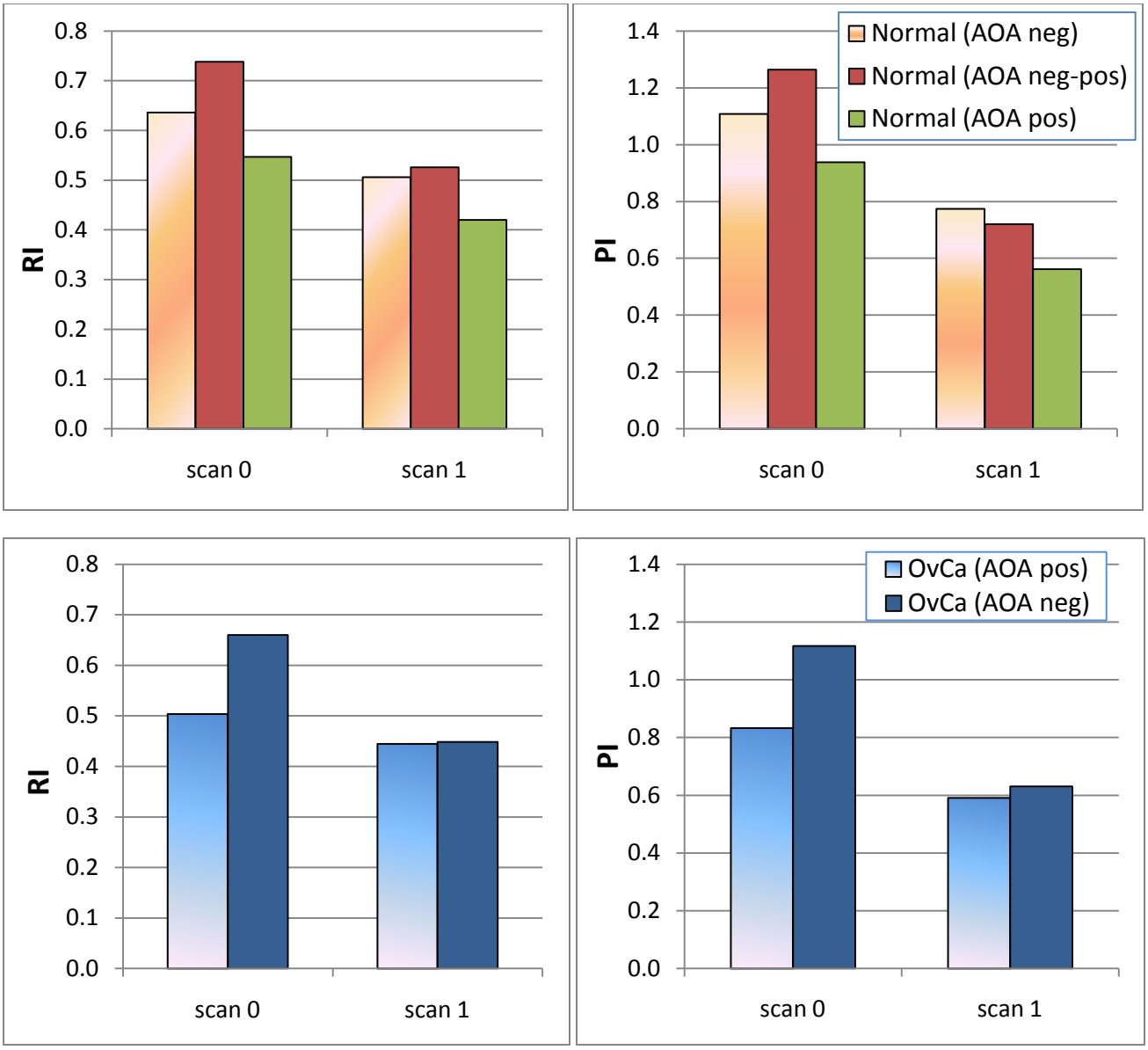

Figure 2. **Comparison of changes in angiogenesis by histology and AOA status.** Histological analysis was performed at sacrifice which occurred from 4-6 months after the second ultrasound scan.

The top panel shows RI and PI values as an indicator of angiogensis for normal ovarian histology; groups are based on the AOA at the first scan (scan 0) and second ultrasound scan (scan 1) which occurred within an interval of 10 months. AOA either remained negative (AOA neg; n=5), changed from negative to positive (AOA neg-pos; n=5) or remained positive (AOA pos; n=6). The RI/PI values were unchanged in AOA negative hens. The key decline in RI/PI values occurred in the group that switched from negative to positive, with a similar but smaller decline in the AOA positive group suggesting neo-angiogenesis may occur about the same time as the appearance of AOA in hens with normal ovaries.

The bottom panel shows RI and PI values as an indicator of angiogenesis for hens with ovarian tumor histology. Hens either remained AOA positive (AOA pos; n=11) or AOA negative (AOA neg; n=11). Overall the RI and PI values are lower than for hens with normal histology which is consistent with previous data that angiogenesis is an early indicator of tumors. The RI/PI values did not change for AOA positive hens with OvCa, while AOA negative to positive hens showed evidence of neo-angiogenesis from the first to the second ultasound scan ($p=0.002$ from 1st to 2nd ultrasound scan; Wilcoxon signed rank test). This is a critical group in which negative hens with normal RI/PI values converted to positive with evidence of angiogenesis and ovarian tumors.

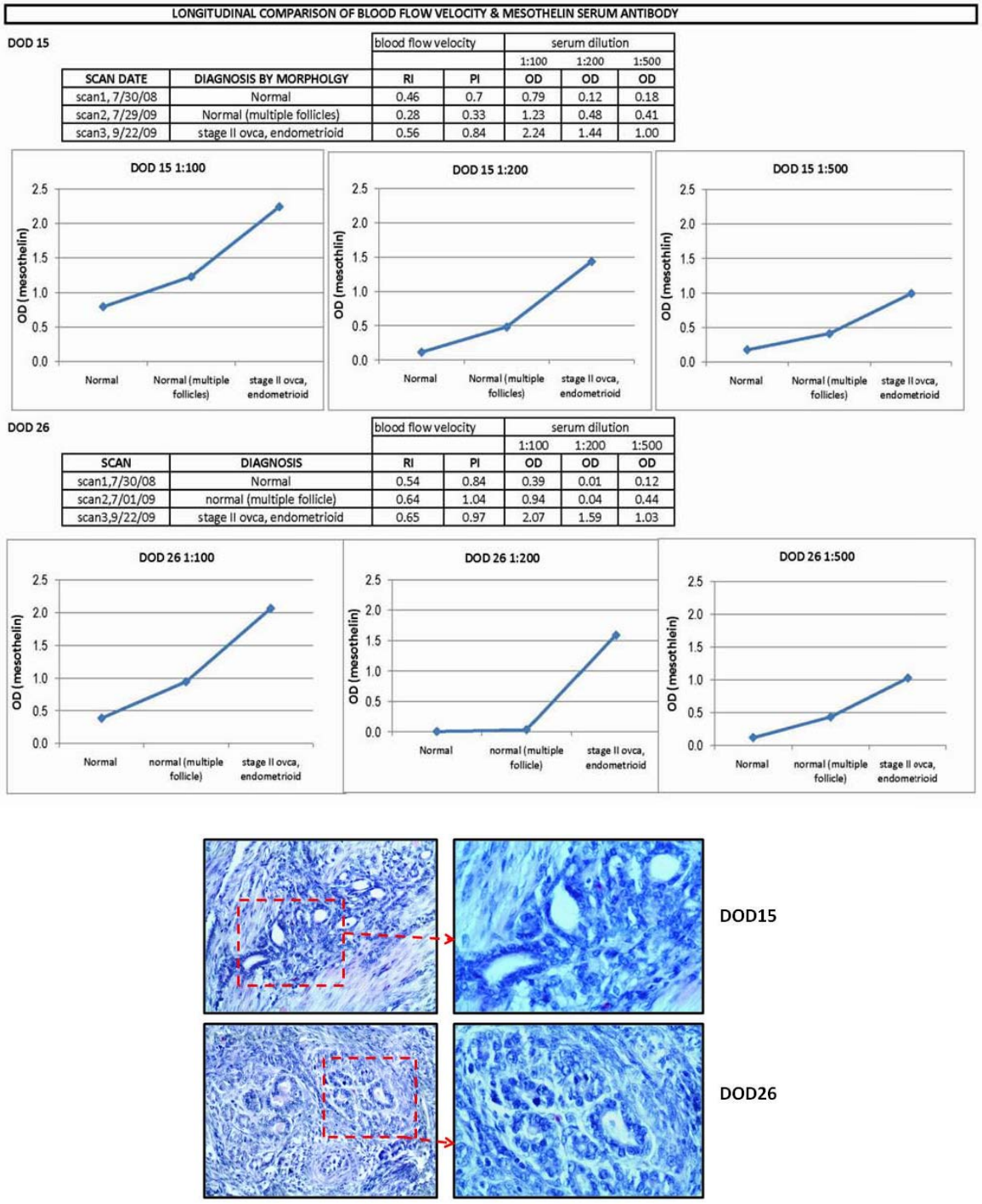

Figure 3. Longitudinal Comparison of Changes in Mesothelin antibody and Angiogenesis during ovarian tumor appearance. Two examples of hens that developed tumors expressing mesothelin determined by RT-PCR are shown (Yi, 2010). Hens were assessed for mesothelin antibody using a previously described immunoassay (Hellstrom et al, 2008). Serum was also assessed for anti-ovarian antibodies in the same sera by a previously described immunoassay (Barua et al, 2008). Angiogenesis (RI value below 0.4) was assessed using color Doppler ultrasound and serum was obtained before each reading. Hen DOD15 was initially positive for anti-ovarian antibodies and mesothelin antibodies began to appear after evidence of angiogenesis (decreased RI). Hen DOD26 was initially negative for anti-ovarian antibodies and developed both anti-mesothelin and anti-ovarian antibodies before evidence of angiogenesis or tumor morphology. Both hens developed mucinous ovarian tumors.

Detection of Tumor-Associated Neoangiogenesis by Doppler Ultrasonography During Early-Stage Ovarian Cancer in Laying Hens

A Preclinical Model of Human Spontaneous Ovarian Cancer

Animesh Barua, PhD, Pincas Bitterman, MD, Janice M. Bahr, PhD, Michael J. Bradaric, BS, Dale B. Hales, PhD, Judith L. Luborsky, PhD, Jacques S. Abramowicz, MD

Objective. Tumor-associated neoangiogenesis (TAN) is one of the earliest events in ovarian tumor growth and represents a potential target for early detection of ovarian cancer (OVCA). Because it is difficult to identify patients with early-stage OVCA, the goal of this study was to explore a spontaneous animal model of in vivo ovarian TAN associated with early-stage OVCA detectable by Doppler ultrasonography (DUS). ***Methods.*** White Leghorn laying hens were scanned transvaginally at 15-week intervals up to 45 weeks. Gray scale ovarian morphologic characteristics and Doppler indices were recorded. Hens were euthanized at diagnosis for ultrasonographic morphologic/vascular abnormalities or at the end of the study (those that remained normal). Ovarian morphologic and histologic characteristics were evaluated. Vascular endothelial growth factor (VEGF) and $\alpha_v\beta_3$-integrin expression was assessed by immunohistochemical analysis. Doppler ultrasonographic observations were compared with histologic and immunohistochemical findings to determine the ability of DUS to detect ovarian TAN. ***Results.*** Significant changes in ovarian blood flow parameters were observed during transformation from normal to tumor development in the ovary ($P < .05$). Tumor-related changes in ovarian vascularity were identified by DUS before the tumor became detectable by gray scale imaging. Increased expression of VEGF and $\alpha_v\beta_3$-integrins was associated with tumor development. Ovarian TAN preceded tumor progression in hens. ***Conclusions.*** The results suggest that ovarian TAN may be an effective target for the detection of early-stage OVCA. The laying hen may also be useful for studying the detection and inhibition of ovarian TAN using various means, including the efficacy of contrast agents, targeted molecular imaging, and antiangiogenic therapies. ***Key words:*** Doppler ultrasonography; early detection; ovarian cancer; ovarian neoangiogenesis; spontaneous animal model.

Abbreviations
AI, angiogenesis index; CA-125, cancer antigen 125; DUS, Doppler ultrasonography; OVCA, ovarian cancer; PI, pulsatility index; RI, resistive index; TAN, tumor-associated neoangiogenesis; TVUS, transvaginal ultrasonography; VEGF, vascular endothelial growth factor

Received August 10, 2009, from the Departments of Pharmacology (A.B., M.J.B., J.L.L.), Pathology (P.B.), and Obstetrics and Gynecology (P.B., J.L.L., J.S.A.), Rush University Medical Center, Chicago, Illinois USA; Department of Animal Science, University of Illinois at Urbana-Champaign, Urbana, Illinois (J.M.B.); and Department of Physiology, Southern Illinois University, Carbondale, Illinois USA (D.B.H.). Revision requested August 24, 2009. Revised manuscript accepted for publication October 19, 2009.

We thank Sanjib Basu, PhD (Department of Preventive Medicine, Rush University Medical Center), for help regarding statistical analysis of the data and the staff of the University of Illinois at Urbana-Champaign Poultry Farm, including Chet and Pam Utterback and Doug Hilgendorf, for maintenance of the hens. This study was supported by the Prevent Cancer Foundation (Dr Barua), a University Research Committee grant (Dr Barua), the Segal Women's Cancer Research Fund (Dr Barua), Pacific Ovarian Cancer Research Consortium Career Development Program grant P50 CA83636 (Dr Barua), and US Department of Defense grant OC073325 (Dr Luborsky).

Address correspondence to Jacques S. Abramowicz, MD, Department of Obstetrics and Gynecology, Rush University Medical Center, 1653 W Congress Pkwy, Chicago, IL 60612 USA.

E-mail: jacques_abramowicz@rush.edu

CME *Article includes CME test*

Ovarian cancer (OVCA) remains a fatal malignancy of women and is responsible for the third highest rate of mortality due to gynecologic cancers, after breast and cervical cancers.[1] In contrast to OVCA, the availability of early-detection tests for other gynecologic malignancies, including breast and cervical cancers, has contributed in part to the gradual decline in death rates due to these malignancies.[1]

Because of the lack of an effective screening tool or an early diagnostic method, it is difficult to detect OVCA at an early stage, and, in most cases it is detected at late stages, when the 5-year survival rate of patients is less than 10% compared with greater than 90% when detected at early stages.[2,3] The nonspecificity of OVCA symptoms at early stages reduces the accessibility to a patient's specimens. It is therefore difficult to validate potential targets for early diagnosis and to establish an effective method to detect those targets.[4] Consequently, this represents one of the main obstacles to the development of an early-detection test for OVCA.

Substantial studies have been described, involving 3 different approaches to develop an effective early-detection test for OVCA, including a serum marker (cancer antigen 125 [CA-125]), traditional transvaginal ultrasonography (TVUS), and their combination.[5,6] Although circulating levels of CA-125 have proven useful in determining the prognosis and response to treatment for patients undergoing chemotherapy, elevated CA-125 levels are also associated with many benign gynecologic conditions. In addition to mucinous OVCA, in which elevation of CA-125 levels is less frequent, 20% of patients with OVCA do not show elevated CA-125 levels.[7] On the other hand, the effectiveness of the Doppler indices (resistive index [RI] and pulsatility index [PI]) from TVUS scanning has been tested extensively to detect early-stage OVCA in humans without any success because of limited resolution and overlap between normal and abnormal indices. Improvement in the overall level of OVCA detection was not observed even with the use of TVUS together with CA-125 because no imaging target in the ovary (indicative of early OVCA-associated morphologic or cellular changes) corresponding to the serum CA-125 level has been defined. Therefore, appropriate changes in the ovarian morphologic, cellular, or molecular architecture associated with early-stage OVCA need to be identified.

Tumor-associated neoangiogenesis (TAN) is one of the earlier events in tumor development. Similar to cancer of other organs, neoangiogenesis is an early event in ovarian malignancy and is a critical determinant of tumor growth, invasion, progression, and metastatic potential.[8,9] Therefore, ovarian TAN represents a potential target for early detection of OVCA, and noninvasive diagnostic techniques to assess in vivo TAN are needed to detect OVCA at an early stage. Ultrasonography is the currently recommended noninvasive method for the evaluation of ovarian abnormalities, but the difficulty in diagnosing early-stage OVCA impedes conduction of studies to improve the ability of Doppler ultrasonography (DUS) to detect early-stage OVCA in humans. Animal models have been useful for preclinical testing of diagnostic paradigms,[10] but the often-used rodent models of OVCA do not develop OVCA spontaneously, and the histopathologic characteristics of induced OVCA differs from those of spontaneous OVCA in humans.[10,11] Laying hens (*Gallus domesticus*) develop OVCA spontaneously[12,13] with similarities to human OVCA in histopathologic characteristics[12,13] and expression of several markers. The objective of this study was to examine the suitability of ovarian TAN as an in vivo detection target of early-stage OVCA by DUS and to further explore the feasibility of the laying hen as a preclinical model to elucidate the ovarian vascular changes relative to OVCA development.

Materials and Methods

Animals

A flock of 110 commercial strains of White Leghorn laying hens (*G domesticus*) was reared under standard poultry husbandry practices with the provision of feed and water ad libitum. Egg production and mortality rates of hens (if any) were recorded daily. On the basis of their egg-laying rates and ultrasound scans, 3-year-old apparently healthy hens with low or irregular egg-laying rates (n = 15) were selected from the flock to monitor prospectively. The incidence of OVCA in laying hens of this age group is approximately 15% to 20% and is associated with low or complete cessation of egg laying. A low egg-laying rate indicates reduced ovarian function, and hens that lay 50% less eggs than their peers are considered to have abnormal ovarian function. The normal egg-laying rate for a commercial laying hen is more than 250 eggs per year, and a rate of less than 50% of the normal laying rate is considered a low egg-laying rate.

Ultrasound Scanning

Hens were scanned by TVUS (both B-mode and Doppler) as reported previously,[14] and hens with apparently normal health without any ultrasonographic ovarian abnormality were selected for the study. All hens with suspected ovarian abnormalities on gray scale ultrasonography were excluded from prospective monitoring and euthanized immediately, and ovarian tissues were processed for routine histologic and immunohistochemical evaluation. All procedures were performed according to Institutional Animal Care and Use Committee–approved guidelines. After initial scans, hens were monitored by gray scale ultrasonography and DUS at 15, 30, and 45 weeks using an instrument equipped with a 5- to 7.5-MHz endovaginal transducer (z.one ultrasound system; Zonare Medical Systems, Inc, Mountain View, CA). Briefly, each hen was immobilized by placing the breast up with the legs gently restrained by an assistant. Transmission gel was applied to the surface of the transducer, which was then covered with a probe cover, and gel was reapplied to the covered probe to ensure uninterrupted conductance of the sound waves. The transducer was inserted transvaginally approximately at a 30° angle to the body and 3 to 5 cm into the cloaca (place of vaginal opening). Two-dimensional transvaginal gray scale ultrasonography and color and pulsed DUS were performed. Young egg-laying hens (the ovaries of these hens contain more developing eggs compared with old hens) were used as standard controls for mechanical adjustment to reveal and characterize the fully functional normal ovary. The laying hen contains one functional ovary (left ovary), and the region surrounding the ovary was scanned. Once the ovary was located, the transducer was swept through the entire area for complete scanning of the ovary. Gray scale B-mode morphologic evaluation of the ovary was performed with attention to the follicular development and the presence of any abnormality, including cysts, septations, papillary projections or solid areas, and variation in echogenicity.

After morphologic evaluation, the color Doppler mode was activated for identification of vascular color signals. If blood flow was detected, it was shown as either "peripheral" (color signals in the ovarian periphery) or "central" (blood flow detected in septa, papillary projections, or solid areas). Once a vessel was identified on color Doppler imaging, the pulsed Doppler gate was activated to obtain a flow velocity waveform. The RI ([systolic velocity – diastolic velocity]/systolic velocity) and PI ([systolic velocity – diastolic velocity]/mean) were automatically calculated from at least 2 consecutive samples, and the average RI and PI values were used for analysis. In the stroma of hens with normal ovaries, high blood flows with prominent vascular areas were observed on the surface of developing preovulatory follicles, and data from these areas were excluded from the study. In addition to the blood flow patterns mentioned above, abnormal ovarian Doppler patterns (suggestive of ovarian TAN) were characterized by evaluating intratumoral blood flow and RI and PI values. Hens with higher intratumoral blood flow as well as lower RI and PI values than their normal counterparts were predicted to have ovarian TAN. All images were processed and archived for future reference.

Ovarian Morphologic and Histologic Evaluations

All hens were euthanized at diagnosis of ovarian TAN or at the end of the study, and gross ovarian morphologic specimens were examined, recorded, compared with the ultrasonographic evaluations, and photographed. Normal ovarian function was judged on the basis of the number of large preovulatory follicles (described in detail previously[15]) without any ovarian abnormality such as a cyst or solid mass. Abnormal ovaries were characterized by the presence of cysts, a shrunken ovarian volume, or a higher number of bloody, discolored, involuted, or atretic small and pearlike follicles. Tumor staging was performed as reported previously,[15] and the early stage of ovarian tumors was characterized by a detectable solid tissue mass within the ovary, followed by histologic observation. Ovarian tissues were fixed in buffered formalin or optimal cutting temperature compound and snap frozen as reported previously. To detect microscopic OVCA lesions in any part of the ovary, the whole ovary was sampled. The tissue blocks were sectioned (5 μm for paraffin and 10 μm for frozen). Sections from each tissue block (paraffin or frozen) were stained with hematoxylin-eosin and observed

under a light microscope to determine the microscopic features, including tumor lesions and types, and compared with the ultrasonographic evaluations.

Immunohistochemical Analysis

Tissue expression of TAN markers, including vascular endothelial growth factor (VEGF) and $\alpha_v\beta_3$-integrins, was examined by routine immunohistochemical analysis to assess angiogenesis using rabbit polyclonal antihuman VEGF (Abcam, Inc, Cambridge, MA) and mouse antihuman $\alpha_v\beta_3$-integrins (CD51/CD61, clone 23C6; BioLegend, San Diego, CA) according to the manufacturers' protocols. The densities of VEGF- and $\alpha_v\beta_3$-integrin-positive microvessels were counted from the tumor vicinity or stroma of normal hens (excluding the follicular areas) using a light microscope attached to digital imaging stereologic software (MicroSuite version 5; Olympus Corporation, Tokyo, Japan) and were expressed as the number of positive vessels in a 20,000-μm^2 area of the normal or tumor ovary. The index for TAN (angiogenesis index [AI]) was calculated for hens with early- and late-stage OVCA as a ratio of the frequency of VEGF-expressing vessels to that in normal ovaries (number of ovarian VEGF-expressing microvessels in each tumor hen/average of ovarian VEGF-expressing microvessels in normal hens; the AI for a normal ovary is considered 1).

Statistical Analysis

Differences in ultrasonographic measurements between two scans of the same group of hens were analyzed by paired sample *t* tests. Differences between two groups (normal and OVCA) of hens (for ultrasonographic indices and the number of microvessels positive for angiogenic markers) were analyzed by 2-sample *t* tests and Mann-Whitney tests. All reported *P* values are 2 sided, and $P < .05$ was considered significant. Statistical analyses were performed with SPSS version 15 software (SPSS Inc, Chicago, IL).

Results

Gray Scale Ultrasonography

No significant changes were detected in the ovarian morphologic characteristics of hens at the second scan (15 weeks from the initial scan) on gray scale ultrasonography. Similar to the initial scan, all hens had a normal-appearing ovary containing 2 or 3 preovulatory follicles with developing eggs at the second scan (Figure 1A). At the third scan, 30 weeks from the initial scan, substantial changes in the gray scale ovarian morphologic characteristics were observed in 4 of 15 hens (Figure 1C), including the absence of preovulatory large follicles with the appearance of solid tissue masses. However, no such changes were observed in the ovaries of the remaining 11 hens. At the final scan (45 weeks from the initial scan), 5 of the remaining 11 hens developed ovarian abnormalities with no detectable large preovulatory follicles.

Doppler Ultrasonography and Detection of Ovarian TAN

The blood flow patterns at the initial scan were located in ovarian "periphery," mostly on the surface of large preovulatory follicles and small growing follicles in the stroma of hens with normal ovarian morphologic characteristics selected for prospective monitoring. Confluent blood flow in areas surrounding the small developing follicles and the walls of the larger preovulatory follicles was observed in these hens. Although no detectable change in ovarian morphologic characteristics was identified (by gray scale imaging mentioned above), blood flow patterns changed from peripheral to a mixture of peripheral (on the surface layer of large ovarian follicles) and central at the second scan (after 15 weeks; Figure 1B) in 6 hens. In 9 hens, RI (mean ± SD, 0.42 ± 0.03) and PI (0.54 ± 0.07) values at the second scan were significantly lower compared with the initial scan (mean RI, 0.52 ± 0.05; mean PI, 0.70 ± 0.1; $P < .001$ for both RI and PI based on paired sample *t* tests; Table 1). At the third scan, with the changes in gray scale morphologic characteristics (including the reduction in the number of detectable follicles and appearance of solid tissue masses), flow patterns changed from mixed to central in these hens (Figure 1D). The RI and PI in these hens decreased further from the second to third scan (mean RI, 0.32 ± 0.09; mean PI, 0.40 ± 0.11; $P < .008$ and .005 for RI and PI, respectively, based on paired sample *t* tests; Table 1). The

ovaries of the remaining 6 hens had a normal appearance on DUS throughout the monitoring period (mean RI, 0.56 ± 0.08; range, 0.47–0.69; mean PI, 0.84 ± 0.2; range, 0.63–1.21). Thus, 9 of 15 hens showed changes in their ovarian blood flow patterns and were suspected to have ovarian TAN by 45 weeks from the initial scan.

Ovarian Morphologic and Histologic Characteristics

Gross ovarian morphologic findings were consistent with the ultrasonographic observations. No detectable tissue mass was found in 6 hens predicted to have normal ovarian morphologic characteristics and vascularity on gray scale ultrasonography and DUS, respectively, at the final 45-week scan (Figure 2A). In contrast, hens with the diagnosis of ovarian TAN and tumor-related morphologic characteristics during or at the end of the study on ultrasonography had tumor-related solid tissue masses (Figure 2C). These hard and solid tissue masses were found to be limited in 1 or 2 areas of the ovary only, although other parts were normal. In addition, no accompanying ascites was found at euthanasia.

Figure 1. Changes in ovarian morphologic characteristics with blood flow patterns leading to tumor development in laying hens. **A**, Gray scale sonogram of a normal hen ovary at the second scan (15 weeks after first scan). The presence of multiple preovulatory follicles (asterisks) of various sizes with no solid mass indicates the functionally normal ovary. **B**, Doppler sonogram of the same ovary imaged in **A** showing blood flows on the follicular wall of the larger preovulatory as well as small stromal follicles, suggesting active follicular growth in the ovary. **C**, Gray scale sonogram of the same hen ovary shown in **A** at the third scan (after 30 weeks from first scan). No developing follicle is seen, and the ovary appears to have solid tissue masses, indicating abnormal morphologic characteristics suggestive of an ovarian tumor. **D**, Doppler sonogram of the same ovary shown in **C**. A central pattern of blood flow is seen on the solid ovarian mass, suggesting the presence of an ovarian tumor. EDV indicates end-diastolic velocity; PSV, peak systolic velocity; and S, stroma.

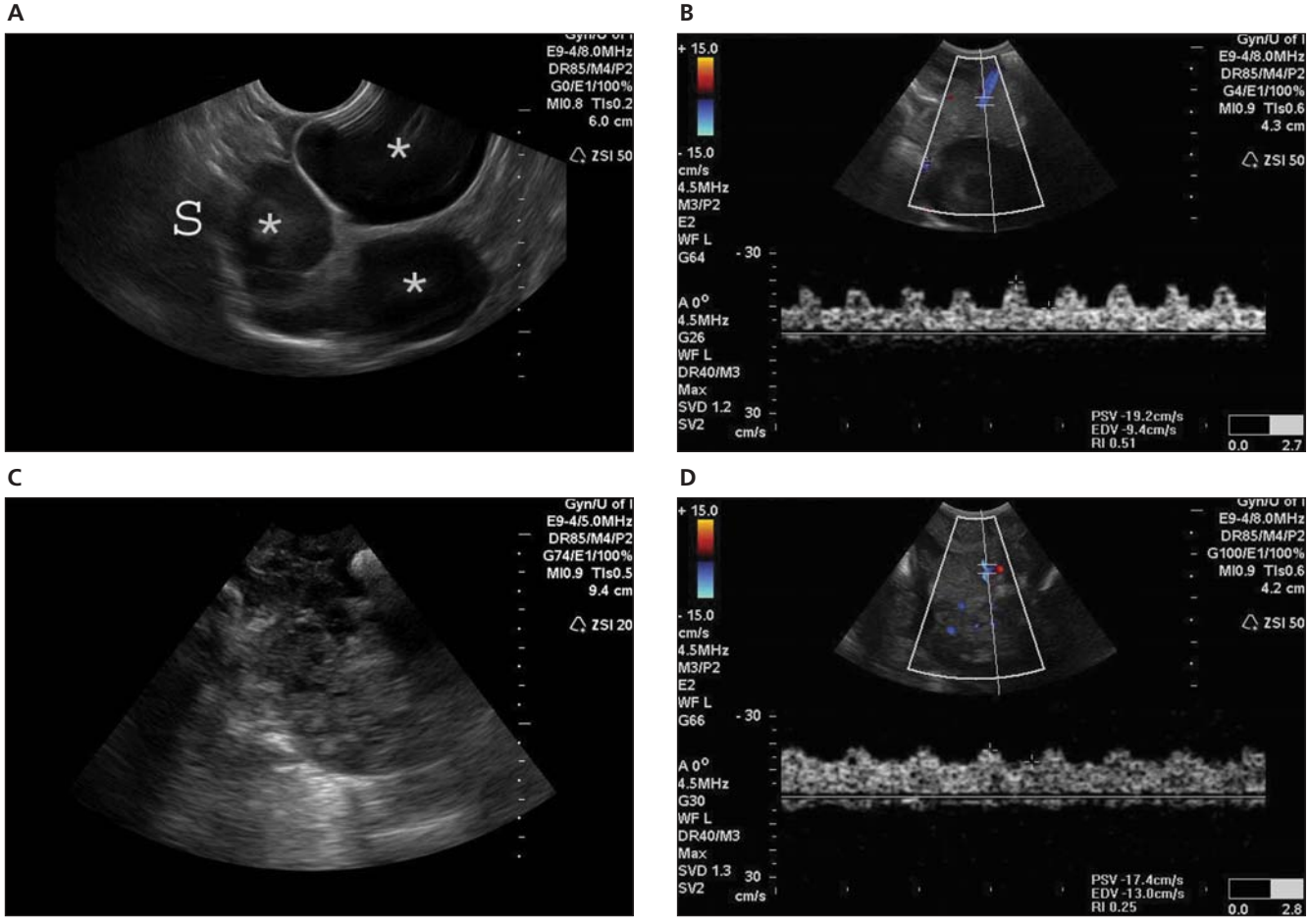

Table 1. Changes in DUS Indices in Association With the Development of Ovarian TAN in a Laying Hen Model of Spontaneous OVCA (n = 9 Hens)

	1st Scan (Initial Scan)		2nd Scan (After 15 wk)		*P* (Between 1st and 2nd Scans)	3rd Scan (After 30 wk)		*P* (Between 2nd and 3rd Scans)
Parameter	Range	Mean ± SD	Range	Mean ± SD		Range	Mean ± SD	
RI	0.43–0.60	0.52 ± 0.05	0.36–0.46	0.42 ± 0.03	<.001	0.18–0.48	0.32 ± 0.09	<.008
PI	0.56–0.84	0.70 ± 0.1	0.42–0.62	0.54 ± 0.07	<.001	0.21–0.54	0.40 ± 0.11	<.005

Histologic evaluation confirmed the presence of ovarian tumors (Figure 2D) in 9 hens suspected to have ovarian TAN and tumor-related hardened tissue masses as detected by DUS and gross morphologic evaluation. Glandular tumor structures containing a single layer of epithelial cells or lacelike papillary projections or glands with secretory ciliated goblet cells as well as many blood vessels of different sizes were seen in hens with the diagnosis of ovarian TAN (Figure 2D). However, such tumor-associated microscopic features, together with hyperplasia and dysplasia, were also found by histologic examinations in 3 additional hens that were not suspected to

Figure 2. Gross and microscopic appearance of a normal ovary and an early-stage ovarian tumor in laying hens. The predicted presence of ovarian TAN by ultrasonography was confirmed by gross and histopathologic examination after euthanasia. **A**, Normal hen ovary showing preovulatory follicles (developing eggs). **B**, Ovarian stroma of the same hen containing embedded follicles (paraffin section stained with hematoxylin-eosin; original magnification ×100). **C**, Ovary showing a solid tumor mass (early stage without ascites). **D**, Corresponding paraffin section stained with hematoxylin-eosin showing confluent tumor glands in the stroma (original magnification ×100). F indicates follicle; G, granulosa layer; O, ovary; OV, oviduct; S, stroma; SM, solid mass; and TG, tumor gland.

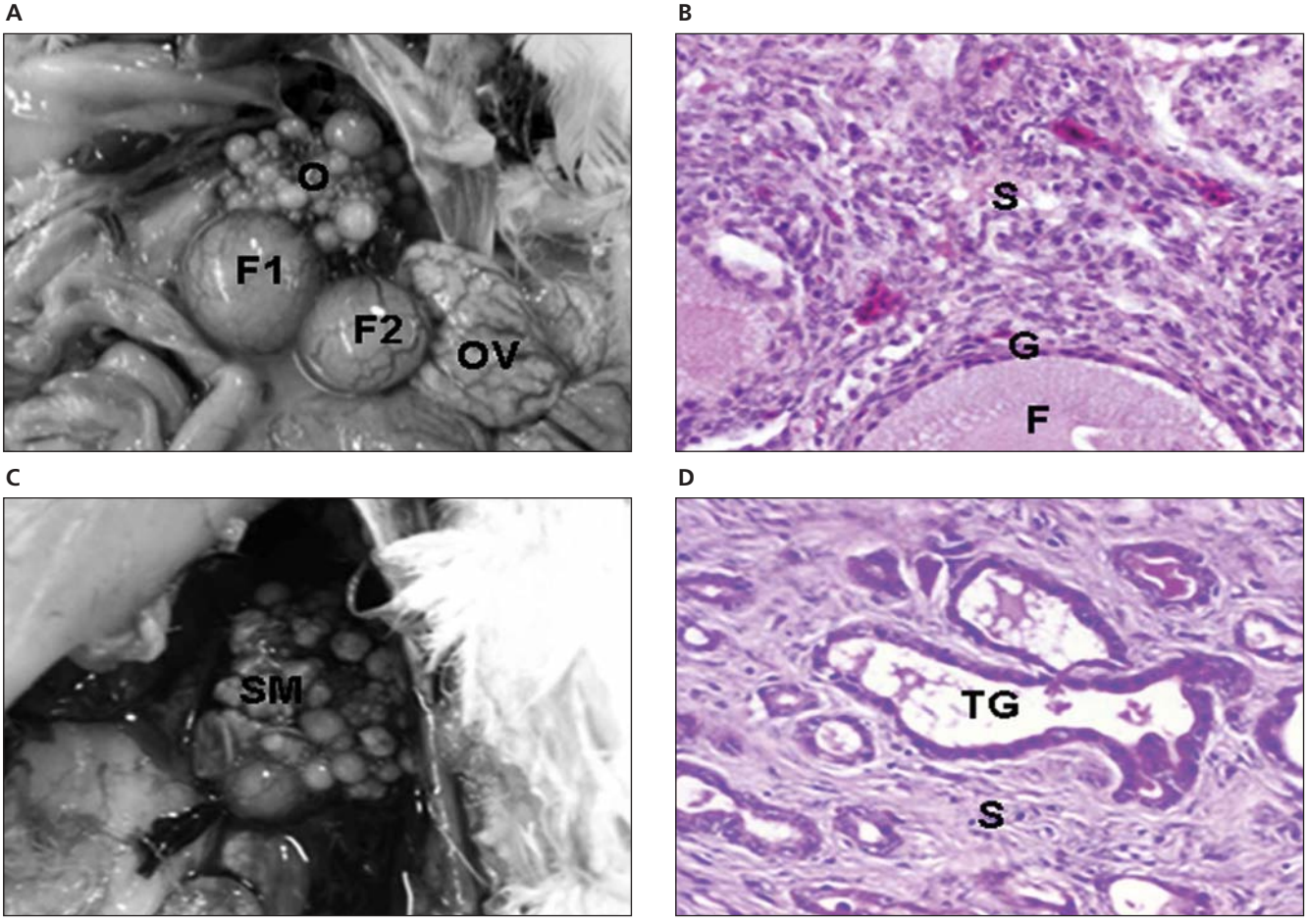

have TAN by ultrasonography. Thus, of 15 hens, 9 had DUS-detectable ovarian TAN and small tumor masses, and 3 had microscopic tumor lesions that remained undetectable by DUS monitoring up to 45 weeks. In contrast, no such change was detected in 3 of the remaining 6 hens that appeared normal at the end of 45 weeks of monitoring (Figure 2B).

Expression of Angiogenic Markers

Intense staining for VEGF was observed in the tumor epithelium and microvessels at the tumor vicinity in hens suspected to have ovarian TAN with a subsequent diagnosis of early-stage OVCA by histologic evaluation (Figure 3B, dotted line). In addition to the tumor vicinity, many microvessels expressing VEGF were also seen in the stroma preceding tumor glands (Figure 3B). Similar patterns were also observed for $\alpha_v\beta_3$-integrin expression in tumor glands as well as stromal blood vessels (Figure 3C). These immunopositive microvessels appeared to be leaky without any well-organized continuous smooth muscle layer surrounding them and stained intermittently. In normal ovaries, immunopositive vessels were seen in and around the developing stromal follicles with very few in the stroma outside the follicles (Figure 3A). The frequency of ovarian VEGF-expressing microvessels was significantly higher ($P < .002$, Mann-Whitney exact test) in hens with TAN (mean, 3.7 ± 0.58, 6.89 ± 0.73, and 9.8 ± 1.1 microvessels/20,000-μm^2 area of ovarian

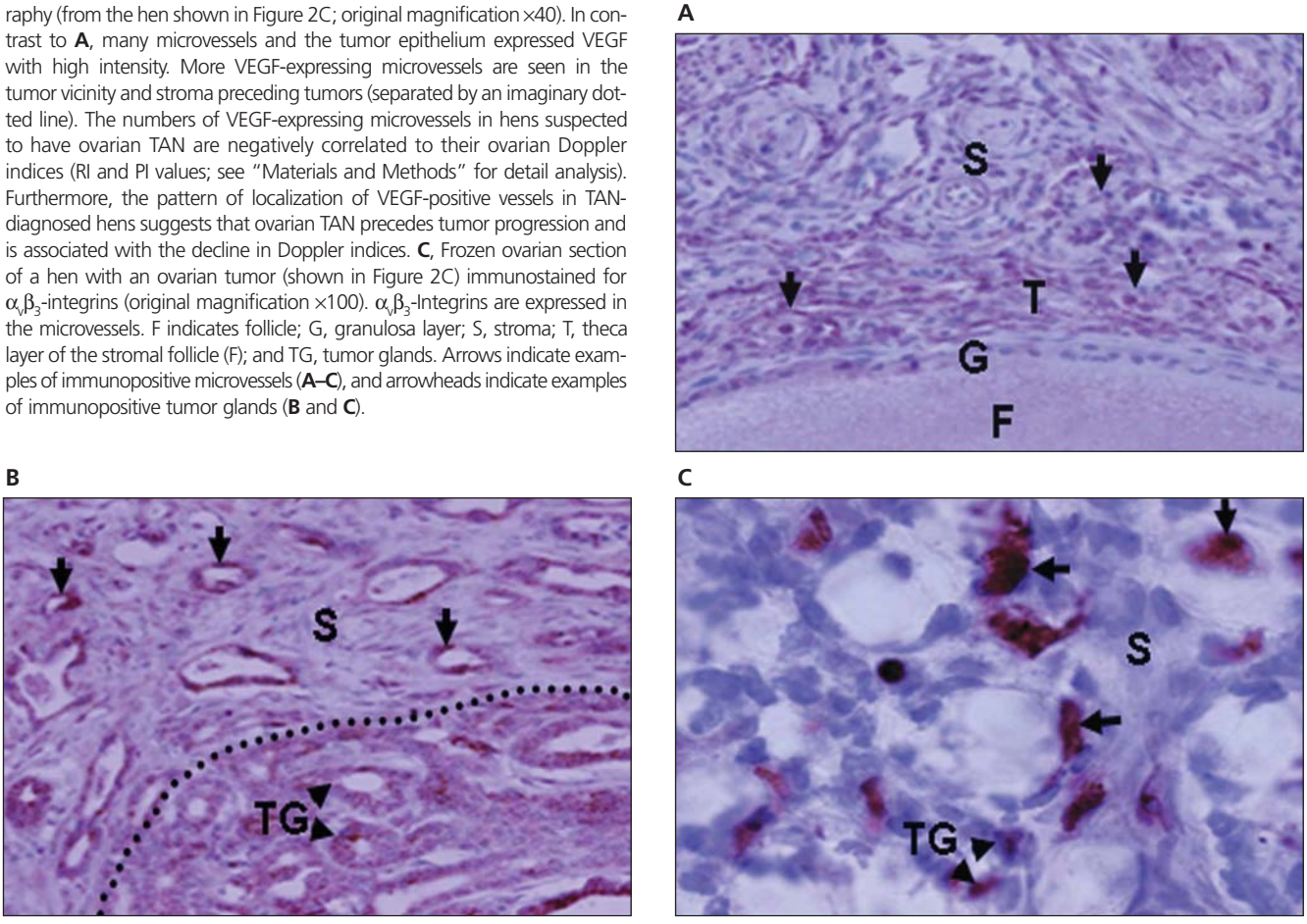

Figure 3. Expression of neoangiogenic markers in hen ovaries predicted to be normal and with ovarian TAN by ultrasonography. **A**, Section showing normal vasculature with few VEGF-stained vessels in the follicular theca and stroma of a hen monitored prospectively by ultrasonography up to 45 weeks (from the hen shown in Figure 2A; original magnification ×40). **B**, Ovarian section of a hen suspected to have ovarian TAN by ultrasonography (from the hen shown in Figure 2C; original magnification ×40). In contrast to **A**, many microvessels and the tumor epithelium expressed VEGF with high intensity. More VEGF-expressing microvessels are seen in the tumor vicinity and stroma preceding tumors (separated by an imaginary dotted line). The numbers of VEGF-expressing microvessels in hens suspected to have ovarian TAN are negatively correlated to their ovarian Doppler indices (RI and PI values; see "Materials and Methods" for detail analysis). Furthermore, the pattern of localization of VEGF-positive vessels in TAN-diagnosed hens suggests that ovarian TAN precedes tumor progression and is associated with the decline in Doppler indices. **C**, Frozen ovarian section of a hen with an ovarian tumor (shown in Figure 2C) immunostained for $\alpha_v\beta_3$-integrins (original magnification ×100). $\alpha_v\beta_3$-Integrins are expressed in the microvessels. F indicates follicle; G, granulosa layer; S, stroma; T, theca layer of the stromal follicle (F); and TG, tumor glands. Arrows indicate examples of immunopositive microvessels (**A–C**), and arrowheads indicate examples of immunopositive tumor glands (**B** and **C**).

tumor tissues in microscopic, early-stage, and late-stage OVCA, respectively) than normal hens (mean, 2.4 ± 0.51 microvessels/20,000 μm^2 area of ovarian tissues). Similar trends were also observed in the frequency of ovarian $\alpha_v\beta_3$-integrin-positive vessels with respect to the different OVCA stages. The AI for early-stage OVCA was significantly higher than in hens with normal ovaries (2.83 versus 1; $P < .01$, Mann-Whitney exact test). The AI was highest in hens with late-stage OVCA (4.08 versus 1; $P < .04$, for hens that had a diagnosis of late-stage OVCA at the first scan and were euthanized immediately instead of prospective monitoring). Tumor volumes were not examined in this study; hence, no correlation between tumor size and Doppler intensity was evaluated. However, Doppler signals were significantly lower with advancing tumor stages. Moreover, we evaluated the correlation between abnormal versus normal Doppler patterns and immunohistochemical findings, and tissue expression of angiogenic markers and AI values were inversely correlated (r = –0.90 and –0.88 for RI and PI, respectively) to Doppler indices (the higher the AI, the lower the RI and PI), indicating that establishment of ovarian TAN is associated with an increase in blood flow to the tumor vicinity.

Discussion

To our knowledge, a study reporting the detection of ovarian TAN during the early stage of the disease by gray scale ultrasonography and DUS in an animal model of human spontaneous OVCA has not been reported previously. This study revealed that ovarian TAN is initiated after neoplastic cellular transformation in the ovary even before the tumor becomes detectable by traditional TVUS. The results of this study suggest that ovarian TAN can be a potential target for the detection of early-stage OVCA by noninvasive ultrasonography if its current detection limit can be improved. Because of the difficulty in identifying patients with early-stage OVCA, the laying hen model can be used to study methods to enhance the detectability of early-stage OVCA on ultrasonography.

The fatality of OVCA is due in part to the lack of a reliable and effective early-detection method. A plethora of serum tumor markers have been reported, and given the heterogeneity of OVCA in different women, none of these markers are routinely effective in detecting early-stage OVCA.[7] Moreover, the association of any of these makers with early tumor-related changes in ovarian morphologic characteristics has not been reported. Furthermore, despite extensive efforts, the use of CA-125, with or without ultrasonography, to detect early-stage OVCA remains ineffective.[7] Use of a morphologic index of the architectural features of ovarian neoplasms on pelvic ultrasonography to predict a probability of ovarian malignancy without the use of CA-125 has been shown to have positive predictive values of up to 0.45.[16] However, this morphologic index requires information on tumor parameters, including tumor size and the presence of ascites (which in most cases is associated with advanced OVCA), to effectively predict tumor malignancy. Consequently, this method is unable to detect early-stage OVCA. Previous studies reported the expression of VEGF and $\alpha_v\beta_3$-integrins in tumor epithelia and blood vessels in patients with OVCA.[9] Similarly, these markers of ovarian TAN were also detected in hens with early- and late-stage OVCA. In addition, in hens with early-stage OVCA (including hens in which tumors were not detected by DUS), the expression of VEGF and $\alpha_v\beta_3$-integrins in many blood vessels in the tumor vicinity (Figure 3, B and C) as well as in the stroma adjacent to the tumor suggests that ovarian TAN precedes tumor progression. Thus, ovarian TAN represents an effective target for the detection of early-stage OVCA if it can be detected. Because it is difficult to study patients with early-stage OVCA, laying hens can be used to determine the ultrasonographic parameters indicative of early-stage OVCA-related neoangiogenesis.

Doppler ultrasonography is related to the vascular architecture of a tissue and is currently an accepted method for in vivo imaging of tissue vascularity. In this study, we monitored healthy laying hens with reduced ovarian function by DUS methods until they developed ovarian TAN or up to 45 weeks at 15-week intervals. Hens with reduced ovarian function compared with their peers of a similar genetic background and reared under similar conditions are considered to be at risk of developing OVCA, as reported earlier.[14,15]

Detection of changes in ovarian vascularity before the tumor became detectable by gray scale ultrasonography in 9 of 15 hens suggests that ovarian TAN can be detected by prospective monitoring of hens. However, this study also confirmed some limitations of DUS in detecting early-stage OVCA-related ovarian TAN. Although DUS detected 9 hens with early-stage OVCA (hens with a small solid ovarian mass and a larger area of the ovary that remained normal at detection), it failed to detect ovarian TAN in 3 hens with microscopic OVCA without any detectable mass. We believe that had we continued to monitor beyond 45 weeks, we would have been able to detect OVCA in these hens also. This failure of DUS reveals its limited capability in detecting ovarian TAN related to microscopic OVCA. It is known that Doppler sensitivity is limited for distinction of OVCA, but in this study, we analyzed changes in the indices, each hen serving as its own control. Although Doppler indices obtained by traditional ultrasonography do not confirm the in vivo detection of microvessels, immunohistochemical detection of VEGF expression indicates the presence of an increased number of microvessels in hens with OVCA compared with normal hens. Ultrasonographic contrast agents have been used to enhance the detection limits of DUS in other organs, and few studies of patients with advanced stage OVCA have shown improvement in the detection of ovarian tumor-related vascularity.[17–21]

The lack of a suitable animal model of spontaneous OVCA is also a reason for fewer studies with contrast agents and presents a considerable barrier to developing effective contrast media for diagnosing early-stage OVCA. With our imaging methods, a laying hen can be scanned repeatedly with DUS in a short interval without affecting it physiologically. This animal model can also be useful in testing which contrast agents show early-stage ovarian tumor-related vascularity better than others. Because ovarian tumors in laying hens also express VEGF and $\alpha_v\beta_3$-integrins, this spontaneous animal model of OVCA can be used to determine the efficacy of molecularly targeted imaging using microbubbles conjugated with anti-$\alpha_v\beta_3$-integrins or anti-VEGFR-2 against ovarian $\alpha_v\beta_3$-integrins and VEGFR-2. Similarly, it may also be useful in determining the efficacy of in vivo imaging-guided, ovary-targeted antiangiogenic therapy in the future.

This was a pilot study, and the small sample size was a limitation. On the basis of our results, however, we conclude that neoangiogenesis may be detected by DUS in the laying hen model of spontaneous OVCA. Expression of relevant markers is associated with the detection of very early ovarian tumors, suggesting that neoangiogenesis may be a feasible target for the detection of early-stage OVCA. Furthermore, this study showed that progression from normal to abnormal ovaries could be followed in the hen model, supporting its utility as a preclinical model of OVCA.

References

1. Jemal A, Siegel R, Ward E, et al. Cancer statistics, 2008. CA Cancer J Clin 2008; 58:71–96.
2. Goodman MT, Correa CN, Tung KH, et al. Stage at diagnosis of ovarian cancer in the United States, 1992–1997. Cancer 2003; 97(suppl):2648–2659.
3. Ries LA. Ovarian cancer: survival and treatment differences by age. Cancer 1993; 71(suppl):524–529.
4. Holschneider CH, Berek JS. Ovarian cancer: epidemiology, biology, and prognostic factors. Semin Surg Oncol 2000; 19:3–10.
5. Moore RG, Bast RC Jr. How do you distinguish a malignant pelvic mass from a benign pelvic mass? Imaging, biomarkers, or none of the above. J Clin Oncol 2007; 25:4159–4161.
6. Bosse K, Rhiem K, Wappenschmidt B, et al. Screening for ovarian cancer by transvaginal ultrasound and serum CA125 measurement in women with a familial predisposition: a prospective cohort study. Gynecol Oncol 2006; 103:1077–1082.
7. Bast RC Jr, Urban N, Shridhar V, et al. Early detection of ovarian cancer: promise and reality. Cancer Treat Res 2002; 107:61–97.
8. Folkman J. What is the evidence that tumors are angiogenesis dependent? J Natl Cancer Inst 1990; 82:4–6.
9. Ramakrishnan S, Subramanian IV, Yokoyama Y, Geller M. Angiogenesis in normal and neoplastic ovaries. Angiogenesis 2005; 8:169–182.
10. Vanderhyden BC, Shaw TJ, Ethier JF. Animal models of ovarian cancer. Reprod Biol Endocrinol 2003; 1:67.
11. Stakleff KD, Von Gruenigen VE. Rodent models for ovarian cancer research. Int J Gynecol Cancer 2003; 13:405–412.
12. Damjanov I. Ovarian tumours in laboratory and domestic animals. Curr Top Pathol 1989; 78:1–10.

13. Fredrickson TN. Ovarian tumors of the hen. Environ Health Perspect 1987; 73:35–51.

14. Barua A, Abramowicz JS, Bahr JM, et al. Detection of ovarian tumors in chicken by sonography: a step toward early diagnosis in humans? J Ultrasound Med 2007; 26:909–919.

15. Barua A, Bitterman P, Abramowicz JS, et al. Histopathology of ovarian tumors in laying hens: a preclinical model of human ovarian cancer. Int J Gynecol Cancer 2009; 19:531–539.

16. DePriest PD, Shenson D, Fried A, et al. A morphology index based on sonographic findings in ovarian cancer. Gynecol Oncol 1993; 51:7–11.

17. Abramowicz JS. Ultrasonographic contrast media: has the time come in obstetrics and gynecology? J Ultrasound Med 2005; 24:517–531.

18. Testa AC, Ferrandina G, Fruscella E, et al. The use of contrasted transvaginal sonography in the diagnosis of gynecologic diseases: a preliminary study. J Ultrasound Med 2005; 24:1267–1278.

19. Testa AC, Timmerman D, Exacoustos C, et al. The role of CnTI-SonoVue in the diagnosis of ovarian masses with papillary projections: a preliminary study. Ultrasound Obstet Gynecol 2007; 29:512–516.

20. Cosgrove D. Ultrasound contrast agents: an overview. Eur J Radiol 2006; 60:324–330.

21. Fleischer A, Lyshchik A, Jones HJ, et al. Contrast-enhanced transvaginal sonography of benign versus malignant ovarian masses: preliminary findings. J Ultrasound Med 2008; 27:1011–1018.

Contrast Enhanced Ultrasonography Detects Spontaneous Ovarian Cancer at Early Stage in a Preclinical Animal Model

Animesh Barua, PhD[1,2,3], Pincas Bitterman, MD[3], Janice M. Bahr, PhD[4], Sanjib Basu, PhD[5], Eyal Sheiner, MD[6], Michael J. Bradaric, BS[1], Dale B. Hales, PhD[7], Judith L. Luborsky, PhD[1,2], Jacques S. Abramowicz, MD[2]

Departments of [1]Pharmacology, [2]Obstetrics and Gynecology and [3]Pathology, [5]Preventive Medicine (Biostatistics), Rush University Medical Center, Chicago, Illinois; Department of [4]Animal Sciences, University of Illinois at Urbana-Champaign, Urbana, Illinois; Department of [6]Physiology, Southern Illinois University, Carbondale, Illinois, USA. Department of [5]Obstetrics and Gynecology, Soroka University Medical Center, Be'er Sheva, Israel

Corresponding Author: Animesh Barua, Ph.D.
Laboratory for Translational Research on Ovarian Cancer
Departments of Pharmacology, Obstetrics & Gynecology and Pathology
Room # 456, Cohn Building,
Rush University Medical Center
1735 W. Harrison St., Chicago IL 60612
Tel. 312-942-6666
Fax: 312-563-3552
e-mail: Animesh_Barua@rush.edu

Objective*.** Our goal was to examine the feasibility of using laying hens, a preclinical model of human spontaneous ovarian cancer (OVCA), in determining the kinetics of ultrasound contrast agent indicative of ovarian tumor associated neoangiogenesis (TAN) at early stage OVCA. ***Methods. Three years old White Leghorn laying hens with decreased ovarian function were scanned before and after intravenous injection of Optision^{TM} at a dose of 5 μL/kg body weight. Gray scale morphology, Doppler indices, arrival time, peak intensity and Wash-out of contrast agent was recorded and archived on still images and video clips. Hens were euthanized thereafter and ultrasound prediction was compared at gross examination and ovarian tissues were collected. Archived clips were analyzed to determine contrast parameters and Doppler intensities of vessels. A time-intensity curve per hen was drawn and area under the curve (AUC) was derived. Tumor types and the density of ovarian microvessels were determined by histology and immunohistochemistry and compared with ultrasound predictions. ***Results***. Contrast agent significantly (P<0.05) enhanced the visualization of microvessels which was confirmed by immunohistochemistry. Contrast parameters including *Time of Wash-out and AUC* were significantly different (P<0.05) between ovaries of normal hens and hens with OVCA and correctly detected OVCA at early stages than the *time of peak*. ***Conclusions.*** The laying hen may be a useful animal model to determine ovarian tumor associated vascular kinetics diagnostic of early stage OVCA using a contrast agent. This model may also be useful to test the efficacy of different contrast agents in a preclinical setting.

Key words: Contrast enhanced ultrasonography; early detection; ovarian cancer; ovarian tumor associated neoangiogenesis; spontaneous animal model.

Neovascularization, preceded by malignant cellular transformation, is an early event during tumor development [1, 2]. Tumor associated neo-angiogenesis (TAN) has been shown to be a critical requirement for the progression and metastasis of malignant tumors of the ovary as well as other organs [1, 3, 4]. Therefore, ovarian TAN represents the potential to be an early detection target for ovarian cancer (OVCA), a fatal disease responsible for the highest death rate of women from all gynecological malignancies[5]. Previous reports on the immunohistochemical localization of tumor microvessels in post operative surgical specimens have shown a positive relationship between tumor progression and tumor associated neo-angiogenesis and suggested the utility of ovarian TAN as a tool for the detection of OVCA at an early stage [6-8]. Therefore, an *in vivo* non-invasive method of detecting ovarian TAN relative to early stage OVCA is highly desirable.

Gray scale and Doppler ultrasound imaging are the non-invasive and currently recommended modalities for the evaluation of gynecologic abnormalities including ovarian tumors. Although Doppler ultrasound can detect large intratumoral blood vessels, in many cases including early stage OVCA, it cannot detect neoangiogenic smaller vessels [9, 10]. Failure to distinguish benign from malignant ovarian tumors and detecting OVCA at early stages are the two main limitations of current Doppler ultrasound imaging [11, 12]. This failure of detection is either because of the smaller sizes of tumor associated microvessels or the Doppler shifts in these vessels are too small or too weak to be detected by the current detection limit of the ultrasound scanner [13]. Therefore, Doppler ultrasound may be an effective method for early detection of OVCA if its current detection limit can be improved to detect ovarian TAN. A moderate number of studies have shown the efficacy of ultrasound contrast agents (UCAs) to enhance the sensitivity of traditional Doppler ultrasound to visualize blood vessels and distinguish malignant tumors from

benign ones on the basis of intratumoral microvascular architecture [13-16]. There is limited literature evaluating contrast enhancement in adenexal masses and, to our knowledge, most of the reported studies on the ovarian imaging by contrast enhanced ultrasound were based on patients with late stage OVCA as difficulty to obtain access to patients with early stage OVCA may be one of the reasons [13, 14, 17, 18]. Thus observations on contrast enhanced ultrasound imaging of these studies may not be useful as-such for the early detection of OVCA. As the 5-year survival rates of OVCA patients is remarkably high when the disease is detected at early stage, studies on the contrast enhanced ultrasound imaging with early stage OVCA cases are needed to establish an early detection method for OVCA. Animal models serve as surrogates to elucidate information on the etiology and mechanism of human diseases especially for those which are difficult to access in patients including OVCA [19]. However, the lack of a feasible spontaneous model of human OVCA represents one of the principal barriers to the understanding of early ovarian tumor development and its detection. Rodents do not develop OVCA spontaneously and the histopathology of induced OVCA in these animals does not resemble that of spontaneous OVCA [19, 20].

The laying hens (*Gallus domesticus*) have been shown to be the only widely available animal that develop OVCA spontaneously[21] with similar histopathology [22] and expression of several cellular and molecular makers common to human ovarian tumors [23-26]. Moreover, the incidence rate increases with age (10-40% between 2.5 to 6 years of age)[21]. The high ovulation rate in commercial strains of laying hens (a hen lays an egg almost every day with an ovulatory cycle of about 24-26 hours during its reproductive life) also mimics the *incessant ovulation theory (a condition referring to the frequent ovulation resulting in repeated trauma as well as wear and tear of the ovarian surface epithelium)[27]*) a much accepted risk factor for

OVCA in humans (a detailed description of the reproductive physiology of laying hens can be found in ref nos. 20, 25). Recently, a transvaginal Doppler ultrasound imaging method for hen ovarian tumors using a transducer similar to that used for humans has been reported [28]. As in humans, tissue expression of vascular endothelial growth factor (VEGF), a marker of ovarian TAN, has also been shown to be increased in association with tumor progression in hens [4, 26]. In addition, laying hens are easily accessible especially because commercial poultry farms maintain large population of hens which they usually cull when hens get older. Therefore, the laying hen represents a potential feasible surrogate to explore information related to the contrast enhanced ultrasound imaging diagnostic of OVCA at early stages which is difficult to perform in humans.

The goal of this pilot study was to examine the feasibility of using laying hens to determine the kinetics of ultrasound contrast agents indicative of ovarian TAN at early stage OVCA. We hypothesized that the ultrasound contrast agent Optison^{TM} would enhance the visualization of ovarian vascularity in the laying hen relative to OVCA.

Methods and Materials

Animals

Approximately 150 three years old (commercial strains of) White Leghorn laying hens (*Gallus domesticus*) were maintained in individual cages with standard poultry husbandry practices including the provision of feed and water *ad libitum*. Egg laying rates (an indicator of ovarian function; low egg laying rate indicates decreased ovarian function) of hens were recorded on daily basis. The normal rate of egg laying by a commercial laying hen is >250 eggs/year and <50% of normal laying rate is considered as low egg laying rate [4, 29]. Hens (n=46) with low,

irregular egg laying rates or those stopped egg laying and with or without any abdominal distention (a sign of possible ovarian tumor associated ascites) were selected randomly from a layer flock for ultrasound scanning. The incidence of OVCA in laying hens of this age group was reported to be approximately 15-20% and is associated with the low or complete cessation of egg laying[22, 30].

Preparation of Optison™ contrast agent

Optison™ (GE Healthcare, St Louis, MO) is a sterile non-pyrogenic suspension of microspheres of human serum albumin with perflutren Protein-Type A of 3.0-4.5 μm in size that create an echogenic contrast effect in blood. Optison™ was prepared prior to injection according to the manufacturer's direction. Briefly, the vial containing Optison™ suspension was inverted and gently rotated to resuspend the microspheres completely. The suspension was transferred from the vial by an injection syringe with a 19 gauge needle to a angiocatheter (small vein infusion set, female luer, 12" tubing, needle of 27 gauge, Kawasumi Laboratories, FL) containing 100 μL of 0.9% sodium chloride previously inserted into the left wing vein (brachial vein) of the hen and followed by the reloading of 1mL 0.9% sodium chloride solution. The loading of sodium chloride solution pre and post injection of Optison™ helped to maintain the vascular patency and air tight condition, in addition to the flushing of the Optison™ from the hen's circulation. The dosage of Optison™ was determined after prior attempts with several dosages using 5 laying hens with fully functional ovaries and 5μL/kg body weight was considered optimal for better resolution. With the dosage higher than 5μL/kg body weight, the initial arrival of Optison™ caused an excessive broadening of color areas (blooming; due to increase in flow signal strength) [13, 31, 32]. Blooming effect was detected when gray scale pixels change to a color display in regions where no flow, in fact, exists. Although in few hens, 5μL/kg body weight dosage, the

exact border of enhanced vessels often vanished blooming was not so intense that it would disturb the counting of the vessels number. Blooming effects were also reported in previous studies.

Ultrasound scanning

Pre-contrast scanning

All procedures were performed according to Institutional Animal Care and Use Committee approval. Ultrasound scanning was performed in a continuous pattern before and after the injection of Optison™ [4, 28] (GE Healthcare, St Louis, MO) with the mechanical set up reported previously. Briefly, all hens were scanned using an instrument equipped with a 5- to 7.5-MHz endovaginal transducer (MicroMaxx; SonoSite, Inc, Bothell, WA). Each hen was immobilized by placing hen with the breast up with legs gently restrained by an assistant. Transmission gel was applied to the surface of the transducer; a probe cover was applied; and gel reapplied to the covered probe to ensure uninterrupted conductance of the sound waves. The transducer was inserted approximately at a 30° angle to the body, 3 to 5 cm into the cloaca (transvaginal), and 2-dimensional transvaginal gray scale sonography as well as pulsed Doppler sonography were performed. Young egg-laying hens (as the ovaries of these hens contain more developing follicles compared to old hens) were used as standard controls for mechanical adjustment to reveal and characterize the fully functional normal ovary of hens. The area of a tumor to be imaged was determined according to three conditions: (1) the whole tumor should be seen on the image, if possible; (2) the sectional plane should contain the solid part (wall, septae and papillae) of the tumor; and (3) the most vascularized area was selected. For normal ovaries, ovaries without any detectable tumor or atrophied ovaries, the region surrounding the ovary was scanned and the transducer was swept through the entire area for complete scanning of the ovary.

Gray scale morphologic evaluation of the ovarian mass was performed with attention to the number of large preovulatory follicles, the presence of abnormal-looking follicles, bilaterality, septations, papillary projections or solid areas, and echogenicity. After morphologic evaluation, the color Doppler mode was activated for identification of vascular color signals. If blood flow was detected, it was shown as either "peripheral" (color signals in the wall or periphery of a follicle or a suspected mass) or "central" (blood flow detected in septa, papillary projections, or solid areas). Once a vessel was identified on color Doppler imaging, the pulsed Doppler gate was activated to obtain a flow velocity waveform. The resistive index (RI: [systolic velocity – diastolic velocity]/systolic velocity) and the pulsatility index (PI: [systolic velocity – diastolic velocity]/mean) were automatically calculated from at least 2 consecutive samples (two separate images from the same ovary), and the lower RI and PI values were used for analysis. All images were processed and digitally archived.

Post-contrast scanning

Post-Optison™ injection scanning was performed in a similar and continuous manner with identical mechanical settings as described above. The same pre-contrast imaged area was imaged after Optison™ injection in post-contrast scanning. All images were archived digitally in still format as well as real time clips (6 min for each hen)in single sided recordable digital video discs (DVD + R format, Maxell Video/Data Media, Maxell Corporation of America, Fair Lawn, NJ) readable with personal computer later.

Evaluation of contrast agent effect

The effect of Optison™ contrast agent was evaluated: a) visually during the examination and b) afterwards from reviewing the archived video clips. The time of arrival of contrast agent [time

interval in seconds from administration of the contrast agent to its visual observation (in seconds)] in the normal or tumor ovarian vessels was recorded on a real time basis. After review of complete clip, the region of interest (ROI) was selected by drawing around the area of solid tissue containing the largest number of vessels with minimal artifacts similar to those reported earlier [14, 17]. For normal or apparently normal (without detectable tumor mass at gray scale) ovaries, stomal but not follicular vessels were counted. A colored area separated from others with a distinct wall typical of blood vessel was assesed before and after the injection of the contrast agent. Therefore, post-contrast appearing of blood vessels in this study could be either a new vessel or a branch of a vessel already recognized before administration of the contrast agent. Analysis of pixel intensities of blood vessels was carried out with a computer assisted software program (MicroSuite version 5; Olympus Corporation, Tokyo, Japan). Using the software, the intensity of the ROI (sum of the pixel values within the ROI) was measured before contrast agent administration and at intervals of 5 seconds after the arrival of contrast agent up to 6 minutes. Then the peak intensity, the time of peak intensity (secs), intensity at wash-out and the time of wash-out (secs) were determined. Total number of blood vessels from each ROI was counted when the intensity was at peak. In addition, the resistive and pulsatility indices (RI and PI, respectively) were calculated before and after the contrast injection using the formula reported earlier [28].

The data were then transferred to a computerized spreadsheet program (Excel 2003, Microsoft, Redmond, Washington) and a time-intensity curve was derived for each hen. The time-intensity curves were analyzed to calculate area under the curve (AUC). The AUC diagnostic of OVCA in hens was derived from the arrival of the contrast agent and the end of the wash-out period minus the area under the baseline in time-intensity curve.

Ovarian morphology

Following ultrasound scanning, all hens were euthanized and examined for the presence of solid tumor mass in the ovary and/or in any other organs, ascitic fluid, large preovulatory follicles or atrophy of the ovary as reported previously[22]. Gross ovarian status was recorded and compared with sonographic evaluations, and photographed. At gross examination, an ovary is considered normally functional if it contains viable large preovulatory follicles for laying hens (for more detail information on the hen ovarian physiology, see references (20, 26) or atrophy of ovary without any large follicles or visible lesions in hens out of egg laying. In contrast to the normal ovary, the abnormal ovary was characterized by the presence of cysts, bloody, discolored, involuted or atretic large preovulatory, small and pear-shaped follicles. Tumor staging was performed based on gross metastatic status and histological observation as reported previously [22]. Briefly, early OVCA (stage 1 or 2) was characterized by detectable formation of a solid tumor in the ovary or extensive tumors but still restricted to the ovary. Late stages of OVCA were characterized when the tumor metastasized to distant organs with moderate to extensive ascites.

Ovarian histopathology and immunohistochemical detection of ovarian microvessel density

Representative portions of a solid ovarian mass or the whole ovary (in case of atrophied or apparently normal appearing ovaries) were divided into several blocks, processed for paraffin sections and stained with hematoxylin & eosin (H&E). Microscopic tumor lesions in any part of the ovary were detected by routine histology with H&E staining and tumor types were determined by light microscopy as reported previously [22].

Following histopathological examination, paraffin sections (5μm thick) of normal and tumor ovaries of all stages and types were processed for routine immunohistochemistry to assess the tumor associated microvessel density using monoclonal anti-α smooth muscle actin antibodies (primary antibody, Invitrogen, Carlsbad, CA) according to manufacturer's protocols. The densities of immunopositive microvessels were counted from the tumor vicinity or stroma of normal hens (excluding the follicular areas) as reported earlier [33, 34] using a light microscope attached to digital imaging stereologic software (MicroSuite version 5; Olympus Corporation, Tokyo, Japan) with a little modification. Briefly, immunostained slides were examined at low power magnification (X10 objective and X10 ocular) to identify the areas of maximum neovascularization of the tumor. Vessels with thick, regular and complete muscular wall as well as vessels with large lumina were excluded from the count as reported previously [34]. Brown stained leaky smaller vessels with discontinuous or incomplete vessel wall, clearly separated from adjacent microvessels, tumor cells or other connective tissue elements were considered to be a single, countable vessel. In each section, 5 most vascular areas were chosen. The number of microvessels in a 20,000-μm^2 area was counted at X40 objective and X10 ocular magnification. The averages of these counts were expressed as the number of immunopositive microvessels in 20,000-μm^2 area of normal or tumor ovaries. Tumor histology and immunohistochemical observations were compared to the ultrasound predictions.

Statistical analysis

Descriptive statistics for contrast parameters were determined and statistical analysis was performed by SPSS 15 (SPSS, Chicago, IL) statistical software. The differences between the power Doppler intensity changes before and after contrast injection were analyzed by the paired t-test and the (exact) sign test. The differences in the contrast parameters and the density of

256 immunopositive microvessels between the normal and tumor ovaries were analyzed by the two-
257 sample t-test and the (exact) Mann-Whitney test. The χ^2 test was used to investigate the
258 association between the contrast parameters including the Wash-out time or AUC (area under the
259 curve) with the presence or absence of tumor lesion. *P* values less than 0.05 were considered
260 significant. All reported *P*-values are two-sided.

261 **Results**

262 ***Ultrasonography***

263 Optison™ injected at a dosage of 5μL/kg body weight was well tolerated and none of the hens
264 showed any adverse condition.

265 *Normal and tumor ovaries in hens*

266 Normal ovaries in healthy hens (n = 24) were found to have multiple preovulatory follicles with
267 many small growing stromal follicles by gray scale ultrasound imaging. Blood vessels were
268 detected in the ovarian stroma by Doppler ultrasound (Figure 1A). In addition, confluent blood
269 flows were detected on the surfaces of the large preovulatory follicles. As compared to pre-
270 contrast scan, Optison™ injection enhanced visualization of ovarian blood vessels in the same
271 area of the ovary (Figure 1B). Solid ovarian masses with or without projected septa and papillary
272 structures and/or accompanied ascites were observed in the ovaries of 15 hens by gray and
273 Doppler ultrasound scan and these hens were "predicted to have ovarian tumors" (Figure 1C).
274 No large preovulatory follicles were observed in these hens. Out of these 15 hens, 11 had solid
275 masses in the ovary together with profuse ascites and were categorized to have late stage OVCA.
276 In the remaining 4 hens, solid masses were found to be limited to a part of the ovary without any
277 detectable ascites and they were categorized provisionally as early stage OVCA (final diagnosis

was performed upon gross examination). Optison™ injection remarkably enhanced the visualization of ovarian tumor associated vascular network in all hens predicted to have OVCA (Figure 1D).

The ovary in few hens (n=7) appeared regressed with only one or no large preovulatory follicles. Although no detectable solid ovarian mass was observed at gray scale ultrasound in these hens, their RI and PI values were lower than the hens with normal ovary. These hens were termed as "hens with abnormal ovarian morphology" as their diagnosis was not conclusive by ultrasound scanning (Figure 2A-D) and subsequent histopathological examinations (detailed below) showed the presence of microscopic malignant tumor lesions in a portion of the ovary of these hens. Thus these hens were finally categorized as "hens with microscopic OVCA". The pre- and post-contrast RI and PI values were significantly lower in hens suspected to have OVCA compared to their normal counter parts (P<0.01 from Exact Mann-Whitney test) (Table 1).

Contrast parameters

Number of blood vessels

Overall, as compared with pre-contrast, the number of detectable blood vessels in the normal as well as in the ovaries with tumor was significantly increased following the injection of Optison™ (P<0.05) (Table 1). As compared to normal hens, significantly more blood vessels were observed in hens predicted to have ovarian tumors (P <0.05) and their frequencies increased as the tumor progressed from microscopic to later stages (Table-1).

Doppler intensity and contrast kinetics

Optison™ injection, as compared with the pre-contrast, significantly enhanced the power Doppler intensity signal to more than two-fold in all hens irrespective of their pathological status (P <0.05) (Figure-3). Compared to hens with normal ovaries, the intensity of post-contrast Doppler signals was highest in hens predicted to have ovarian tumors (P <0.05) (Figure-3).

Although the time of arrival and the time to reach peak intensity of contrast agent were tended to be faster in hens predicted to have ovarian tumors than normal hens, the difference was not statistically significant (Table 2). The wash-out of contrast agent had two phases: a fast initial decrease and a second was slower decrease approximately to the baseline. The wash-out of Optison™ was shorter in normal hens and was significantly longer in hens predicted to have ovarian tumors (P<0.05) (Table 2). As compared to hens with normal ovary, significantly greater AUC was observed in hens predicted to have ovarian tumors (P< 0.05) (Table 2). Differences were not observed among hens of different tumor types (serous, endometrioid, mucinous and sero-mucinous mixed) with respect to their contrast parameters.

Histopathology and Microvessel Density

Gross examination of hens at necropsy confirmed ultrasound prediction. Ovarian tumors, their stages and types were confirmed at necropsy and by routine histology with H&E staining, respectively (Figure 4A-D). As observed in ultrasound scanning, late stage OVCA (n = 11 hens, 4 serous, 5 endometrioid, 1 mucinous, 1 sero-mucinous mixed) was associated with moderate to profuse ascites and metastasis to distant organs. Early stage OVCA (n=4 hens) was limited to the ovary (1 serous, 1 endometrioid, 2 sero-mucinous mixed) with little or no ascites. The seven hens initially diagnosed as “hens with abnormal ovarian morphology’ without any grossly detectable solid ovarian mass during gray scale ultrasound had microscopic malignant ovarian lesions upon

H&E staining in one or more areas of the ovary and thus were classified as hens with microscopic OVCA.

Immunopositive microvessels were detected in both normal ovaries and ovarian tumors (Figure 5). In normal hens most of the immunopositive ovarian vessels had thick, complete and continuous vessel walls with intense staining. In contrast, most of the vessels in ovarian tumors were leaky, discontinuous or incomplete with thin vessel walls (Figure 5). In normal hens, most of the immunopositive microvessels were localized in the follicular theca with few positive blood vessels in the ovarian stroma. The densities of ovarian immunopositive microvessels were significantly higher ($P < 0.01$, Mann-Whitney exact test) in hens predicted to have ovarian TAN at contrast enhanced ultrasonography (mean, 8.0 ± 0.53, 13.0 ± 0.84, and 19.0 ± 1.3 microvessels/20,000-μm^2 area of ovarian tumor tissues in microscopic, early-stage, and late-stage OVCA, respectively) than normal hens (mean, 4.0 ± 0.55 microvessels/20,000 μm^2 area of ovarian tissues). In addition to immunopositive microvessels, smooth muscle fibers surrounding the tumor glands but not the tumor epithelium were also stained positively. However, differences were not observed among different tumor types with regard to their immunopositive microvessel densities. Thus increased number of ovarian microvessels in ovaries with tumor compared to normal ovaries confirmed the *in vivo* prediction of ovarian tumor associated neoangiogenesis by contrast enhanced ultrasonography.

In vivo detection of ovarian tumor associated neoangiogenesis

Pathological status of hens including tumor staging (by histopathology) and tissue expression of ovarian microvessels (by immunohistochemistry) were compared with contrast parameters. Data on 3 contrast parameters including the *Peak post-contrast Doppler intensity*, *Wash-out time of contrast agent* and *the AUC* were used retrospectively to determine the efficacy of contrast

parameters in detecting *in-vivo* ovarian tumor associated neo-angiogenesis. Two cut-off values for each of these 3 contrast parameters namely, the mean + 2 standard deviations (SD) and the mean + 3 SD of peak intensity value and Wash-out time or AUC of normal (control) hens were used to examine the detectablity of ovarian TAN at early stage of OVCA. All three parameters with both the cut-off values detected in all hens with OVCA at early stage (tumor detected at gross examination and limited to the ovary) or late stage. The cut-off value of *Peak post-contrast Doppler intensity* with 2 SD detected 86% of (6 of 7) hens with microscopic tumor lesion (without any detectable tumor by gray scale or gross at euthanasia) whereas those with 3 SD detected only 43% of (3 of 7) these hens (Figure 3). On the other hand, cut-off value for *AUC* with 3 SD detected 86% of hens with microscopic OVCA (Table 2). However, *Wash-out time of contrast agent* detected all hens with microscopic OVCA using both cut-off values (Table 2 and Figure 6). Thus, the AUC and the Wash-out time of contrast agent were found more efficient in the detection of microscopic OVCA than other contrast parameters.

Discussion

This is the first study on the improvement of *in vivo* detection of ovarian tumor associated vascular architecture by the ultrasound contrast agent Optison™ contrast agent in laying hens, a spontaneous animal model of human OVCA. Our goals were to test the efficacy of a contrast agent in enhancing the visualization of ovarian tumor associated blood vessels in laying hens and to determine the contrast kinetics associated with early stage OVCA in laying hens. The results of the present study suggest that the contrast agent enhanced the detection of the hen ovarian vascular network. Our results also suggest that laying hens provide a new and valid platform to study kinetic parameters relative to early stage OVCA using a contrast agent. The translational significance of this study is that the laying hen may be a suitable preclinical model of

spontaneous human OVCA for the study of contrast enhanced ultrasound imaging to establish an early detection test for OVCA. This animal model of spontaneous OVCA may also be useful to test *in vivo* the efficacy of different contrast agents in a preclinical setting.

In the present study, as compared to pre-contrast scanning, significant enhancement in the detection of ovarian microvessels by power Doppler ultrasound using a contrast agent without any adverse physiological effect suggests the utility of this contrast agent in hens as reported in humans. The time of washout of the contrast agent and the AUC were significantly different between hens with ovarian tumors and hens with normal ovaries. Similar patterns were also reported in OVCA patients [13, 14]. Ovarian RI and PI values decreased in hens with normal or tumors ovaries following the contrast agent injection irrespective of their disease status. Although the precise reason(s) is not known, it is possible that the increase in the amount of recognizable vessels as well as increased blood flow may be the factors for such decrease in RI and PI values following the injection of contrast agent. Lower RI and PI values in hen ovarian tumors than in hen normal ovaries also support previous findings that lower RI and PI values are associated with OVCA [4, 28] and thus these indices may be used together with the contrast parameters to distinguish malignant ovarian vasculature from that of the normal ovary. Decreased RI and PI values in association with increased number of blood vessels (immunohistochemical observation) confirmed the enhanced detection of ovarian tumor associated vascular network by contrast parameters using Optison^{TM}. Thus the tolerance as well as the enhanced detection of ovarian blood vessels by contrast agent in hens as in humans suggests the suitability of laying hens as a preclinical animal model to study the contrast kinetics diagnostic of early stage OVCA.

Ovarian TAN is the hallmark of tumor development and progression. Contrast parameters including the time of wash-out of the contrast agent and the AUC, as observed in the present study, may be useful in distinguishing normal ovarian physiological angiogenesis from the ovarian tumor associated neo-angiogenesis at the early stage of OVCA. An increase in ovarian leaky and immature microvessels as observed in this study is one of the characteristics of ovarian TAN [1, 35]. These increased microvessel densities were associated with contrast parameters predictive of ovarian tumors. Recently, we have reported that ovarian tumor progression in hens is associated with increased frequency of VEGF-expressing ovarian blood vessels [4]. Thus an increase in ovarian microvessel frequency (as observed in this study) together with the increased expression of VEGF by these microvessels [4] may suggest that VEGF also plays a critical role in ovarian tumor progression in laying hens as in humans. Therefore, VEGF represents an additional marker of OVCA. Elevated concentrations of circulatory VEGF have been reported to be associated with OVCA in humans. Although not determined in the current study, a serum VEGF concentration may identify which hens are at risk of developing OVCA and may be followed prospectively with ultrasound monitoring for detecting the OVCA related morphological changes in the ovary. Because VEGF is not specific for ovarian TAN only, it is possible that circulatory VEGF (marker of TAN) in association with other techniques like contrast enhanced ultrasound imaging may constitute an effective early detection test for OVCA. The laying hen may be useful in establishing this early detection test. Recently, we have generated anti-chicken VEGF antibodies to detect the serum concentrations of VEGF by immunoassay in chickens. Thus, the findings of the current study may facilitate future studies with the elevated circulatory VEGF concentrations to monitor hens prospectively to detect the

development of OVCA at an early stage and to establish an early detection test in this preclinical model.

The small number of hens (total = 46 hens, 24 normal, 7 microscopic, 4 early stage and 11 late stages of OVCA) used is a limitation of the current study. We have used both the paired t-test and its nonparametric equivalent, the exact sign test for before and after comparison of Optison effects. Similarly, we have used both the two-sample t-test as well as, its nonparametric equivalent, the exact Mann-Whitney test for comparing normal versus tumor ovaries. The reported significant results were typically found in both the t-test (paired or two-sample, as appropriate) as well as the nonparametric test (sign test or the Mann-Whitney test). The p-values for the exact sign test and exact Mann-Whitney test are computed by numerical methods without any large sample approximations and are valid in small samples. Thus the remarkable increase in the intensity of ovarian vascular architecture as well as the number of blood vessels following contrast agent injection may form the foundation for a larger study to establish an effective early detection test for OVCA. Furthermore, laying hens may also be useful in developing the ovarian TAN targeted molecular imaging and in monitoring the effects of anti-angiogenic drugs related to the recession or relapse of ovarian tumors.

Few reports have described that Doppler imaging using contrast agent to assess tumor enhancement has low contrast and resolution, substantial background noise, and considerable operator dependence and suggested that these limitations can be addressed by new sonographic imaging methods, such as pulse inversion harmonic (PIH) imaging. [11, 14, 35]. Although we have not used PIH method, we adjusted the dosage of Optison^{TM} for optimal contrast and resolution with minimum background noise in our initial studies in this model.

In conclusion, the results of this pilot study showed that the laying hen, a pre-clinical spontaneous animal model of human OVCA may be useful to understand and determine ovarian tumor associated vascular kinetics during early and late stage OVCA using contrast enhanced ultrasonography. Information on contrast enhanced ultrasound imaging for the detection of early stage OVCA in laying hens will also provide the foundation for clinical studies.

Acknowledgement

We thank Chet and Pam Utterback and Doug Hilgendorf, staff of the University of Illinois at Urbana-Champaign (UIUC) Poultry Research Farm for maintenance of the hens. We also thank Sergio Abreu Machado, graduate student, Department of Animal Sciences, UIUC for his help in injecting hens with Optison™. This study was supported by the Prevent Cancer Foundation (Dr Barua), Rush University Research Committee grants-in-Aid (Dr Barua), The Brian Piccolo Cancer Research Fund (grants for purchasing ultrasound machine, Dr Barua), NCI-Pacific Ovarian Cancer Research Consortium Career Development Program grant P50 CA83636 (to Dr Barua, PI: Dr. Urban) and Elmer Sylvia and Sramek Foundation (Dr. Barua).

References:

1. Folkman, J. *What is the evidence that tumors are angiogenesis dependent?* J Natl Cancer Inst, 1990; **82**: 4-6.
2. Shubik P. *Vascularization of tumors: a review.* J Cancer Res Clin Oncol, 1982; **103**: 211-226.
3. Ramakrishnan S, Subramanian IV, Yokoyama Y, Geller M. *Angiogenesis in normal and neoplastic ovaries.* Angiogenesis, 2005; **8**: 169-182.
4. Barua A, Bitterman P, Bahr JM, Bradaric MJ, Hales DB, Luborsky JL, Abramowicz JS. *Detection of tumor-associated neoangiogenesis by Doppler ultrasonography during early-stage ovarian*

cancer in laying hens: a preclinical model of human spontaneous ovarian cancer. J Ultrasound Med, 2010; **29**:173-182.

5. Jemal A, Siegel R, Ward E, Hao Y, Xu J, Thun MJ, *Cancer statistics, 2009.* CA Cancer J Clin, 2009. **59**(4): p. 225-249.

6. Hata K, Fujiwaki R, Maede Y, Nakayama K, Fukumoto M, Miyazaki K. *Expression of thymidine phosphorylase in epithelial ovarian cancer: correlation with angiogenesis, apoptosis, and ultrasound-derived peak systolic velocity.* Gynecol Oncol, 2000; **77**: 26-34.

7. Hata K, Fujiwaki R, Nakayama K, Maede Y, Fukumoto M, Miyazaki K. *Expression of thymidine phosphorylase and vascular endothelial growth factor in epithelial ovarian cancer: correlation with angiogenesis and progression of the tumor.* Anticancer Res, 2000; **20**: 3941-3949.

8. Bamberger ES. Perrett CW. *Angiogenesis in epithelian ovarian cancer.* Mol Pathol, 2002; **55**: 348-359.

9. Bosse K, Rhiem K, Wappenschmidt B, Hellmich M, Madeja M, Ortmann M, Mallmann P, Schmutzler R. *Screening for ovarian cancer by transvaginal ultrasound and serum CA125 measurement in women with a familial predisposition: a prospective cohort study.* Gynecol Oncol, 2006; **103**: 1077-1082.

10. Moore RG, Bast RC, Jr. How do you distinguish a malignant pelvic mass from a benign pelvic mass ? Imaging, biomarkers or none of the above. J Clin Oncol,2007; 25:4159-4161

11. Fleischer AC, Lyshchik A, Jones HW, Crispens MA, Andreotti RF, Williams PK, Fishman DA. *Diagnostic parameters to differentiate benign from malignant ovarian masses with contrast-enhanced transvaginal sonography.* J Ultrasound Med, 2009; **28**: 1273-1280.

12. Fishman DA, Cohen L, Blank SV, Shulman L, Singh D, Bozorgi K, Tamura R, Timor-Tritsch I, Schwartz PE. *The role of ultrasound evaluation in the detection of early-stage epithelial ovarian cancer.* Am J Obstet Gynecol, 2005; **192**: 1214-1221; discussion 1221-1222.

13. Orden MR, Gudmundsson S, Kirkinen P. *Contrast-enhanced sonography in the examination of benign and malignant adnexal masses.* J Ultrasound Med, 2000; **19**:783-788.

14. Marret H, Sauget S, Giraudeau B, Brewer M, Ranger-Moore J, Body G, Tranquart F. *Contrast-enhanced sonography helps in discrimination of benign from malignant adnexal masses.* J Ultrasound Med, 2004; **23**: 1629-1639; quiz 1641-1642.

15. Leen, E. *Ultrasound contrast harmonic imaging of abdominal organs.* Semin Ultrasound CT MR, 2001. **22**(1): p. 11-24.

16. Fleischer, A.C., A. Lyshchik, H.W. Jones, Jr., M. Crispens, M. Loveless, R.F. Andreotti, P.K. Williams, D.A. Fishman. *Contrast-enhanced transvaginal sonography of benign versus malignant ovarian masses: preliminary findings.* J Ultrasound Med, 2008. **27**(7): p. 1011-8; quiz 1019-21.

17. Orden, MR, Jurvelin JS, Kirkinen PP. *Kinetics of a US contrast agent in benign and malignant adnexal tumors.* Radiology, 2003; **226**: 405-410.

18. Suren A, Osmers R, Kulenkampff D, Kuhn W. *Visualization of blood flow in small ovarian tumor vessels by transvaginal color Doppler sonography after echo enhancement with injection of Levovist.* Gynecol Obstet Invest, 1994; **38**: 210-212.

19. Vanderhyden BC. Shaw TJ, Ethier JF. *Animal models of ovarian cancer.* Reprod Biol Endocrinol, 2003; **1**: 67.

20. Stakleff KD, Von Gruenigen VE. *Rodent models for ovarian cancer research.* Int J Gynecol Cancer, 2003; **13**: 405-412.

21. Fredrickson TN.*Ovarian tumors of the hen.* Environ Health Perspect, 1987; **73**: 35-51.

22. Barua A, Bitterman P, Abramowicz JS, Dirks AL, Bahr JM, Hales DB, Bradaric MJ, Edassery SL, Rotmensch J, Luborsky JL. *Histopathology of ovarian tumors in laying hens: a preclinical model of human ovarian cancer.* Int J Gynecol Cancer, 2009; **19**: 531-539.

23. Rodriguez-Burford C, Barnes MN, Berry W, Partridge EE, Grizzle WE. *Immunohistochemical expression of molecular markers in an avian model: a potential model for preclinical evaluation of agents for ovarian cancer chemoprevention.* Gynecol Oncol, 2001; **81**: 373-379.

24. Jackson E, Anderson K, Ashwell C, Petitte J, Mozdziak PE. *CA125 expression in spontaneous ovarian adenocarcinomas from laying hens.* Gynecol Oncol, 2007; **104**: 192-198.

25. Hales DB, Zhuge Y, Lagman JA, Ansenberger K, Mahon C, Barua A, Luborsky JL, Bahr JM. *Cyclooxygenases expression and distribution in the normal ovary and their role in ovarian cancer in the domestic hen (Gallus domesticus).* Endocrine, 2008; **33**: 235-244.

26. Urick ME, Giles JR, Johnson PA.*VEGF expression and the effect of NSAIDs on ascites cell proliferation in the hen model of ovarian cancer.* Gynecol Oncol, 2008; **110**: 418-424.

27. Fathalla MF. *Incessant ovulation--a factor in ovarian neoplasia?* Lancet, 1971; **2**: 163.

28. Barua A, Abramowicz JS, Bahr JM, Bitterman P, Dirks A, Holub KA, Sheiner E, Bradaric MJ, Edassery SL, Luborsky JL. *Detection of ovarian tumors in chicken by sonography: a step toward early diagnosis in humans?* J Ultrasound Med, 2007; **26**: 909-919.

29. Bahr JM, Palmer SS. *The influence of ageing on ovarian function.* Crit Rev Poul Biol, 1989: **2**: 8-14.

30. Damjanov I. *Ovarian tumours in laboratory and domestic animals.* Curr Top Pathol, 1989; **78**: 1-10.

31. Forsberg F, Liu JB, Burns PN, Merton DA, Goldberg BB. *Artifacts in ultrasonic contrast agent studies.* J Ultrasound Med, 1994; **13**: 357-365.

32. Orden MR, Gudmundsson S, Kirkinen P. *Intravascular ultrasound contrast agent: an aid in imaging intervillous blood flow?* Placenta, 1999; **20**: 235-240.

33. Weidner N, Folkman J, Pozza F, Bevilacqua P, Allred EN, Moore DH, Meli S, Gasparini G. *Tumor angiogenesis: a new significant and independent prognostic indicator in early-stage breast carcinoma.* J Natl Cancer Inst, 1992; **84**: 1875-1887.

34. Bosari S, Lee AK, DeLellis RA, Wiley BD, Heatley GJ, Silverman ML. *Microvessel quantitation and prognosis in invasive breast carcinoma.* Hum Pathol, 1992; **23**: 755-761.

35. Schiffenbauer YS, Abramovitch R, Meir G, Nevo N, Holzinger M, Itin A, Keshet E, Neeman M. *Loss of ovarian function promotes angiogenesis in human ovarian carcinoma.* Proc Natl Acad Sci U S A, 1997; **94**: 13203-13208.

Table 1: Changes in Doppler indices and the number of blood vessels in hen ovaries following the injection of Optison™.

Ovarian pathology	RI values		PI Values		Number of blood vessels	
	Before	After	Before	After	Before	After
Normal	0.68 ± 0.05 (0.60-0.80)	0.56 ± 0.05 (0.49-0.74)	1.05 ± 0.21 (0.83-1.46)	0.80 ± 0.11 (0.68-1.12)	3.29 ± 1.04 (2.00-5.00)	6.17 ± 1.31 (4.00-9.00)
Microscopic OVCA	0.59 ± 0.04 (0.54-0.66)	0.47 ± 0.03 (0.43-0.53)	0.88 ± 0.10 (0.74-1.08)	0.65 ± 0.08 (0.58-0.78)	5.14 ± 0.90 (4.00-6.00)	13.71 ± 3.90 (7.00-18.00)
Early stage OVCA	0.43 ± 0.01 (0.42-0.44)	0.33 ± 0.04 (0.29-0.38)	0.56 ± 0.02 (0.54-0.58)	0.44 ± 0.07 (0.36-0.53)	8.50 ± 1.00 (7.00-9.00)	18.50 ± 5.20 (15-26)
Late stage OVCA	0.36 ± 0.04 (0.30-0.40)	0.25 ± 0.04 (0.18-0.32)	0.46 ± 0.07 (0.34-0.56)	0.33 ± 0.07 (0.22-0.41)	12.91 + 2.43 (10.00-18)	24.09 + 4.61 (20-32)

Table 2: Kinetics of contrast agent relative to stages of ovarian cancer in hens.

Ovarian pathology	Time of arrival of contrast agent (secs)	Time to reach peak intensity (secs)	Time of wash-out (secs)	Percentage of hens with OVCA detected by Time-of-Washout*	Area under the curve (AUC)	Number of hens with OVCA detected by AUC*
Normal	15 ± 0.82 (14-16)	21 ± 0.81 (20-22)	51 ± 2.44 (48-56)	Ref	5496.94 ± 1439.80	Ref
Microscopic OVCA	14± 1.21 (12-15)	20 ± 2.04 (17-22)	72 ± 4.24 (69-81)	100% (*P*<0.01)	15310.86 ± 2771.64	86% (*P*<0.05)
Early stage OVCA	14 ± 0.96 (13-15)	19 ± 1.29 (17-20)	120 ± 11.15 (108-135)	100% (*P*<0.01)	49404.00 + 10957.71	100% (*P*<0.05)
Late stage OVCA	13 ± 1.12 (11-14)	18 ± 0.94 (17-19)	150 ± 4.94 (142-156)	100% (*P*<0.01)	80607.00+ 15247.76	100% (*P*<0.05)

Ref = reference

* above the cut-off value (mean of normal + 3SD) for Time-of-Washout and AUC.

Figure Legends:

Figure 1: Pre- and post-contrast Doppler ultrasonograms of hen ovaries with or without tumors. Scanning of hens was performed in a continuous manner before and after the injection of the Optison™. Images including still and movie clips were digitally archived. Contrast kinetics namely, the time of arrival, time to reach peak intensity and time of wash-out as well as pre-and post-contrast Doppler indices (RI and PI values) were recorded. A) Pre-contrast sonogram of a normal appearing ovary showing a preovulatory follicle and few small follicles without any solid mass and B) is the corresponding post-contrast sonogram of the same hen. As compared to pre-contrast, more vesssels are seen in the post-contrast sonogram. C) Pre-contrast sonogram of a hen predicted to have ovarian tumor. Solid tumor-like mass is seen in the ovary and a central blood flow pattern with a few vessels is detected in and around the mass. D) Post-contrast sonogram of the ovary shown in C). The Contrast agent remarkably enhanced the intensity of blood vessels as well as visualization of more blood vessels. As compared to pre-contrast, many blood vessels are seen in the post-contrast scan. Ultrasound predictions were confirmed at gross (euthanasia) and histopathological examination. S = Stroma of ovary, SM = Solid tissue mass in the ovary.

Figure 2. Contrast agent (Optison™) enhanced the ability of Doppler ultrasound to detect microscopic ovarian tumor associated vasculature in laying hens. A) Pre-contrast sonogram of an ovary without detectable solid ovarian mass or abnormality. Only a few blood vessels are seen in this ovary with no preovulatory follicle. B) Corresponding sonogram of the same ovary showing the arrival of contrast agent Optison™. As compared to pre-contrast, the number of detectable blood vessels is increased and as compared to pre-contrast, the vessels appear more dilated in the post-contrast sonogram. C) Post-contrast sonogram of the same ovary showing peak level of

enhancement. As compared to pre-contrast and post-contrast at arrival of Optison, more vessels are detected at peak enhancement. Although no solid ovarian mass is detected but the central pattern of vascular arrangement indicates a potential ovarian abnormality. D) Gross appearance of the same ovary at euthanasia. As predicted, neither large preovulatory follicle nor detectable solid mass is seen. However, subsequent histopathological examination showed the presence of an endometrioid tumor lesion (termed as microscopic ovarian tumor) confirming the prediction of contrast enhanced ultrasound scanning. Scanning of hens and their subsequent processing were similar to those mentioned in Figure 1. S= Stroma; Dotted circle indicates the ovary.

Figure 3. Detection of ovarian tumor associated neo-angiogenesis by post-contrast Doppler intensity of blood vessels. A flock of 150 hens were monitored for their ovarian function and their egg laying rates were recorded on a daily basis. Hens with low egg laying rates (n=46) were selected for sonography. Based on gray scale sonography, gross and histopathological examinations, hens were grouped to have normal ovary (n=24 hens), microscopic OVCA (n=7), early stage OVCA (n=4) and late stage OVCA (n=11). Post-contrast Doppler intensities of ovaries or ovarian tumors were measured by power Doppler sonography following the injection of Optison^{TM}. Cut-off lines [mean peak Doppler intensity values of normal hens with 2 or 3 standard deviation (SD)] indicate the detectability of OVCA by post contrast peak Doppler intensities.

Figure 4. Gross and histological sections of ovarian tumors in hens scanned with contrast enhanced ultrasound. Following contrast enhanced Doppler ultrasound, hens were euthanized and examined grossly for the presence of tumor-related solid ovarian mass which was confirmed by routine histology with hematoxylin and eosin (H&E). A) Ovary of a hen with early stage of ovarian cancer (OVCA). Few small solid tumor masses with no preovulatory follicles are

present. The tumor is limited to a part of the ovary. B) Section taken from a normal and uninvolved portion of an ovary in which a tumor was detected in the other part of the ovary (early stage OVCA). Stromal follicles are embedded in the normal appearing stroma. No invasion of tumor cells is seen in this portion of the ovary. C) An ovarian tumor in hens with late stage of OVCA. The solid tumor mass appears like a cauliflower. The tumor metastasized to distant organs and was associated with extensive ascites. D) Section of a serous ovarian tumor from a hen with late stage OVCA. The tumor has a compact sheath of tumor cells with pleomorphic nuclei and tumor glands are surrounded by fibromuscular layers (H&E). All sections are of 20X magnification; F = follicle, G = granulosa layer of follicle, S = ovarian stroma, SM = solid tumor mass, T = theca layer of follicle, Tu = tumor

Figure 5. Immunohistochemical detection of ovarian microvessels in laying hens with or without ovarian cancer (OVCA). Paraffin sections were immunostained with monoclonal anti-α smooth muscle actin. A) Section of a hen's normal ovary. Immunopositive microvessels are seen in the follicular theca and few in the adjacent stroma. Most of the immunopositive vessels have a thick vessel wall. B) Section of hen's ovary with early stage OVCA [ovary shown in Fig 4(A)]. As compared to the normal ovary, more immature immunopositive microvessels with leaky, thinner, incomplete or discontinuous vessel walls are present between tumor glands. The fibrous connective tissue of the tumor glands are also stained positive. C) Section of an ovarian tumor from a hen with late stage OVCA [ovary shown in Fig 4(C)]. As compared to normal and early stage OVCA, many leaky and immature microvessels with discontinuous or attenuated staining are seen in vicinity of the tumor. Arrows indicate examples of immunopositive microvessels. F = follicle; G = granulosa layer; S = stroma; T = theca layer. Dotted circles indicate examples of tumor glands.

Figure 6. Detection of ovarian tumor associated neo-angiogenesis by Wash-out time of contrast agent. Other information is similar to the legend of Fig 3. Cut-off lines [mean of Wash-out time (seconds) of normal hens with 2 or 3 SD] indicate the detectability of OVCA by the Wash-out time of contrast agent.

Abbreviations

AUC, area under the curve; OVCA, ovarian cancer; PI, pulsatility index; RI, resistive index; TAN, tumorassociated, neoangiogenesis; VEGF, vascular endothelial growth factor

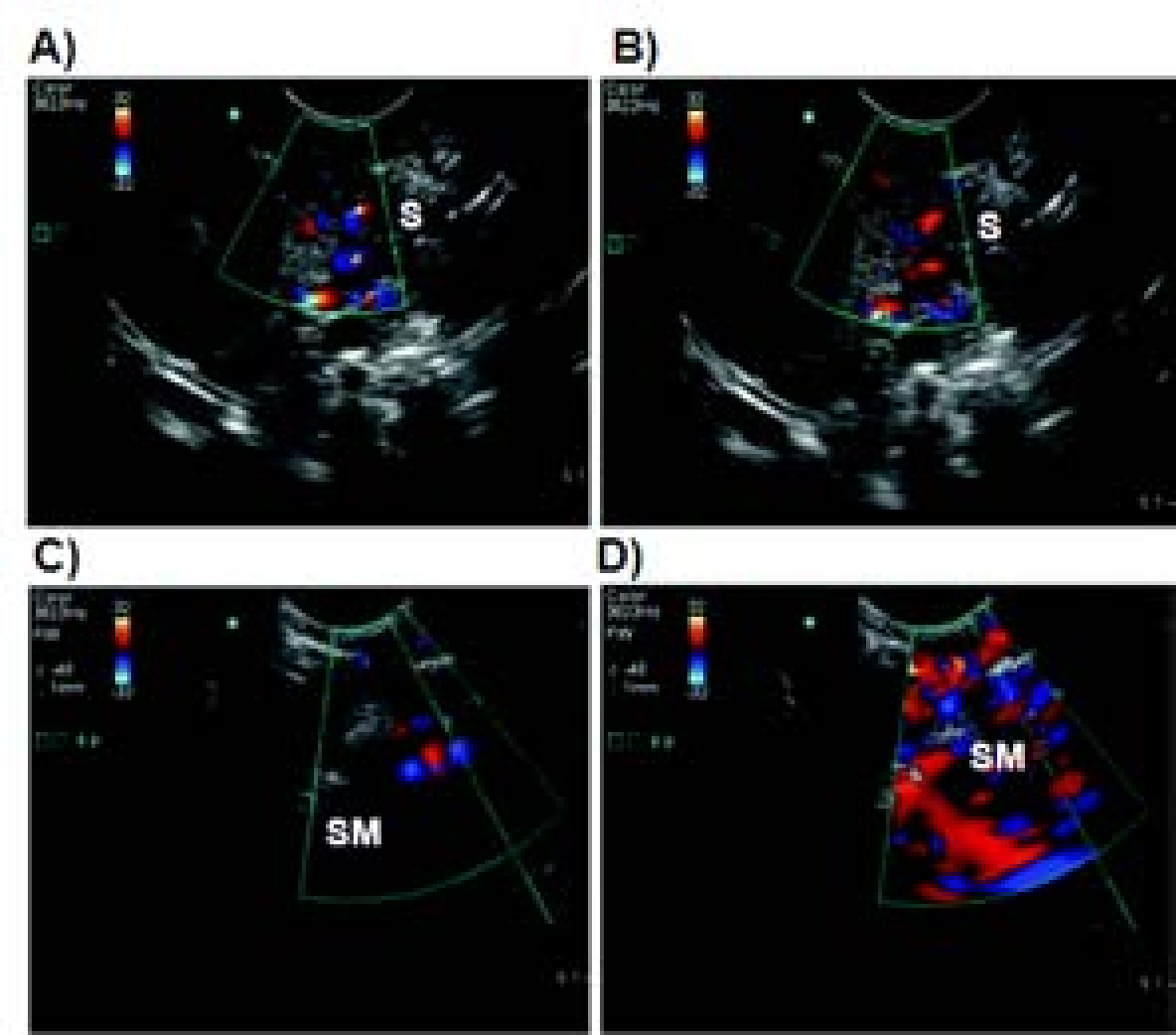
A)
S
B)
S
C)
SM
D)
SM

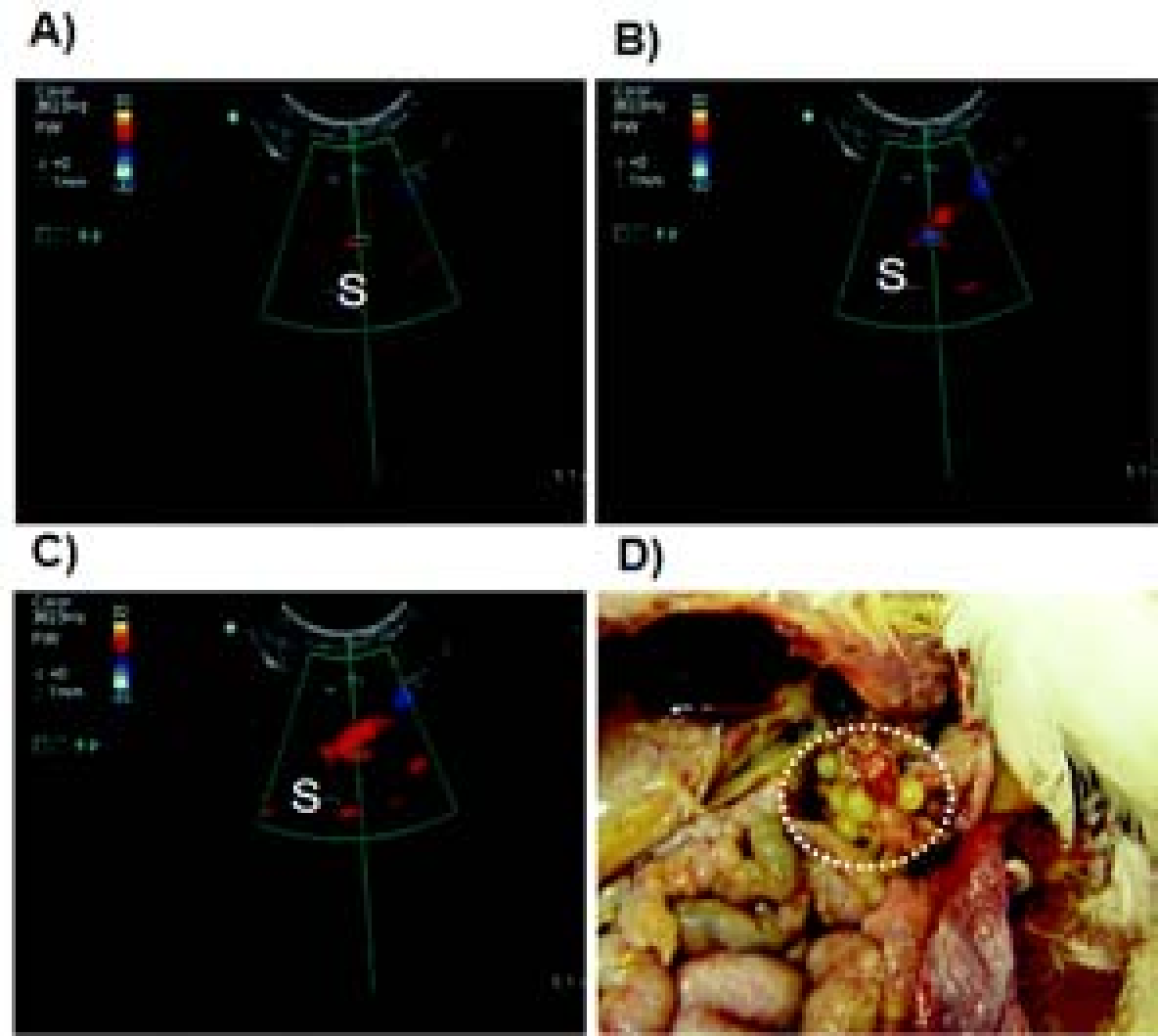
A)
B)
S
S
C)
D)
S

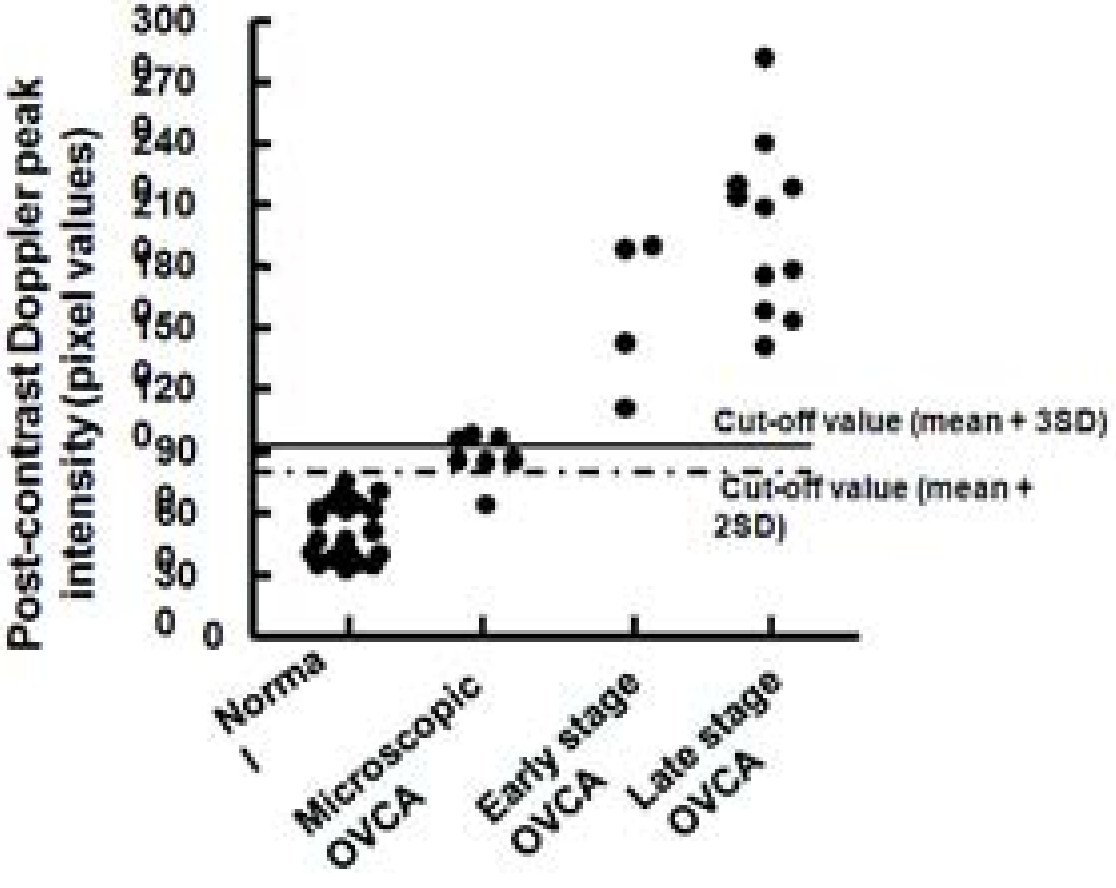
Post-contrast Doppler peak intensity (pixel values)
300
270
240
210
180
150
120
90
80
30
0
0
Cut-off value (mean + 3SD)
Cut-off value (mean + 2SD)
Normal
Microscopic OVCA
Early stage OVCA
Late stage OVCA

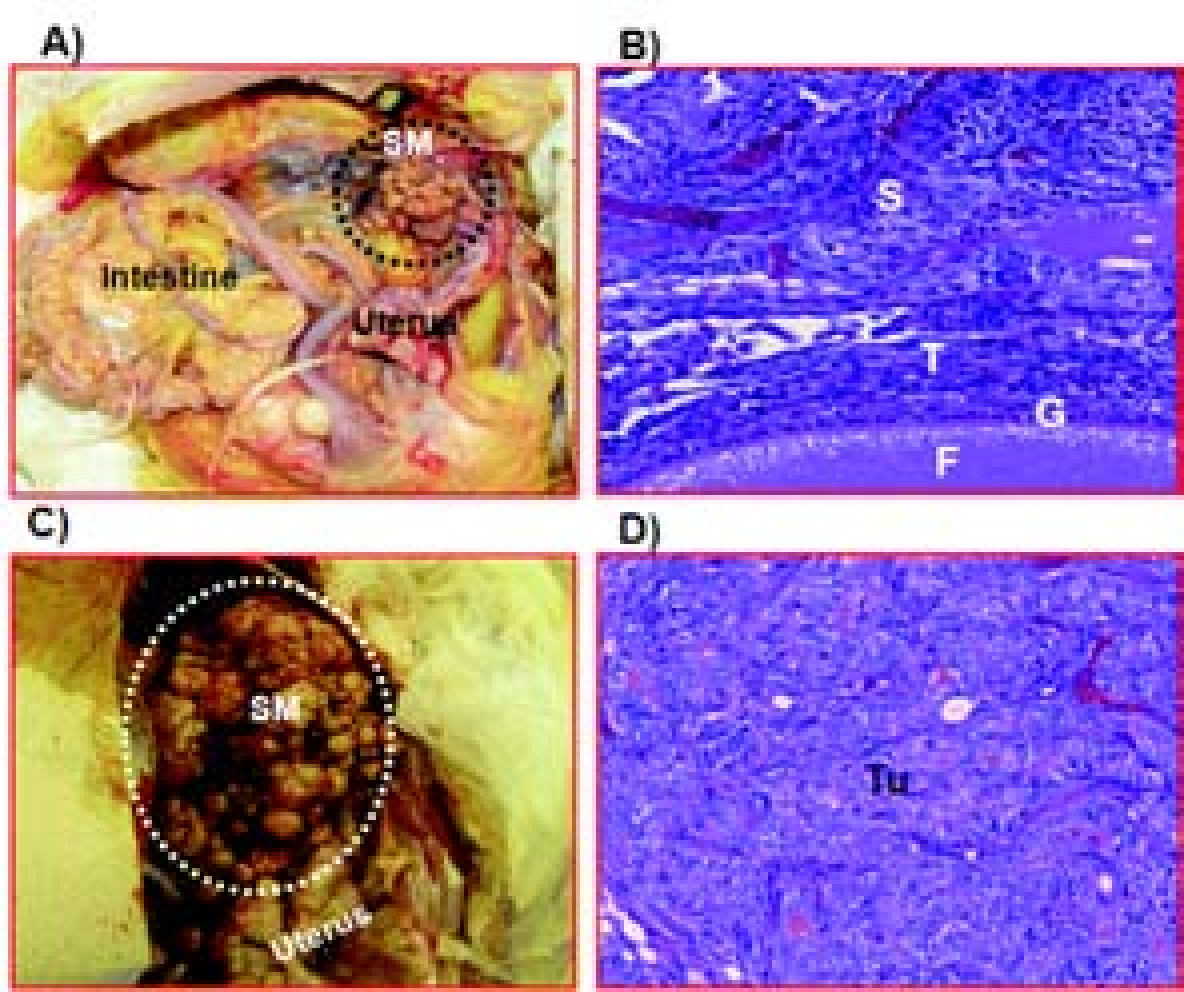
A)
SM
Intestine
Uterus
B)
S
T
G
F
C)
SM
Uterus
D)
Tu

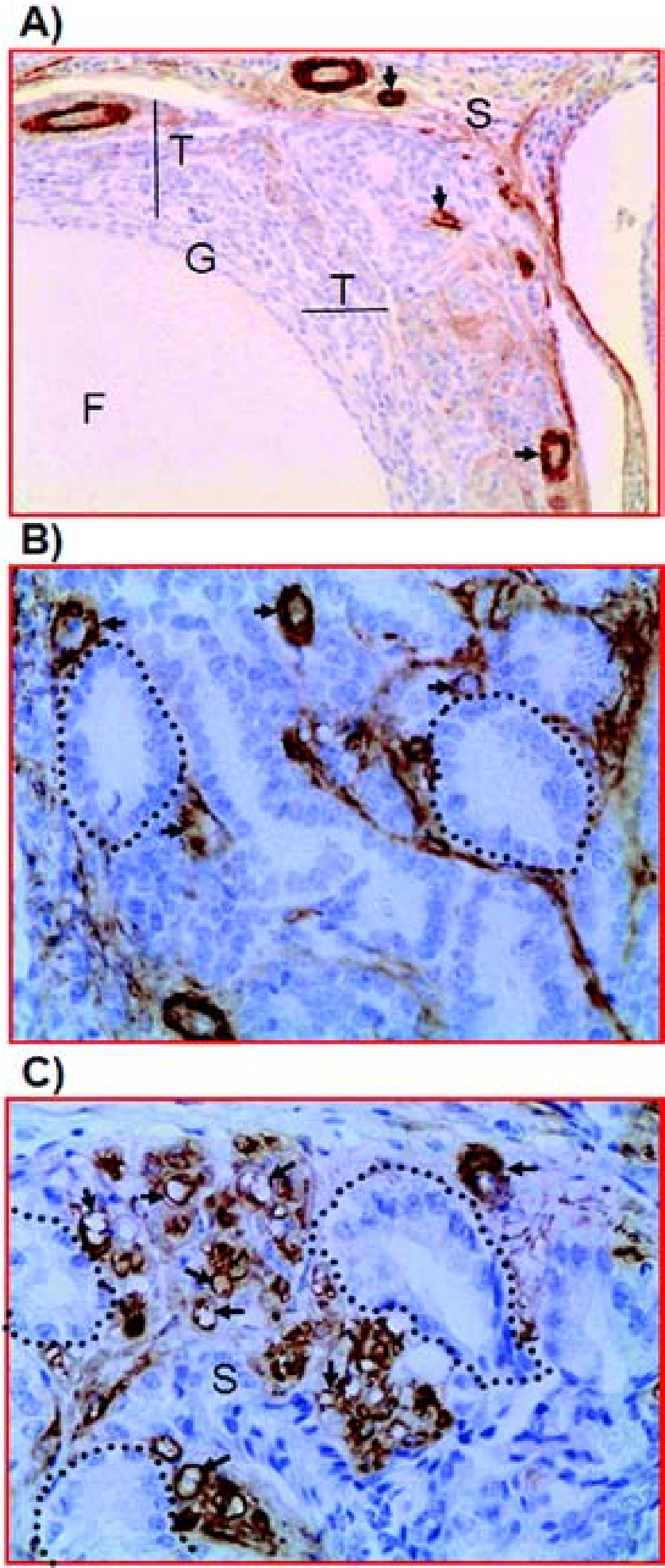
A)
T
G
T
S
F
B)
C)
S

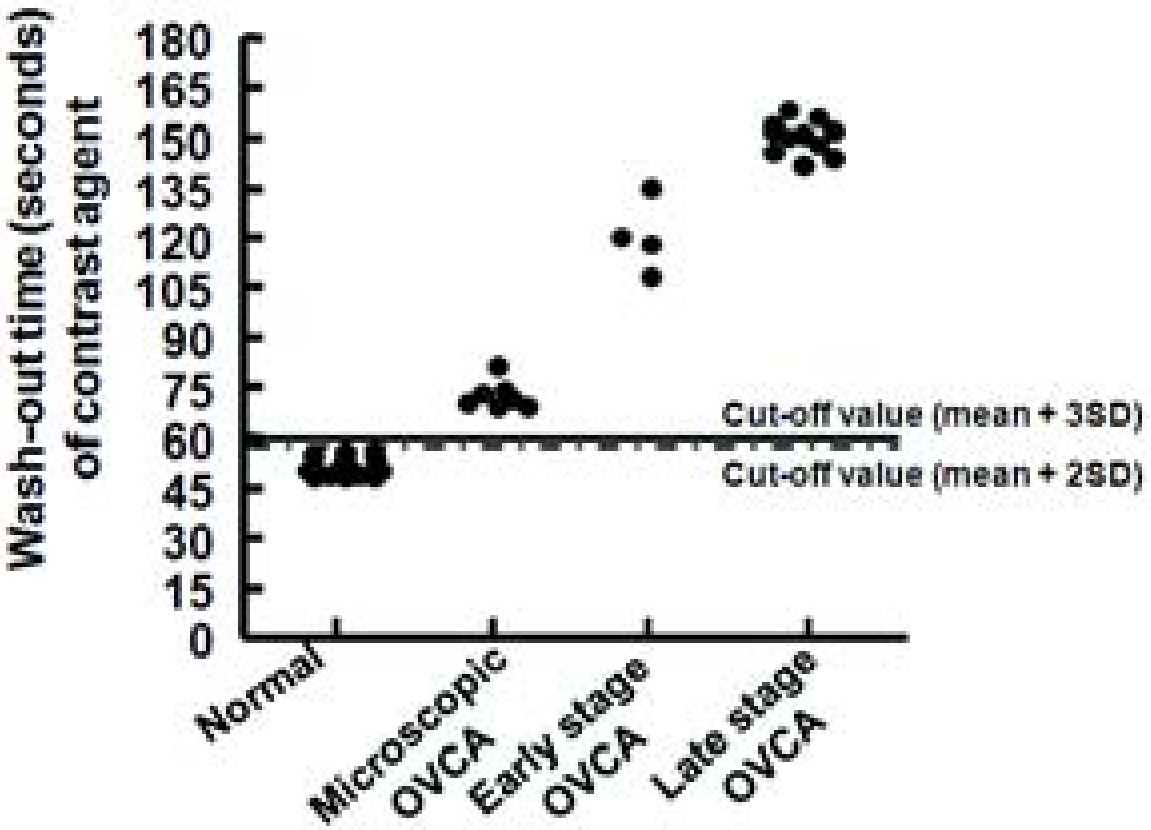
Wash-out time (seconds) of contrast agent
180
165
150
135
120
105
90
75
60
45
30
15
0
Cut-off value (mean + 3SD)
Cut-off value (mean + 2SD)
Normal
Microscopic OVCA
Early stage OVCA
Late stage OVCA

Sphingosine-1 Phosphate Receptor (S1p1), a Critical Receptor Controlling Human Lymphocyte Trafficking, is Expressed in Hen and Human Ovaries and Ovarian Tumors

Michael J Bradaric, BS[1]; Animesh Barua, PhD[1,2,3]; Krishna Penumatsa, MS[1]; Yu Yi, MS[1]; Seby L Edassery, MS[1]; Sameer Sharma MD[2,4]; Jacques S Abramowicz, MD[2]; Janice M Bahr, PhD[5]; Judith L Luborsky, PhD [1,2,§]

[1]Department of Pharmacology, Rush University Medical Center, Chicago, IL
[2]Department of Obstetrics & Gynecology, Rush University Medical Center, Chicago, IL
[3]Department of Pathology, Rush University Medical Center, Chicago, IL
[4]Department of Obstetrics & Gynecology, Section of Gynecologic Oncology, John Stroger Hospital, Chicago IL
[5]Department of Animal Sciences, University of Illinois Urbana – Champaign, IL

Email Addresses/ phone numbers

MJB: michael_bradaric@rush.edu	(312) 563-2204
AB: animesh_barua@rush.edu	(312) 942-6666
KP: krishna_penumatsa@rush.edu	(312) 563-2204
YY: Yu_Yi@rush.edu	(312) 942-4842
SE: seby_l_edassery@rush.edu	(312) 563-2628
SS: Sameer_Sharma@rush.edu	(219) 864-2580
JSA: Jacques_Abramowicz@rush.edu	(312) 942-9428
JMB: jbahr@uiuc.edu	(217) 503-0657
JLL: jluborsk@rush.edu	(312) 942-6602

§ Corresponding Author: Judith L Luborsky, PhD

ABSTRACT

Background. Sphingosine-1 receptor 1 (S1P1) plays a major role in regulating lymphocyte egress from peripheral lymph tissue. Lymphocyte trafficking is potentially a critical response to tumors and to tumor vaccines. Also, the receptor has been shown to influence metastasis. However, there is little information on its expression in the aged ovary or ovarian tumors. As a basis for further studies in the laying hen model of spontaneous ovarian cancer, the objective of this study was to determine if S1P1 is expressed in hens, and if the morphological distribution of S1P1 is similar in hen and human ovary and ovarian tumors.

Methods. S1P1 mRNA was ascertained in hen tissue by RT-PCR using hen specific primers. S1P1 protein expression and localization was evaluated in hen and human tissue with a human S1P1 antibody by Western blot and immunohistochemistry.

Results. S1P1 mRNA was expressed in all hen tissues examined. Protein was detected in human and hen ovary and ovarian tumors at 47, 72 and 108 kDa in Western blots. S1P1 was similarly expressed on endothelial cells, lymphocytes and surface epithelial cells in normal ovaries and tumor-containing ovaries. In addition, S1P1 distribution was heterogeneous in ovarian tumors by immunohistochemistry.

Conclusion. The results show that S1P1 is expressed in the hen and human ovary as well as in ovarian tumors. These findings support the use of the hen in further studies of the role of S1P1 in metastasis and immune cell trafficking in ovarian tumor development.

Key words: ovary, ovarian cancer, chicken, human, S1P1 (EDG-1).

Background

Sphingolipids acting through sphingosine-1-phosphate receptors are involved in embryogenesis, angiogenesis, vascular homeostasis and immune cell trafficking [1;2]. There are five isoforms of sphingosine receptors (S1P1 – S1P5) [3]. Sphingosine receptors are members within a larger family of G-Protein Coupled Receptors (GPCR) that are expressed on leukocytes and on vascular endothelial cells. The ligand, sphingosine-1 phosphate (S1P), binds to several of the sphingosine 1-phosphate receptors with higher affinity to the S1P1 and S1P3 isoforms [4]. The S1P1 regulates lymphocyte egress from lymphoid organs [5;6] and is necessary for lymphocyte recirculation from thymus and peripheral lymphoid organs. In addition to a critical role in regulating immune cell trafficking, activation of S1P1 can promote or inhibit apoptosis of immune cells depending on the balance of cytokines [7]. Knockout of S1P1 (LP(B1)/EDG-1) in mice is embryologically lethal [8]. S1P1 also has a role in inflammatory disease such as graft versus host disease and multiple sclerosis [9]. The drug FTY720 binds to S1P1 as a high affinity agonist and causes down-regulation and internalization of S1P1. This drug has been used as novel immunosuppressive agent to inhibit S1P1-mediated immune cell migration from lymph to sites of inflammation and is of particular interest in transplant and in treatment of autoimmune diseases such as multiple sclerosis [9] and more recently, cancer.

The endogenous ligand (S1P) was recently shown to play an important role in ovarian cancer invasiveness and ovarian tumor cell migration [10;11]. It also appears to protect ovaries from the effects of chemotherapy [12] and radiation [13] and therefore is potentially a therapeutic target to preserve fertility in patients undergoing therapy for cancer. While there are several studies of S1P involvement in ovarian cancer models and ovarian tumor-derived cell lines there is no information on the expression of its receptor, S1P1, in normal human (aged) ovary or in naturally occurring ovarian tumors in humans or animal models.

We [14-18] and others [19-21] reported that the laying hen, which spontaneously develops ovarian tumors [22] is useful for studies of ovarian cancer. The normal hen ovary has been used

extensively to understand ovarian physiology [23;24] because it shares many features of normal human ovary including similar cyclic hormone regulation of follicle development and ovulation [25]. Like human ovaries, hen ovaries express receptors for follicle stimulating hormone (FSH) and luteinizing hormone (LH) and produce inhibins, estrogen, and progesterone in response to FSH and LH [24]. One difference between human and hen ovarian function is the lack of post-ovulatory development of a progesterone-secreting corpus luteum and the events that lead to implantation because eggs are laid externally.

Likewise, naturally occurring hen ovarian tumors are similar to human tumors [17;22]. Commonly, hen ovarian tumors exhibit epithelial cell histology including serous, endometrioid, clear cell and mucinous histology [17] and less frequently tumors of germ cell origin [22] which is typical of the histology seen in humans [26]. The incidence of both hen and human ovarian tumors increases with age [22;27]. In hens, which are pure bred (rather than inbred), the incidence of ovarian tumors is also strain and flock dependent [20] which suggests a genetic component associated with ovarian cancer, as in humans [28]. As well, many of the same proteins are expressed in human and hen tumors such as CA125 [29], E-cadherin [30], COX [19], p53 [28], SBP-1 [31], mesothelin [32] and several others [21]. Interestingly, progesterone reduced the incidence of ovarian carcinoma in hens which parallels the reduced risk of ovarian cancer associated with oral contraceptive use in women [33]. Recently, we developed the use of ultrasound to assess ovarian morphology and tumor-associated angiogenesis [18] in order to facilitate the selection of hens for studies of ovarian cancer and to be able to monitor hens longitudinally.

A further advantage of the hen as a model for studies of immune mechanisms in ovarian cancer is the well established knowledge of the immune system. In fact, the two different types of immune cells (T and B cells) were first described based on the differences in lymphocytes in the thymus and bursa of Fabricius [34;35]. Also, the first successful anti-tumor vaccine was developed for chickens to prevent Marek's disease, a virally-induced lymphoid neoplasm [36]. Moreover, humans [37;38] and hens [16] develop spontaneous ovarian autoimmunity and circulating anti-ovarian antibodies associated with prematurely reduced ovarian function.

Our future objective is to examine the role of immunity in ovarian tumor development and progression through modification of lymphocyte trafficking. Although the expression and role of S1P1 has been demonstrated in humans, there is little information on its expression in the human or hen ovary. Therefore, the specific objective of this study was to determine if S1P1, a major receptor that regulates lymphocyte trafficking in humans, is expressed in hens, and if the morphological distribution of S1P1 is similar in hen and human ovary and ovarian tumors.

Methods

Animals: White leghorn hens (2-3 years old, strain W/96) were housed at the University of Illinois at Urbana-Champaign (UIUC) at the Poultry Research Farm affiliated with the Department of Animal Science. Food and water were given *ad libitum* and hens were maintained on a 17:7 hour light: dark schedule. Hens this age were used in our study because the proportion of hens with ovarian tumors is about 10-15%, based on our experience. Animals were selected for study based on normal or abnormal ovarian ultrasound as described previously [15;17;18]. Hens were sacrificed at UIUC by cervical dislocation and organs removed. Hen tumors were histologically staged and typed by a pathologist using criteria similar to human tumor type and staging as described previously [17]. All procedures were approved by the University of Illinois Institutional Animal Care and Use Committee (IACUC).

Human Ovarian Tissues: Normal ovaries and ovarian tumors were obtained from the gynecologic oncology clinics at Rush University Medical Center and John Stroger Hospital (Chicago, IL) according to Institutional Review Board (IRB) approved protocols. Normal ovaries were obtained at hysterectomy (n = 5; mean age 54 ± 8 years). Ovarian tumors were obtained from patients with malignant tumors (n = 18; mean age 64 ± 15 years). The tumor histology and tumor grade were determined by a pathologist using standard FIGO criteria [17]. The criterion for inclusion in the study was women ≥45 years old. The criteria for exclusion were previous history of any cancer and prior chemotherapy or radiation treatment. Of the five ovarian

tumors shown in this report, three were serous and two were endometrioid.

Tissue preparation: Hen ovary (n = 20), spleen (n = 5), and ceccal tonsils (peripheral lymphoid organ, n = 4) and brain (n = 2) were cut into three equal portions. Human (normal) ovary (n = 4) and ovarian tumors (n = 4) were similarly prepared. One portion was fixed in 10% PBS-buffered formalin and embedded in paraffin for histology and immunohistochemistry [17]. A second portion was frozen (-80ºC) for cryostat sections for immunohistochemistry. The final portion was washed with cold 1.5mM Tris HCl, homogenized (100mg wet weight tissue/100mL of 40mM Tris HCl, 5 mM $MgSO_4$ buffer), centrifuged (1,000 x g, 10 minutes, 4ºC) and the supernatant stored at -80ºC for Western blot analysis [16;31]. In addition, to enrich for S1P1 receptors, the supernatant was centrifuged again (18,000 x g, 40 minutes, 4ºC) and the pellet was suspended in sample buffer (Bio-Rad Laboratories, Hercules, CA) for one-dimensional gel electrophoresis (1D-PAGE). Rat brain was used for control and was a gift from Dr. Amanda Mickiewicz (Rush University, Chicago).

Reverse transcription-polymerase chain reaction (RT-PCR): To assess S1P1 mRNA expression, RT-PCR was performed as reported previously [38]. Briefly, total RNA (n=40, ovaries = 30, other organs (lymph, muscle, liver) from at least four hens) was extracted using Trizol reagent (Invitrogen, Carlsbad, CA). The RNA content was measured at an optical density (OD) of 260 nm and the purity evaluated using an OD 260/ 280 nm absorbance ratio $\geq$ 1.7. RNA was treated with DNASe (Invitrogen, Carlsbad, CA) to remove trace amounts of genomic DNA before the first strand synthesis. First strand synthesis was performed using 500 ng of RNA according to the manufacturer's protocol (37ºC, 1 hour; High Capacity cDNA RT Kit, (Applied Biosystems, Carlsbad, CA). The PCR amplifications were carried out in a 25 µl reaction volume containing 25 ng of cDNA using Platinum Taq DNA Polymerase (Invitrogen, Carlsbad, CA) according to the manufacturer's recommendation. The PCR cycle consisted of a primary denaturation at 94ºC (3 minutes) followed by 35 cycles of denaturation at 94º C (30 seconds) and 54º C (30 seconds) to anneal and 72 º C (1 minute) for extension followed by a final extension at 72º C (10 minutes) in a programmable Peltier Thermo Cycler (PTC-200, MJ Research Inc., Ramsey, MN). Hen-specific S1P1 primers were designed using Oligoperfect Designer software

(Invitrogen, Carlsbad, CA) using the S1P1 sequence from the NCBI [GeneBank: XM_422305.2]. The forward primer was CCCCAGGAGCATTAAAACTG and the reverse primer was CTGCTGACCACCCTCACTG located between exons 1 and 2. β-actin was used as the endogenous control with a forward primer of TGCGTGACATCAAGGAGAAG and a reverse primer of ATGCCAGGGTACATTGTGGT. The expected base pair size for the S1P1 amplicon was 226 bp and for β-actin was 300 bp. PCR amplicons were visualized in a 2% agarose gel (Pierce/Thermo Fisher, Rockford, IL USA) in T.A.E. buffer (4.84g Tris Base, 1.14mL acetic acid, 2.0 mL 0.5M EDTA/L of buffer) and stained with ethidium bromide. The image was captured using a ChemiDoc XRS system (Bio-Rad, Hercules, CA). Amplicon from a positive sample (endometrioid carcinoma of the ovary) was used for sequence analysis after purification using the Quia-Quick PCR Purification System (Qiagen, Valencia, CA USA) according to manufacturer's instructions. The purified DNA was sequenced at the DNA sequencing facility at the University of Illinois at Chicago using an ABI 3100 Genetic analyzer (Applied Biosystems, Foster City, CA).

One-dimensional (1D) Western Blot: Ovarian tissue samples (n= 15) were homogenized according to a previous protocol [39] and stored at -80ºC. Proteins (10 µg/lane) were separated by 1D gel electrophoresis using 10% gradient Tris-HCl gels (Bio-Rad, Hercules, CA) using standard procedures [31]. MagicMark XP Western blot standards (Invitrogen, Carlsbad, CA) were used to estimate molecular weight. Rat brain (n=3) was used as a positive control (recommended by Cayman Chemical website). Proteins were transferred (18 Volts, 30 minutes) to a nitrocellulose membrane (0.45 µm; Bio-Rad, Hercules, CA). Blots were blocked in 10 x Blocking Buffer (diluted to 1x; Sigma St. Louis, MO) containing 0.05% Tween-20 (4ºC; 16 hours; Sigma, St. Louis, MO), rinsed in Wash buffer (0.15M NaCl in 10mM Tris containing 0.05% Tween-20, pH7.5) and incubated in rabbit anti-S1P1 polyclonal antibody (1:200; Cayman Chemical, Anne Arbor MI) diluted in blocking buffer containing 0.05%Tween-20. The nitrocellulose membrane was washed three times in cold Wash buffer followed by goat anti-rabbit immunoglobulin-HRP (Horseradish-Peroxidase; Pierce/Thermo Fisher, Rockford, IL). The reaction was developed in Super Signal West Dura substrate (Pierce/Thermo Fisher, Rockford, IL) and digital images acquired using a ChemiDoc XRS system (Bio-Rad, Hercules, CA). Digital images were analyzed by Quantity One software (Bio-Rad, Hercules, CA).

Because there are currently no commercially available antibodies against avian S1P1, we used a commercially available polyclonal antibody against human S1P1 for Western blotting and immunohistochemical experiments. There are two serine (S) to threonine (T) substitutions in the chicken S1P1R, within amino acids 241-253 of the epitope, and a high degree of homology (> 85% based on sequence comparisons) between the two proteins.

Immunohistochemistry: Hen ovarian tissue (n = 40) was cut into two equal pieces for paraffin and frozen tissue processing. Ovarian tissue was embedded in paraffin and sectioned (6 μm). Sections of formalin-fixed, paraffin-embedded tissue stained with Hematoxylin and Eosin (H/E) were examined by a pathologist to determine the histological type and stage. For cryostat sections, tissue was washed in cold phosphate buffered saline (PBS, pH 7.0) and placed in 30% sucrose overnight at 4^{o}C. Tissues were washed once more in PBS the following morning, embedded in OCT Compound (Tissue Tek, Sakura, Japan) and flash frozen in dry-ice cooled methanol and stored at -80ºC until use.

Ovarian sections were incubated with rabbit anti-S1P1 (Cayman, Ann Arbor, MI) diluted 1:200 in PBS containing 1% BSA (bovine serum albumin; Fisher, Waltham, MA). The primary antibody was omitted as a control for non-specific antibody binding. Other primary antibodies for immune cell markers include Bu1a (chB6; Abcam, Cambridge, MA) and T cell antibodies (CD3, CD4, and CD8; Southern Biotech, Birmingham, AL). As a control for antibody specificity the anti-S1P1 was pre-absorbed with blocking peptide (Cayman, Ann Arbor, MI) (1:1, v/v; 45 minutes, 22ºC). The absorbed, control anti-S1P1 was diluted to the same concentration as the untreated S1P1 antibody (1:200) in blocking buffer (Sigma, St. Louis MO) supplemented with 0.05% Tween-20 and incubated with sections. Sections were washed and incubated with goat anti-rabbit immunoglobulin-HRP (Pierce/Thermo Fisher, Rockford, IL) (1:10,000 in Sigma Blocking Buffer containing 0.05% Tween-20;1 hour; 22ºC; Sigma, St. Louis, MO). Color was developed with 3, 3-diaminobenzidine (DAB) substrate (Vector Labs; Burlingame, CA). Slides were washed in running water (15 minutes) and counterstained with hematoxylin followed by dehydration with graded alcohol series (70 -100%) and xylene. Sections were examined with an

Olympus light microscope (BX41, Tokyo, Japan) and an Olympus U-CMAD3 camera with Micro Suite #5 software.

Results

S1P1 mRNA is expressed in hen tissues. The mRNA for S1P1 was detected at the predicted amplicon size of 226 bp in hen tissue (Figure 1). Four normal ovaries (no evidence of cancer) and four tumor ovaries with endometrioid, serous and mucinous histology had S1P1 mRNA (Figure 1A). Other tissues, including muscle, oviduct, liver and kidney also contained S1P1 mRNA (Figure 1B). The expression of S1P1 mRNA was confirmed by sequence analysis at University of Illinois at Chicago DNA Services Facility (DNAS). Human tissue was not evaluated for S1P1 mRNA expression because it was demonstrated previously [40].

S1P1 protein is expressed in hen tissues. S1P1 protein was expressed in human and hen ovaries and ovarian tumors with bands at 47, 72 and 108 kDa detected by Western blot (Figure 2). There were variations in the intensity of bands at each molecular size from different preparations in both hen and human tissues. A membrane-enriched fractionation (18,000 x g) did not result in a consistently enhanced 47 kDa band in either the hen tissues or control rat brain. Hen brain showed the same bands as the positive control. Spleen was expected to express S1P1 because it is a major lymphocyte processing organ and the Western blot reactions were the same as the rat and hen brain. The band intensity was reduced using anti-S1P1 antibody pre-absorbed with blocking peptide and was absent when the primary antibody was omitted.

S1P1 localization in hen ovaries and ovarian tumors by immunohistochemistry. S1P1 was expressed in normal hen ovaries in blood vessels in the stromal (Figure 3A and B) and medullary regions (Figure 3 E) of the ovary. S1P1 was also found in mature follicles, but not in early stage follicles (Figure 3A). Within mature follicles, S1P1 was expressed exclusively in the theca externa (Figure 3A). Surface epithelial cells of the ovary also showed intense S1P1 expression (Figure 3C). Atretic follicles (Figure 3D) had S1P1+ immune cells (insert) but S1P1

staining was absent in follicle remnants. The endothelial cells but not the smooth muscle cells of blood vessels were S1P1+ (Figure 3E, insert).

Hen ovarian tumors had varied S1P1 staining (Figure 4). A mucinous ovarian tumor had S1P1 staining associated with mucin-secreting glandular structures (Figure 4A and C). An example of a serous ovarian tumor shows light stromal cell cytoplasmic S1P1 staining but intense staining of the surface epithelium (Figure 4E and 4F). Endometrioid (Figure 4K and 4L) ovarian tumors had similar S1P1+ staining within the tumor; the most intense staining being associated with surface epithelial cells and the area immediately adjacent to it (Figure 4L). Most of the S1P1+ cells associated with clear cell carcinomas were outside the tumor (Figure 4G), while blood vessels in the uninvolved stroma adjacent to the tumor were S1P1+ (Figure 4I).

S1P1 localization in human ovary and ovarian tumors by immunohistochemistry. The staining patterns of S1P1 in human ovarian cancers were heterogeneous, similar to the hen ovarian tumors. Normal ovaries (post-menopausal women, age: 58) had some endothelial cell S1P1 staining around blood vessels as well as light staining of the ovarian stroma (Figure 5A and C). Serous ovarian tumors had some S1P1 staining in the stroma but not the epithelium (Figure 5B). Endometrioid structures were not stained, but surrounding stroma was S1P1 immuno-stained (Figure 5D).

S1P1 expression associated with immune cells in ovaries of hens. Serial frozen sections of ovarian tissue were stained with hen specific antibodies against Bu1a (antigen specific for avian B cells) and CD3 to determine if S1P1 expression was associated with immune cells (Figures 6 and 7). In normal ovaries (Figure 6), S1P1 was expressed on cells both with and without B or T cell markers in the ovarian stroma and was primarily expressed on blood vessels. The B and T cells were found in close proximity to S1P1 stained blood vessels. In tumors (Figure 7) staining patterns were less organized. S1P1 staining occurred in serous tumor cells. While CD4 T cells were more often found scattered around the tumor glands, CD8 T cells and Bu1a+ staining was localized throughout the tissue and in tumor glands.

Discussion

This is the first study reporting the expression of S1P1 in ovarian tissues in the adult laying hen. Although chicken specific primers were used to detect S1P1 mRNA and an anti-human S1P1 antibody was used to detect S1P1 protein, the expression of S1P1 mRNA and protein were correlated. Similarly, S1P1 was detected by immunohistochemistry in tissue positive for S1P1 mRNA and protein. This is consistent with the high degree of amino acid similarity (> 85%) between avian [GenBank ACC#: XP_001231780.1] and human [GenBank ACC#: NP_001391.2] S1P1 protein. Furthermore the location of S1P1 positive cells was similar in hen and human. In normal ovaries and ovarian tumors, S1P1 was expressed in endothelial cells of blood vessels and immune cells. In follicle cells of normal hen ovary, theca externa cells but not ovarian stroma nor other follicular structures were stained. Follicles in normal human ovary were not observed in this study because tissue from post-menopausal women was used and thus it was not possible to compare them with the hen follicles. Tumor cells and surface epithelium in ovaries with tumors were variably stained. Overall the expression of S1P1 in hen and human ovaries and in the ovarian tumors examined was remarkably similar.

Previous reports of S1P1 detected in Western blots indicated various molecular sizes [41], although the expected size is 47 kDa [2]. We observed a 47 kDa species by Western blotting in a membrane-enriched fraction, although it was often faint or undetectable. However, there were two predominant higher molecular weight species (72 and 108 kDa); these are not usually described although they are evident in some reports [42]. Notably, the same molecular sizes were observed in hen and human ovaries and ovarian tumors, hen spleen, and hen and rat brain. Because bands react with S1P1 antibody, the larger size bands may represent aggregates in dimmers or trimers [43]. Alternatively, S1P1 receptor may also be differentially glycosylated, [44] although this would not usually produce proteins double the smaller 50kDa size. When tissues were subjected to deglycosylation enzymes after homogenization (EndoH, New England Bio-Labs, Ipswich, MA USA), the molecular sizes did not change (data not shown) suggesting either the protein is not glycosylated or, more likely, is resistant to EndoH cleavage. Nonetheless,

297 similar protein bands were detected in the human and hen ovary, demonstrating a similar
298 expression pattern.

299

300 The immunohistochemical pattern of S1P1 staining was common to both hen and human
301 ovaries. Normal hen ovary expressed S1P1 in surface epithelial cells, theca cells of the follicle,
302 endothelial cells of blood vessels in the stroma and medullary region, as well as in immune cells
303 such as infiltrating immune cells of atretic follicles. The expression of S1P1 was not confined to
304 immune cells. Because the human ovaries used in this study were from older women, they did not
305 have any follicles for comparison. However, S1P1 was similarly expressed in surface epithelial
306 cells, endothelial cells and immune cells. Likewise, in hen and human ovarian tumors S1P1 was
307 expressed in endothelial cells and immune cells. In addition, tumors cells expressed S1P1 and the
308 expression was dispersed throughout the cytoplasm. Furthermore, S1P1 expression varied
309 among ovarian tumors. This may have been due to variations in expression among tumors or
310 among tumor types or to sampling of individual tumors.

311

312 **Conclusion**

313

314 In summary, S1P1 is expressed on immune cells in the hen. S1P1 is also expressed in
315 ovarian tissues of the laying hen with a distribution in the ovary that is similar to human ovaries.
316 The chicken embryo contains both sphingosine-1 phosphate (ligand for S1P1) and sphingosine
317 kinase; the enzyme responsible for the conversion of sphingosine to sphingosine-phosphate which
318 occurs in the blood [45]. Similarly, chicken embryonic amacrine cells were recently reported to
319 express S1P1 [46], indicating that this receptor can be found in both embryonic and, as our study
320 shows, the adult tissues of the chicken.

321

322 We also show, for the first time, that S1P1 is expressed in both hen and human ovarian
323 tumors. S1P (the ligand for S1P1) has been implicated in the trafficking of immune cells [5].
324 Immune cells are reported to be involved in the progression of tumors of various organs [47].
325 While the role of infiltrating immune cells in ovarian cancer progression is not clearly defined [48]

there clearly is a relationship of infiltrating T cells and survival [48-50]. The hen provides an alternative animal model to engineered rodent models for studies of ovarian cancer. Further studies addressing immune cell infiltration into tumors and the role S1P1 plays in regulating immune cell infiltration into ovarian tumors would be facilitated by use of the hen because all stages of spontaneous tumors in the hen can be readily observed.

Disclosure Statement

The authors have no conflict of interest.

Author Contributions

MJB carried out the molecular and immunohistochemical studies, participated in the sequence alignment, assisted in tissue collection, and drafted the manuscript. AB classified hen ovarian tumors, collected all tissue, prepared tissue for immunohistochemistry and maintained databases. YY reproduced the RT-PCR experiments. KP assisted in Western blotting experiments and maintained the tissue inventory. SLE designed PCR primers, prepared the sequence comparisons and assisted in the molecular biology experiments and their design. SS provided human ovarian tissue used in this study and participated in discussions of the experimental design. JSA assisted AB in detecting potential ovarian tumors with ultrasound. JMB maintained hens, collected tissue with AB and MJB and contributed expertise in avian physiology. JLL conceived the study, participated in its design and coordination, data analysis and preparation of the manuscript with MJB. All authors read and approved the final manuscript

Acknowledgements

This work was supported by NIH R01AI 055060 (JL), DOD OC073325 (JL), the Joy Piccolo O'Connell/Gavers Women's Cancer Award (JL), Prevent Cancer Foundation (AB), National Cancer Institute (AB) and Sramek Foundation (AB). Also, the generous effort and support of Chet and Pam Utterback and Doug Hilgendorf at the UIUC Poultry Farm is acknowledged.

FIGURE LEGENDS

Figure 1. **S1P1 mRNA expression in hen tissues**.

(**A**) S1P1 mRNA (226 bp) is expressed in both normal and tumor ovaries. Examples of mRNA in tumors with endometrioid (En), serous (Sr), and mucinous (Mc) histology are shown. (**B**) Examples of other hen tissues that express S1P1 mRNA (226 bp) include liver (LVR), kidney (KDNY), skeletal muscle (MSCL), oviduct (OVDT) and spleen. Normal ovary and spleen are from the same hens (1-4). β-actin (300 bp) was used as a loading control.

Figure 2. S1P1 protein expression in hen and human tissue.

S1P1 immunoreactions are similar in hen and human ovaries and ovarian tumors. Three bands at 47, 72, 108 kDa were observed. The band at 47kDa was faint, while bands at 72 and 108 kDa were consistently present in all tissues but vary in intensity. The 47kD band was not significantly enhanced using a membrane enriched (18,000xg pellet) fraction. The pattern of immunoreactive bands was identical in the positive control recommended by the manufacturer (rat brain) and in hen brain and spleen. The bands were absent in control incubations in which the primary antibody was pre-adsorbed with a blocking peptide or in which the primary antibody was omitted.

Figure 3. Localization of S1P1 receptor protein expression in normal hen ovary.

(**A**) S1P1+ cells (black arrows) in theca of a mature follicle (F) and within small blood vessels (BV; white arrows) in ovarian stroma (100 x). Primordial follicles (f) have comparatively little S1P1+ expression. (**B**) Endothelial cells of blood vessels (BV) in the theca externa (TE) of a follicle (F) and ovarian stroma are S1P1+ (200 x). (**C**) Surface epithelial cells (EpC) showing intense S1P1+ expression (400 x). (**D**) An atretic follicle (af) with characteristic infiltrating S1P1+ immune cells (100 x). Inset: High magnification of (D) showing an S1P1+ immune cell (1000 x). (**E**) Well developed blood vessels (BV) in the medullary region of the ovary also contain S1P1+ endothelial cells (400 x) but staining is lighter and more diffuse than in stromal blood vessels seen in (A) and (B). Inset: high magnification (800 x) shows detail of smooth

muscle cells (SmC) and endothelial cells (EnC). (**A-C)** are frozen tissues; (**D)** and (**E)** are paraffin-embedded.

Figure 4. Localization of S1P1 receptor protein expression in hen ovarian tumors.

(**A**) An example of a mucinous ovarian tumor with S1P1+ staining associated with surface epithelium (black arrow) and mucin-secreting structures (black arrow) (100 x). (**B**) H& E stained section (100 x) serial to that in (A) shows mucinous histology. (**C**) Higher magnification of (A) showing S1P1+ mucin-secreting glandular (MG) structures (black arrows) (400 x). (**D**) H&E stained section of a serous ovarian tumor (100 x). (**E**) Serial section showing minimal stromal cell stain for S1P1+ but intense surface epithelial cell staining (black arrow) and lighter more diffuse S1P1+ sub-epithelial cells (white arrow) (100 x). (**F**) High magnification (of box) showing S1P1+ surface epithelial cells (EpC) (600 x). (**G**) Clear-cell ovarian tumor (T; left of dotted red line) with negligible S1P1+ in tumor and S1P1+ cells in adjacent uninvolved stroma (100 x). (**H**) H&E-stained serial section from the same tumor region in (G) shows cellular detail of clear cell carcinoma (400 x). (**I**) Higher magnification of box in(G) showing stromal blood vessels (BV) with S1P1+ endothelial cells and stromal cells (S) (200 x). (**J**) H&E stained section of late stage endometrioid tumor (100 x). (**K**) S1P1+ is highly expressed in cells in the tumor periphery and to a lesser extent in tumor stroma (100 x). (**L**) High magnification of box in (K) showing cytoplasmic staining of endometrioid tumor cells (400x). All images are from paraffin-embedded tissue, except clear cell carcinoma (G-I) which is a frozen section.

Figure 5. S1P1 receptor expression in human ovarian carcinomas.

(A) Normal ovary showing diffusely stained S1P+ stromal cells (white arrows) and a blood vessel (BV) with intensely stained S1P1+ endothelial cells (black arrow) (200 x). **(B)** Serous ovarian tumor with S1P1+ stroma (white arrows) and unstained surface epithelium (200 x). **(C)** Normal ovary (BV, arrows) are positive (600 x). **(D)** S1P1+ endometrioid ovarian tumor with patches of intense stain (white arrows) (400 x). (A-D) are paraffin-embedded sections.

Figure 6. In normal hen ovary S1P1 expression was observed in areas of immune cell infiltration. (**Row A)** Immune cells (Bu1a+ and CD3+) are adjacent to the follicle (f) in the ovarian stroma near a transverse blood vessel (arrow in column S1P1). Cells lining the vessel near the follicle (f) are S1P1+ (row A, S1P1) (original magnification 100 x). (**Row B)** High magnification (see red boxes in row A) showing B and T cells clustered within the stroma near S1P1 stained vascular endothelium (arrow). Some immune cells are also S1P1+ (open arrow) (original magnification 400 x). (**Row C)** Cross-section of a large blood vessel shows Bu1a and CD3 positive cells are clustered near the blood vessel. The apical surfaces of endothelial cell express S1P1 (original magnification 100 x).

Figure 7. In ovarian tumors S1P1 expression was observed near T and B cells. Alternate serial sections of a serous ovarian tumor of the hen showing (**A)** Bu1a+ cells in the stroma (arrows) and diffuse tissue stain (open arrow), (**B)** CD4 T cells around tumor glands (arrows), (**C)** S1P1 expression on the epithelium of tumor glands (arrow) and (**D)** CD8 T cells (arrows) in the stroma (original magnification 100 x).

Reference List

(1) Brinkmann V, Pinschewer D, Chiba K, Feng L: **FTY720: a novel transplantation drug that modulates lymphocyte traffic rather than activation.** *Trends Pharmacol Sci* 2000, **21**:49-52.

(2) Brinkmann V: **Sphingosine 1-phosphate receptors in health and disease: mechanistic insights from gene deletion studies and reverse pharmacology.** *Pharmacol Ther* 2007, **115**:84-105.

(3) Brinkmann V, Davis MD, Heise CE, Albert R, Cottens S, Hof R *et al*: **The immune modulator FTY720 targets sphingosine 1-phosphate receptors.** *J Biol Chem* 2002, **277**:21453-21457.

(4) Schmid G, Guba M, Ischenko I, Papyan A, Joka M, Schrepfer S *et al*: **The immunosuppressant FTY720 inhibits tumor angiogenesis via the sphingosine 1-phosphate receptor 1.** *J Cell Biochem* 2007, **101**:259-270.

(5) Chiba K, Matsuyuki H, Maeda Y, Sugahara K: **Role of sphingosine 1-phosphate receptor type 1 in lymphocyte egress from secondary lymphoid tissues and thymus.** *Cell Mol Immunol* 2006, **3**:11-19.

(6) Matloubian M, Lo CG, Cinamon G, Lesneski MJ, Xu Y, Brinkmann V *et al*: **Lymphocyte egress from thymus and peripheral lymphoid organs is dependent on S1P receptor 1.** *Nature* 2004, **427**:355-360.

(7) Goetzl EJ, Kong Y, Mei B: **Lysophosphatidic acid and sphingosine 1-phosphate protection of T cells from apoptosis in association with suppression of Bax.** *J Immunol* 1999, **162**:2049-2056.

(8) Liu Y, Wada R, Yamashita T, Mi Y, Deng CX, Hobson JP *et al*: **Edg-1, the G protein-coupled receptor for sphingosine-1-phosphate, is essential for vascular maturation.** *J Clin Invest* 2000, **106**:951-961.

(9) Brinkmann V: **FTY720: mechanism of action and potential benefit in organ transplantation.** *Yonsei Med J* 2004, **45**:991-997.

(10) Devine KM, Smicun Y, Hope JM, Fishman DA: **S1P induced changes in epithelial ovarian cancer proteolysis, invasion, and attachment are mediated by Gi and Rac.** *Gynecol Oncol* 2008, **110**:237-245.

(11) Smicun Y, Reierstad S, Wang FQ, Lee C, Fishman DA: **S1P regulation of ovarian carcinoma invasiveness.** *Gynecol Oncol* 2006, **103**:952-959.

(12) Hancke K, Strauch O, Kissel C, Gobel H, Schafer W, Denschlag D: **Sphingosine 1-phosphate protects ovaries from chemotherapy-induced damage in vivo.** *Fertil Steril* 2007, **87**:172-177.

(13) Morita Y, Perez GI, Paris F, Miranda SR, Ehleiter D, Haimovitz-Friedman A *et al*: **Oocyte apoptosis is suppressed by disruption of the acid sphingomyelinase gene or by sphingosine-1-phosphate therapy.** *Nat Med* 2000, **6**:1109-1114.

(14) Barua A, Yoshimura Y: **Ovarian autoimmunity in relation to egg production in laying hens.** *Reproduction* 2001, **121**:117-122.

(15) Barua A, Abramowicz JS, Bahr JM, Bitterman P, Dirks A, Holub KA *et al*: **Detection of ovarian tumors in chicken by sonography: a step toward early diagnosis in humans?** *J Ultrasound Med* 2007, **26**:909-919.

(16) Barua A, Edassery SL, Bitterman P, Abramowicz JS, Dirks AL, Bahr JM et al: **Prevalence of antitumor antibodies in laying hen model of human ovarian cancer.** *Int J Gynecol Cancer* 2009, **19**:500-507.

(17) Barua A, Bitterman P, Abramowicz JS, Dirks AL, Bahr JM, Hales DB et al: **Histopathology of ovarian tumors in laying hens: a preclinical model of human ovarian cancer.** *Int J Gynecol Cancer* 2009, **19**:531-539.

(18) Barua A, Bitterman P, Bahr JM, Bradaric MJ, Hales DB, Luborsky JL et al: **Detection of tumor-associated neoangiogenesis by Doppler ultrasonography during early-stage ovarian cancer in laying hens: a preclinical model of human spontaneous ovarian cancer.** *J Ultrasound Med* 2010, **29**:173-182.

(19) Hales DB, Zhuge Y, Lagman JA, Ansenberger K, Mahon C, Barua A et al: **Cyclooxygenases expression and distribution in the normal ovary and their role in ovarian cancer in the domestic hen (*Gallus domesticus*).** *Endocrine* 2008, **33**:235-244.

(20) Johnson PA, Giles JR: **Use of genetic strains of chickens in studies of ovarian cancer.** *Poult Sci* 2006, **85**:246-250.

(21) Rodriguez-Burford C, Barnes MN, Berry W, Partridge EE, Grizzle WE: **Immunohistochemical expression of molecular markers in an avian model: a potential model for preclinical evaluation of agents for ovarian cancer chemoprevention.** *Gynecol Oncol* 2001, **81**:373-379.

(22) Fredrickson TN: **Ovarian tumors of the hen.** *Environ Health Perspect* 1987, **73**:35-51.

(23) Bahr J: **The Chicken as Model Organism.** In: *Sourcebook of Models for Biomedical Research*. Edited by Conn, PM. SpringerLink; 2008:161-167.

(24) Bahr J: **The avian ovary: model for endocrine studies.** *J Exp Zool Suppl* 1990, **4**:192-194.

(25) Lovell TM, Gladwell RT, Groome NP, Knight PG: **Ovarian follicle development in the laying hen is accompanied by divergent changes in inhibin A, inhibin B, activin A and follistatin production in granulosa and theca layers.** *J Endocrinol* 2003, **177:**45-55.

(26) Goodman MT, Howe HL, Tung KH, Hotes J, Miller BA, Coughlin SS et al: **Incidence of ovarian cancer by race and ethnicity in the United States, 1992-1997.** *Cancer* 2003, **97**:2676-2685.

(27) Giles JR, Olson LM, Johnson PA: **Characterization of ovarian surface epithelial cells from the hen: a unique model for ovarian cancer.** *Exp Biol Med* (Maywood) 2006, **231**:1718-1725.

(28) Hakim AA, Barry CP, Barnes HJ, Anderson KE, Petitte J, Whitaker R et al: **Ovarian adenocarcinomas in the laying hen and women share similar alterations in p53, ras, and HER-2/neu.** *Cancer Prev Res* (Phila) 2009, **2**:114-121.

(29) Jackson E, Anderson K, Ashwell C, Petitte J, Mozdziak PE: **CA125 expression in spontaneous ovarian adenocarcinomas from laying hens.** *Gynecol Oncol* 2007, **104**:192-198.

(30) Ansenberger K, Zhuge Y, Lagman JA, Richards C, Barua A, Bahr JM et al: **E-cadherin expression in ovarian cancer in the laying hen, Gallus domesticus, compared to human ovarian cancer.** *Gynecol Oncol* 2009, **113**:362-369.

(31) Stammer K, Edassery SL, Barua A, Bitterman P, Bahr JM, Hales DB et al: S**elenium-Binding Protein 1 expression in ovaries and ovarian tumors in the laying hen, a spontaneous model of human ovarian cancer.** *Gynecol Oncol* 2008, **109**:115-121.

(32) Yi Yu, Edassery, SL Barua A, Bitterman P, Abramowicz JS, Bahr JM, Hellstrom I and Luborsky, JL: **Mesothelin expression in ovarian tumors and serum autoantibodies of the laying hen model is similar to human ovarian cancer [abstract # 3264]:** In: *Proceedings of the 101st Annual Meeting of the American Association for Cancer Research*: 17-21 April 2010; Washington, DC. Cadmus Publishing; 2010:793.

(33) Barnes MN, Berry WD, Straughn JM, Kirby TO, Leath CA, Huh WK et al: **A pilot study of ovarian cancer chemoprevention using medroxyprogesterone acetate in an avian model of spontaneous ovarian carcinogenesis.** *Gynecol Oncol* 2002, **87**:57-63.

(34) Chan MM, Chen CL, Ager LL, Cooper MD: **Identification of the avian homologues of mammalian CD4 and CD8 antigens.** *J Immunol* 1988, **140**:2133-2138.

(35) Cooper MD, Peterson RD, Good RA: **Delineation of the Thymic and Bursal Lymphoid Systems in the Chicken.** *Nature* 1965, **205**:143-146.

(36) Davison TF: **The immunologists' debt to the chicken.** Br Poult Sci 2003, **44**:6-21.

(37) Luborsky J: **Ovarian autoimmune disease and ovarian autoantibodies.** J *Womens Health Gend Based Med* 2002, **11:**585-599.

(38) Barua A, Bradaric MJ, Kebede T, Espionosa S, Edassery SL, Bitterman P et al: **Anti-tumor and anti-ovarian autoantibodies in women with ovarian cancer.** *Am J Reprod Immunol* 2007, **57**:243-249.

(39) Luborsky JL, Visintin I, Boyers S, Asari T, Caldwell B, DeCherney A: **Ovarian antibodies detected by immobilized antigen immunoassay in patients with premature ovarian failure**. *J Clin Endocrinol Metab* 1990, **70**:69-75.

(40) Akiyama T, Sadahira Y, Matsubara K, Mori M, Igarashi Y: **Immunohistochemical detection of sphingosine-1-phosphate receptor 1 in vascular and lymphatic endothelial cells.** *J Mol Histol* 2008, **39**:527-533.

(41) Braun A, Xu H, Hu F, Kocherlakota P, Siegel D, Chander P et al: **Paucity of pericytes in germinal matrix vasculature of premature infants**. *J Neurosci* 2007, **27**:12012-12024.

(42) Ishii I, Friedman B, Ye X, Kawamura S, McGiffert C, Contos JJ et al: S**elective loss of sphingosine 1-phosphate signaling with no obvious phenotypic abnormality in mice lacking its G protein-coupled receptor, LP(B3)/EDG-3.** *J Biol Chem* 2001, **276**:33697-33704.

(43) Van Brocklyn JR, Behbahani B, Lee NH: **Homodimerization and heterodimerization of S1P/EDG sphingosine-1-phosphate receptors.** *Biochim Biophys Acta* 2002, **1582**:89-93.

(44) Kohno T, Wada A, Igarashi Y: **N-glycans of sphingosine 1-phosphate receptor Edg-1 regulate ligand-induced receptor internalization.** *FASEB J* 2002, **16**:983-992.

(45) Choi CH, Jeong JS, Yoo BI, Jin YX, Moon DC, Yoo HS et al: **Sphingosine 1-phosphate and sphingosine kinase activity during chicken embryonic development.** *Arch Pharm Res* 2007, **30**:502-506.

(46) Crousillac S, Colonna J, McMains E, Dewey JS, Gleason E: **Sphingosine-1-phosphate elicits receptor-dependent calcium signaling in retinal amacrine cells.** *J Neurophysiol* 2009, **102**:3295-3309.

(47) de Visser KE: **Spontaneous immune responses to sporadic tumors: tumor-promoting, tumor-protective or both?** *Cancer Immunol Immunother* 2008, **57**:1531-1539.

(48) Milne K, Kobel M, Kalloger SE, Barnes RO, Gao D, Gilks CB et al: **Systematic analysis of immune infiltrates in high-grade serous ovarian cancer reveals CD20, FoxP3 and TIA-1 as positive prognostic factors.** *PLoS One* 2009, **4**:e6412.

(49) Sato E, Olson SH, Ahn J, Bundy B, Nishikawa H, Qian F et al: I**ntraepithelial CD8+ tumor-infiltrating lymphocytes and a high CD8+/regulatory T cell ratio are associated with favorable prognosis in ovarian cancer.** *Proc Natl Acad Sci* U S A 2005, **102**:18538-18543.

(50) Zhang L, Conejo-Garcia JR, Katsaros D, Gimotty PA, Massobrio M, Regnani G et al: **Intratumoral T cells, recurrence, and survival in epithelial ovarian cancer.** *N Engl J Med* 2003, 348:203-213.

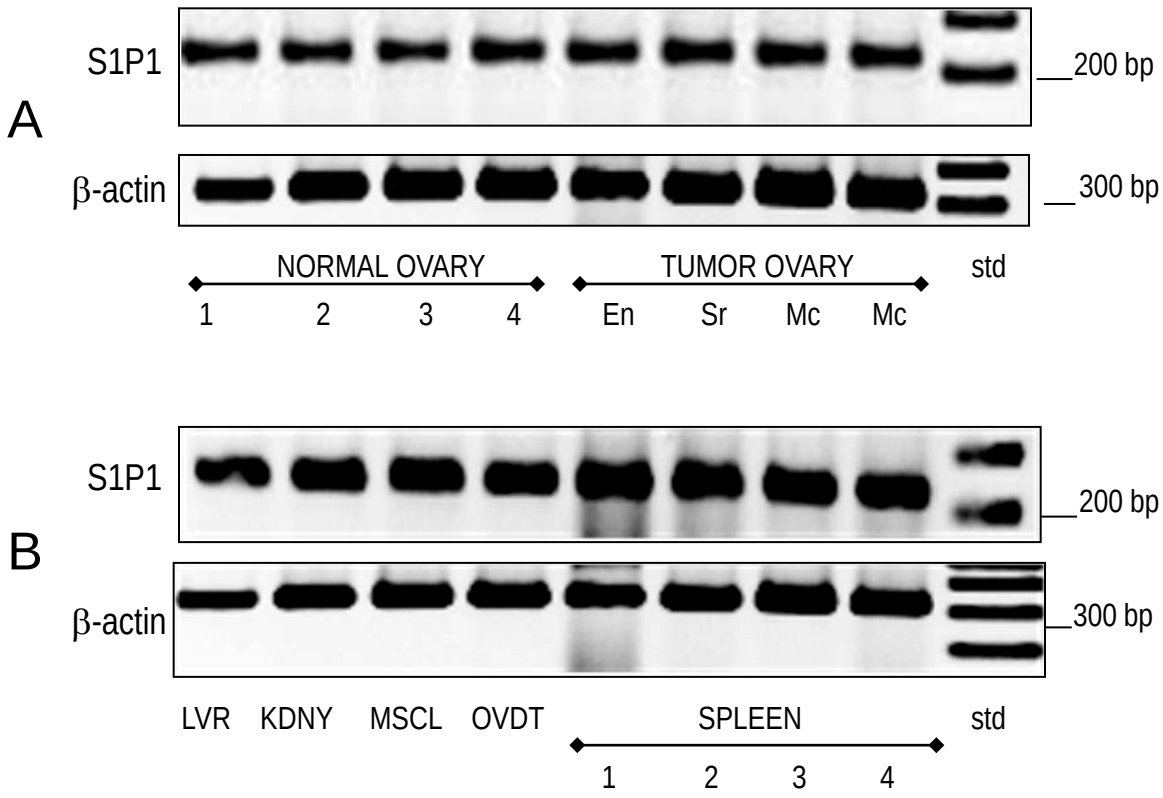
A
S1P1
200 bp
β-actin
300 bp
NORMAL OVARY
TUMOR OVARY
std
1
2
3
4
En
Sr
Mc
Mc
B
S1P1
200 bp
β-actin
300 bp
LVR
KDNY
MSCL
OVDT
SPLEEN
std
1
2
3
4

Figure 1

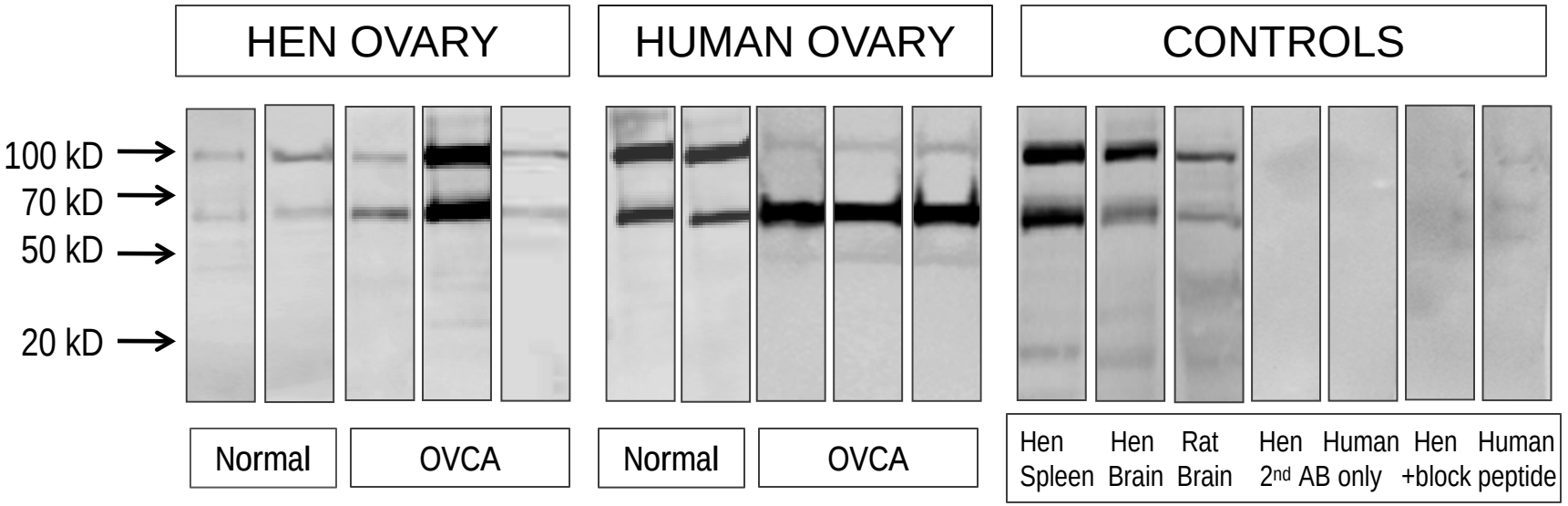
HEN OVARY
HUMAN OVARY
CONTROLS
100 kD
70 kD
50 kD
20 kD
Normal
OVCA
Normal
OVCA
Hen Spleen
Hen Brain
Rat Brain
Hen 2nd AB only
Human +block
Hen peptide
Human

Figure 2

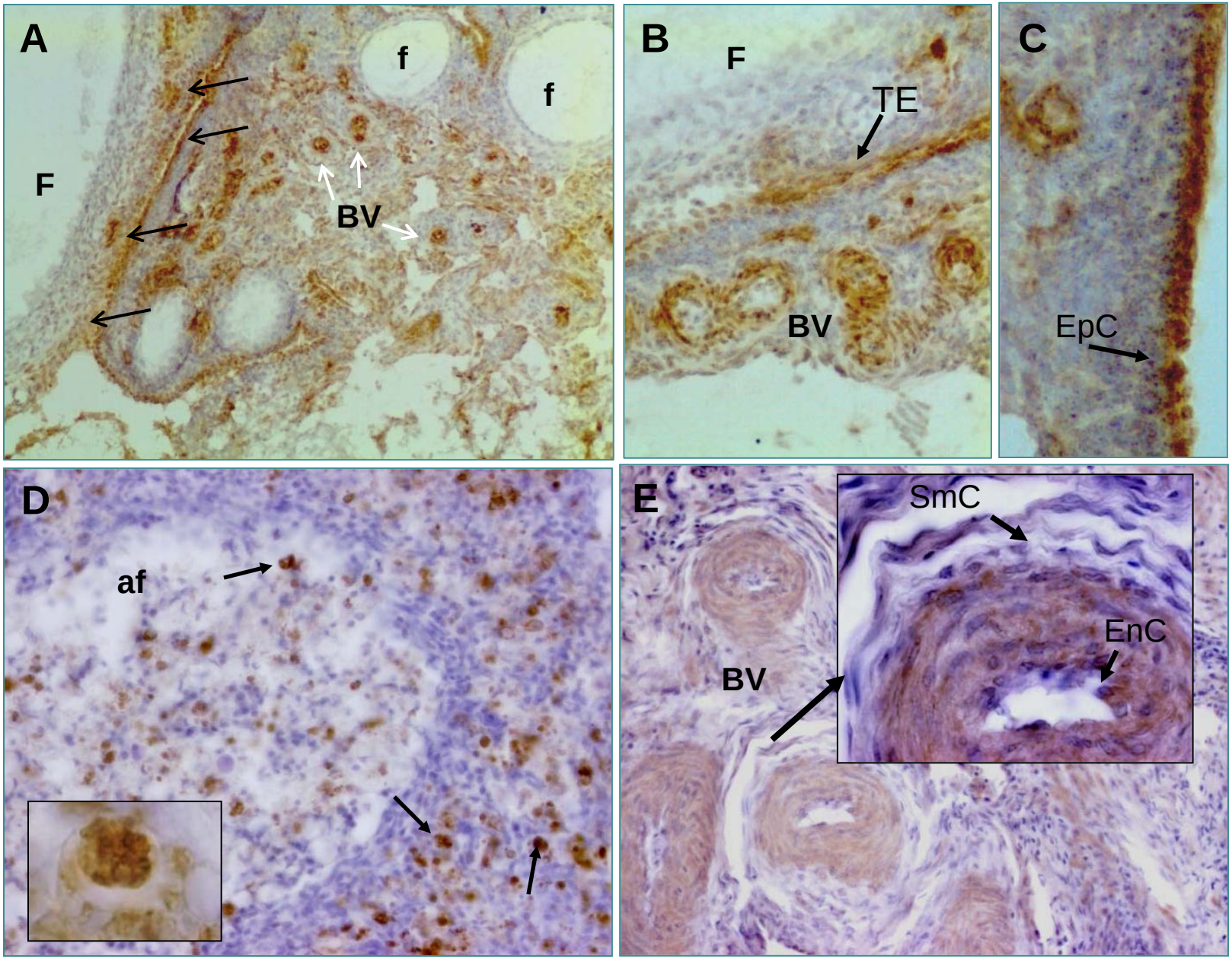

Figure 3

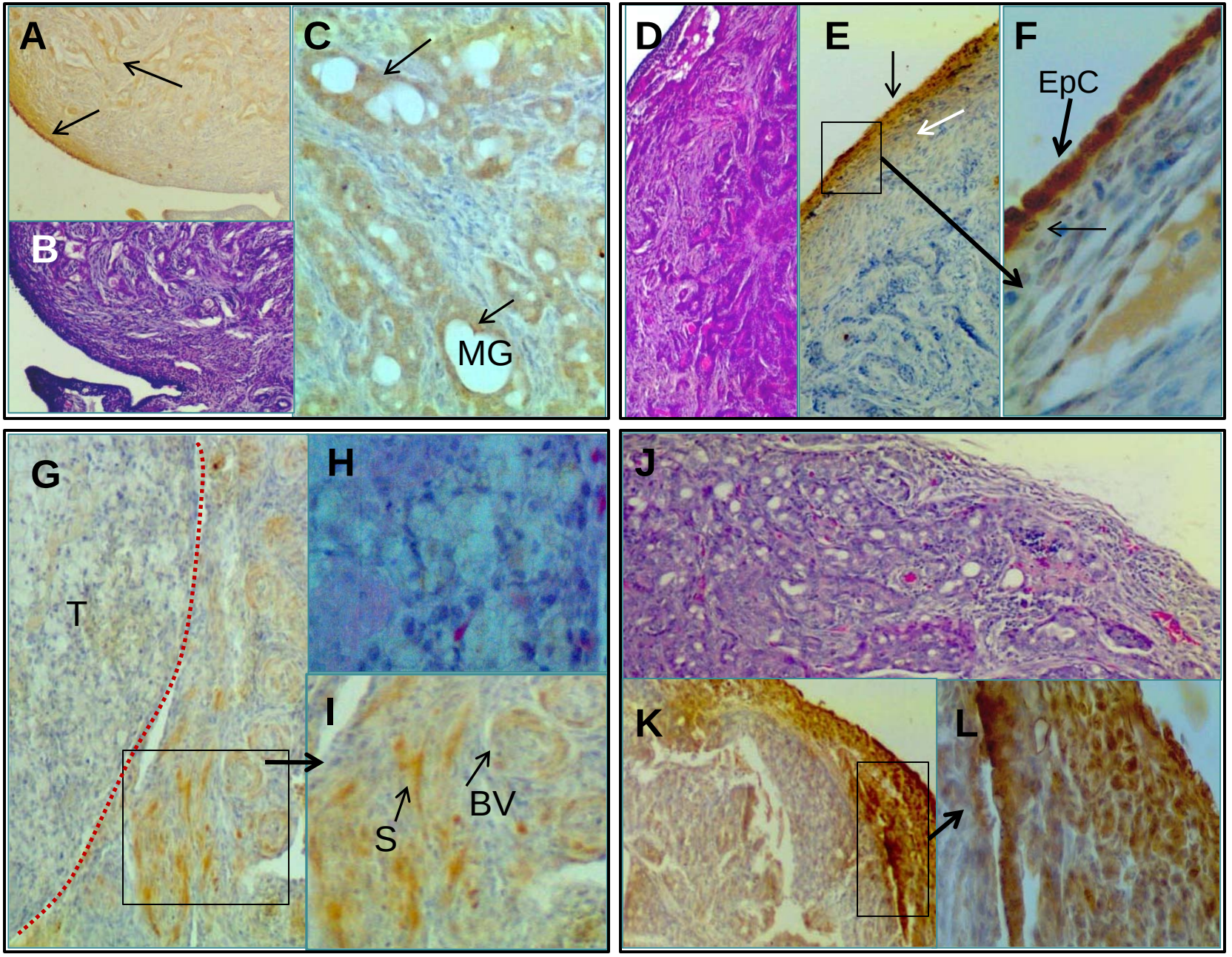

Figure 4

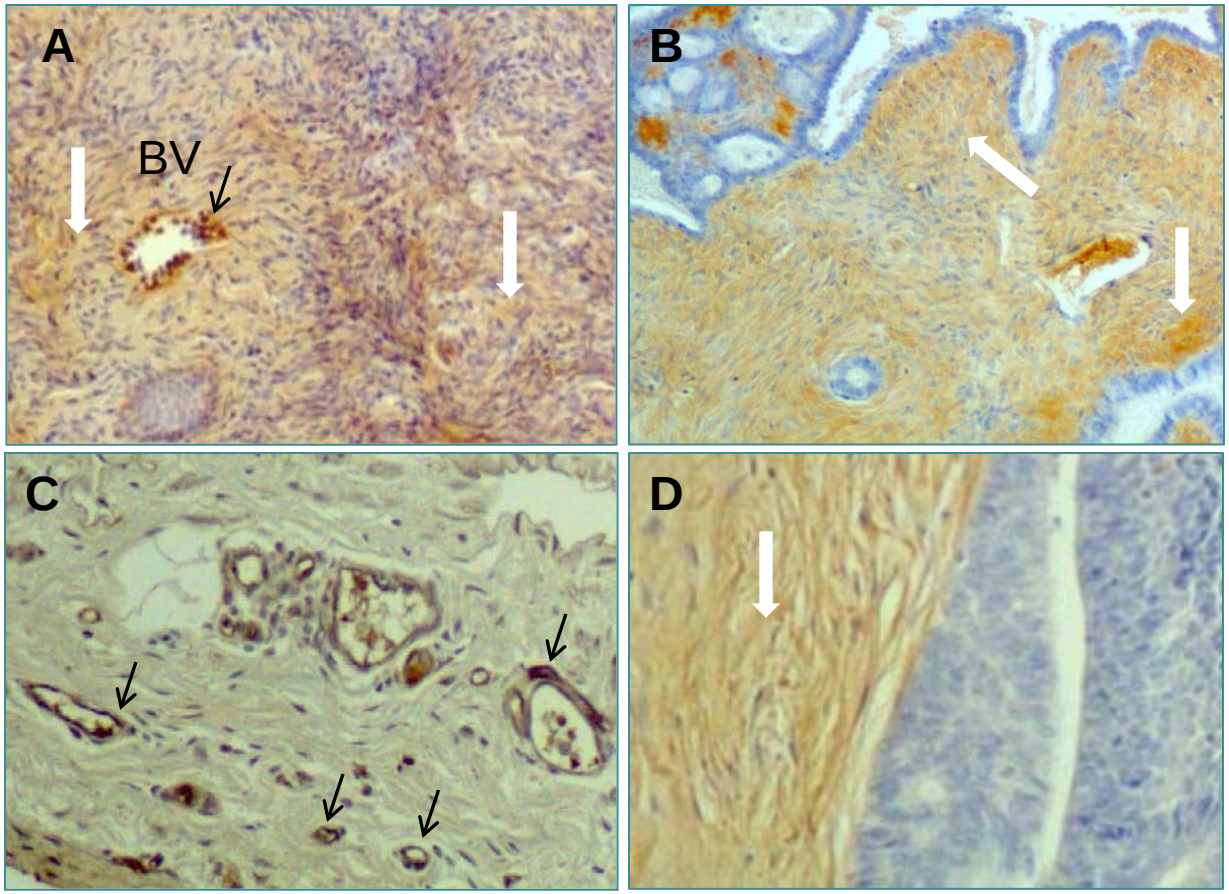

Figure 5

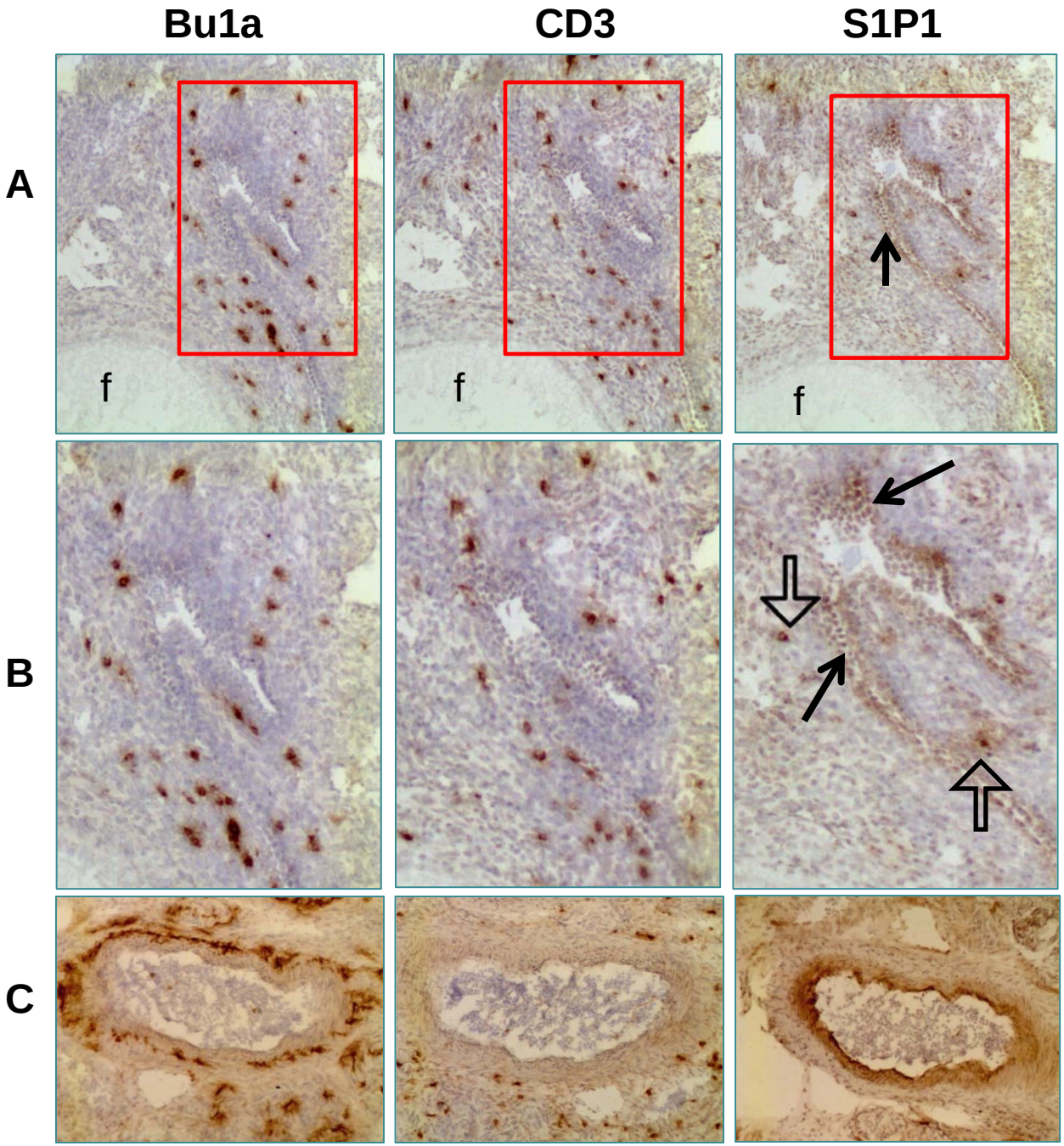

Figure 6

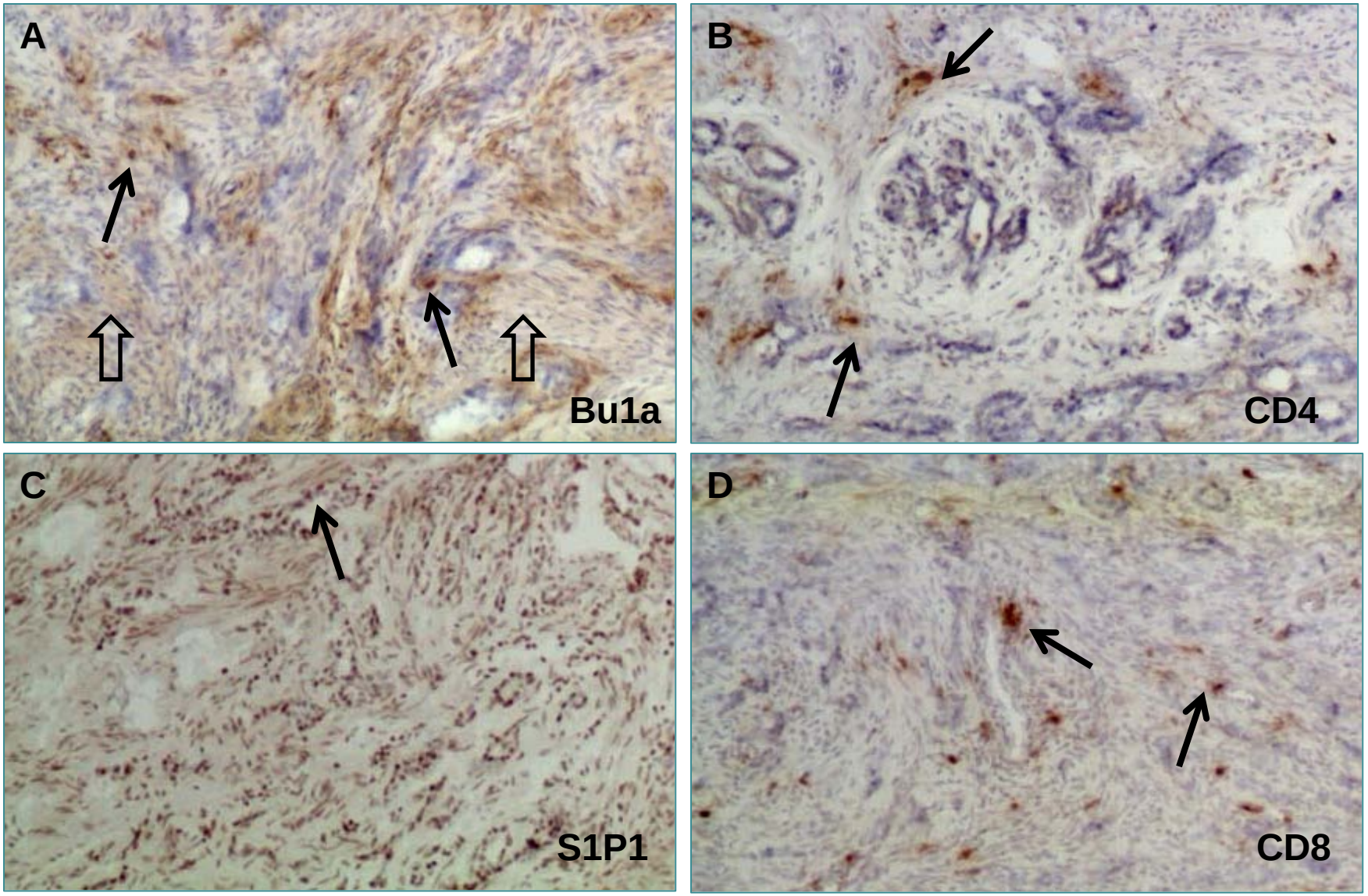

Figure 7

file: All_figs_91410_MB_JL